Analysis of the role of the p47 GTPase IIGP1 in Resistance against Intracellular Pathogens

Inaugural-Dissertation
zur
Erlangung des Doktorgrades
der Mathematisch-Naturwissenschaftlichen Fakultät
der Universität zu Köln

vorgelegt von
Iana Angelova Parvanova
aus Bulgarien

Köln 2005

Berichterstatter: Prof. Dr. Jonathan C. Howard
                      Prof. Dr.Jens Brüning

Tag der mündlichen Prüfung: 19.7.2005

To my family

3   RESULTS   33

ABBREVIATIONS

2'-5'-OAS	2'-5'-oligoadenylate synthetase
ADAR	adenosine deaminases that act on double-stranded RNA
BAC	bacterial artificial chromosome
bp	base pair
BSA	bovine serum albumine
CDS	coding sequence
CFU	colony-froming units
CM	cerebral malaria
cpm	counts per minute
DMEM	Dulbecco Modified Eagles Medium
DMSO	dimethylsulfoxid
EF cells	embryonic feeder cells
ES cells	embryonic stem cells
ER	endoplasmatic reticulum
FCS	foetal calf serum
GAP	GTPase activating protein
GBP	guanylate binding protein
GDP	guanosine diphosphate
GTP	guanosine triphosphate
mHPRT	mouse hypoxanthine guanine phosphoribosyl transferase
IDO	indoleamine 2,3-dioxygenase
IF	immunofluorescence
IFN	Interferon
IFNGR	IFN-γ receptor
IFNAR	IFN-α receptor
iNOS	inducible nitric oxide synthetase
i.p.	intraperitoneal
ISG20	interferon stimulated gene 20
JAK	janus kinase
kb	kilobase
kDa	kilodalton
LPS	lipopolysaccharide
M	molar
MEF	mouse embryonic fibroblats
OD	optical density
PBS	phosphate buffered saline
PCR	polymerase chain reaction
PFA	paraformaldehyde
Phox	phagosome oxidase
p.i.	post infection
PKR	protein kinase R
PML	promyelocytic leukaemia
PV	parasitophorous vacuole
PVM	parasitophorous vacuole membrane
RNAse	ribonuclease
rpm	rounds per minute
RT	room temperature
STAT	signal transducer and activator of transcription
TNF-α	tumor necrosis factor α
TRIM5α	tripartite motif 5α
U	unit
ZAP	Zinc-finger Antiviral Protein

1 INTRODUCTION

1.1 Infection and immunity- the never ending battle

Millions of years of co-evolution and reciprocal adaptation have created a complicated system of interactions between pathogens and their hosts [1, 2]. The aim of all pathogens is to invade the host and successfully establish an infection, which allows them to exploit resources, propagate and eventually spread to other hosts. In order to achieve these goals pathogens have developed numerous evasion mechanisms interfering with host resistance processes [3-8]. To answer the pathogen challenge living organisms have developed a sophisticated multilayer immune system. The function of this system is to recognize invaders, interfere with essential steps in their propagation and destroy them. All multicellular organisms possess a complex of evolutionary conserved immune mechanisms, known as the innate immune system. In vertebrates, there is a second and more sophisticated layer of defense mechanisms, the adaptive immune system. All elements of the immune system, innate and adaptive, are subjected to complex regulation in order to guarantee elimination of invading agents with minimal host damage.

The innate immune system provides the first line of defense against invasion. This system senses the invaders through a variety of germline-encoded pattern recognition receptors (PRRs) recognizing conserved products of microbial metabolism designated as pathogen associated molecular patterns (PAMPs) [9]. The lists of PRRs includes cell surface molecules such as Toll-like receptors (TLRs) [10] and scavenger receptors [11], intracellular receptors like NODs [12], PKR [13], 2'-5'-oligoadenylate synthase (OAS) [14] and some molecules secreted in the bloodstream and tissue fluids, for example mannose-binding protein (MBP) [15] and C-reactive protein (CRP) [16]. Essential components of the innate immune system are numerous cells that bear PRRs; these include macrophages, dendritic cells (DCs), mast cells, neutrophils, eosinophils, natural killer (NK) cells. They can rapidly become activated during an inflammatory response and differentiate to short-lived effector cells whose major role is to fight the infection. Important innate elements of host defense are also the different antimicrobial peptides [17, 18] and the complement system [19]. The mechanisms by which the innate immune system fights infections include

opsonization and phagocytosis, activation of complement and coagulation cascades, induction of apoptosis, activation of proinflamatory signaling pathways.

In vertebrates, the immune system is more complicated. It includes a complex of mechanisms known as the adaptive immune system. It becomes activated with the help of the innate immune system, which induces the production of co-stimulatory molecules, secretion of chemokines and cytokines and triggers DC maturation, thus directing the cells of the adaptive immune system to the place of inflammation. The adaptive immune system provides some big advantages to the host, especially in immune recognition. The cells of the adaptive immune system, T and B-lymphocytes, express surface receptors known as T-cell receptor (TCR) and B-cell receptor (BCR), respectively. The genes encoding these receptors are assembled by recombination of gene segments during lymphocyte development. This assembling process generates a huge variability of receptors, which potentially could recognize every unknown antigen the organism can encounter. The pathogens, which manage to go through the barriers of the innate immune system, meet the pool of lymphocytes and select among them the cells bearing receptors with the right specificity. These cells clonally expand and produce large numbers of effector cells, which fight the invaders. Because of the processes of selection and clonal expansion, the adaptive immune response is very specific but also delayed in time when compared to innate immunity. In the process of clonal expansion the adaptive immune system produces also long-lived cells, thus providing the host with immunological memory and allowing it to mount a stronger and more specific response in case of re-encounter with the same pathogen. The cells of the adaptive immune system are specialized with respect to their anti-pathogenic effector functions. B cells differentiate into plasma cells, which produce antibodies targeting extracellular pathogens. T cells from the CD8+ subset directly lyse infected cells or neutralize pathogens in non-cytolytic manner by secreting cytokines, mainly IFNγ [20]. The CD4+ T cells do not have direct antimicrobial functions but they orchestrate the complicated actions of the immune system by secreting diverse cytokines. Cytokines are small regulatory proteins secreted by various cells of the body in response to activating stimuli. They control important processes such as cell proliferation and chemotaxis, thus contributing to both innate and adaptive immunity. Some cytokines have direct antimicrobial and antiviral functions. In this respect, very important molecules are the IFNs.

1.2 Interferons, the central players in antimicrobial and antiviral immunity

Interferons (IFNs) are members of a multigene family of small inducible cytokines, originally described as substances protecting cells from viral infection [21]. The family subdivides in three groups: IFN type I, II and III. The group of type I IFNs includes multiple IFNα proteins [22-23], as well as IFNβ [24], IFNκ [25], IFNε [26] and IFNτ [27], each with a single member. All proteins from this list are found in both mice and humans. Mouse limitin [28], pig IFNδ [29] and human IFNω [30] also belong to the group of type I IFNs. The IFNα species exhibit antiviral, antiproliferative and immunomodulatory activities. Antiviral activity has also been demonstrated for IFNβ, IFNω and IFNκ. The group of type III IFNs consists of three IFNλ proteins [31-32] which are also induced by virus infection and have antiviral activity.

The type II IFN group has only one member- IFNγ. IFNγ is produced by cells of the immune system (NK cells, CD4 cells, CD8 CTLs, macrophages) [33] in response to diverse activating stimuli. The synthesis of IFNγ is regulated mainly by IL-12 and IL-18, which synergistically induce its production. IFNα/β also can promote IFNγ expression.

IFNγ mediates its functions through the Jak-Stat signaling pathway [34] (Fig. 1). The receptor for IFNγ (IFNGR) is expressed on the cell surface of all nucleated cells and consists of two heterologous subunits, IFNGR-1 and IFNGR-2. Upon binding of the ligand, the IFNGR dimerizes and induces a cascade of intracellular phosphorylation and activation events involving members of the Janus family tyrosine kinases (Jak-1 and Jak-2) and subsequently Stat-1, a transcription factor from the STAT (signal transducer and activator of transcription) family. Phosphorylated Stat-1 forms a homodimer, known as gamma activation factor (GAF); the dimer translocates to the nucleus and binds to the gamma activation site (GAS) response element present in IFNγ-responsive promoters, thus leading to activation of transcription.

IFNα and β also signal through a heterodimeric receptor and a pathway similar of that of IFNγ (Fig.1). Receptor dimerization is, however, not required and the set of Jak and Stat components involved is different. This pathway employs the kinases Jak-1 and Tyk-2 and the transcription factors Stat-1 and Stat-2. Upon activation, the latter two form a trimer with another transcription factor, IRF-9 (IFN regulatory factor 9);

the trimer is known as ISGF3. This trimer translocates to the nucleus, binds to the IFN-stimulated response element (ISRE) promoter sequence and activates transcription of IFNα/β-inducible genes.
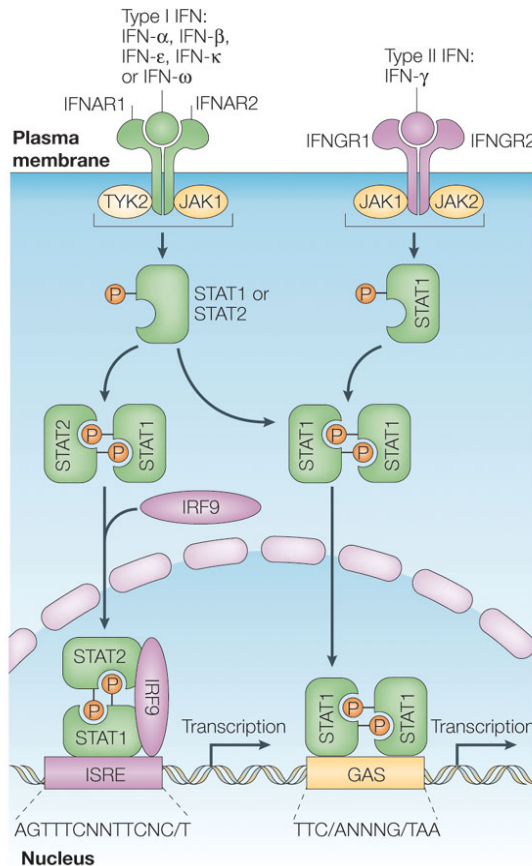
Figure 1. Interferon receptors and activation of the JAK–STAT pathways by type I and type II interferons. (from [219]) Type I interferons (IFNs) bind to a common receptor (type I IFN receptor) The type I IFN receptor is composed of two subunits, IFNAR1 and IFNAR2, which are associated with the tyrosine kinases TYK2 and JAK1, respectively. IFN-γ, binds to a distinct cell-surface receptor (type II IFN receptor). This receptor is also composed of two subunits, IFNGR1 and IFNGR2, which are associated with JAK1 and JAK2, respectively. Activation of the JAKs that are associated with the type I IFN receptor results in tyrosine phosphorylation of STAT2 and STAT1; this leads to the formation of STAT1–STAT2–IRF9 complexes, which are known as ISGF3 complexes. These complexes translocate to the nucleus and bind ISREs in DNA to initiate gene transcription. Both type I and type II IFNs also induce the formation of STAT1–STAT1 homodimers (GAFs) that translocate to the nucleus and bind GAS elements that are present in the promoter of certain ISGs, thereby initiating the transcription of these genes. The consensus GAS element and ISRE sequences are shown.

The cellular response to IFNs and especially to IFNγ in particular, is extremely complex. Current data shows that IFNγ induces the expression of more then 800 genes. The products of these genes mediate the multiple effects of IFNγ on all aspects of immunity [35-38]. The complexity of the IFNγ response, however, makes the analysis of the functions of the individual genes involved in it very difficult. Therefore, the mechanisms by which IFNγ mediates its functions are still largely unknown.

1.3 Antimicrobial functions of IFNγ

Pathogenesis studies using mouse mutants with disrupted genes encoding IFNγ, IFNGR-1, IFNGR-2 and Stat-1 provide strong evidence for the importance of IFNγ in host response to microbial and viral pathogens. If kept in pathogen-free environment these null mutants show no developmental or physiological abnormalities but their ability to mount an immune response against infections is largely compromised. These include infections with a variety of intracellular bacteria, protozoa and viruses some of which are listed in Table 1.

Table1

Pathogens	References
Intracellular bacteria	
Mycobacterium spp.	[41, 42]
Chlamydia spp.	[43, 44]
Salmonella typhimurium	[45, 46]
Listeria monocytogenes	[47-50]
Shigella flexneri	[51]
Yersinia enterocolitica	[52]
Legionella pneumophilla	[53]
Bordetella pertussis	[54]
Intracellular protozoa	
Toxoplasma gondii	[55]
Plasmodium spp.	[56]
Trypanosoma cruzi	[57]
Leishmania major	[58, 59]
Viruses	
herpes simples virus (HSV)	[60]
lymphocytic choriomeningitis virus (LCMV)	[61]
Vaccinia virus	[47]
murine cytomegalovirus (MCMV)	[62]
vesicular stomatitis virus (VSV)	[49]

The classical view about IFNγ is that this cytokine is mainly involved in resistance against bacteria while the antiviral defense is a function of the type I IFNs. IFNγ

indeed plays a critical role in innate host response against microbes but it also contributes to the protection against viruses, especially in long-term control of viral infections. In some diseases, IFNγ plays important role in both protection and pathogenesis. For example, in a *Helicobacter pylori* infection model, increased production of IFNγ in absence of IL-4 promotes mucosal inflammation [39]. IFNγ is also proved to be responsible for persistence of *Chlamydia spp.* infection [40].

In many cases, the antimicrobial and antiviral effects of IFNγ are due to its general immunostimulatory functions. However, there is growing evidence supporting the idea that the potent direct negative effect of many IFNγ-induced proteins on growth of intracellular pathogens is essential for host defense. Extensive data shows that IFNγ directly induces intracellular resistance programs and these cell-autonomous effects play a critical role in resistance against intracellular pathogens from all classes.

1.4   IFN-induced cell-autonomous immunity

By definition, cell-autonomous resistance is mediated by any cell without assistance from specialized cells of the immune system. Such assistance might be needed initially for the induction of a cell-autonomous resistance factor but once induced and synthesized in the cell this factor confers resistance by itself without further specialized help. In recent years, many IFN-induced molecules have been implicated in cell-autonomous resistance mechanisms. The list of such molecules includes well-known and extensively studied antiviral factors as PKR [63, 64] and 2'-5' OAS/RNaseL [65, 66], as well as molecules with activity against a large spectrum of pathogens from all classes, for example iNOS [67, 68, 69], IDO [70, 71, 72] and the phox complex [73]. The list of cell-autonomous resistance factors is still growing, relative newcomers in it being ADAR1 [74], ISG20 [75], ZAP [76] and TRIM5α [77]. It is becoming clear that IFN-induced GTPases also play an important role in cell-autonomous resistance against intracellular pathogens.

1.5   IFN-inducible GTPases as cell-autonomous resistance factors

Among the genes highly induced by IFNs are the members of four families of GTPases. Type I IFNs induce the Mx proteins. Type II IFN induces three other families of GTP binding proteins: the p65 guanylate-binding proteins (GBPs), the

very large inducible GTPases (VLIGs) and the p47 GTPases. Members of all these families except the VLIGs have already been implicated in cell-autonomous resistance mechanisms.

1.5.1 Mx proteins

The first mouse Mx gene was identified as a locus in A2G mice conferring resistance to influenza virus [78]. The gene was subsequently mapped and cloned [79, 80] and is currently known as Mx1. A second mouse family member (Mx2) [81] and two human proteins (MxA and MxB) were identified later [82, 83]. Mx GTPses are strongly induced by IFNα and IFNβ in cultured cells. They are also shown to be abundant in most tissues of mice infected with viruses or treated with IFNα or IFNβ. Other cytokines, including IFNγ are poor inducers of Mx GTPases.

Mx proteins, in particular MxA and Mx1, attract a great deal of attention due to their potent antiviral activity demonstrated in induced or stably transfected cell culture systems. The Mx proteins protect cells against a variety of negative-strand RNA viruses form the families *Orthomyxoviridae*, *Bunyaviridae* and *Hepadnaviridae*. This group of viruses includes some human pathogens causing severe diseases, for example influenza [84], hepatitis B (HBV) [85], hemorrhagic fever with high mortality rate (Hantaan virus and Crimean-Congo hemorrhagic fever virus) [86, 87], fever epidemics (Rift Valley fever virus) [87] or encephalitis (La Crosse virus) [87].

The antiviral activity of the Mx proteins is further demonstrated by extensive *in vivo* studies. It is long known that most inbred mouse strains naturally carry nonfunctional Mx genes [88]. This explains their strong susceptibility to infections with orthomyxoviruses [89, 90]. The higher resistance of MxA-transgenic mice to certain viral infections [91] also confirms the function of human MxA as a potent antiviral effector in vivo. Furthermore, MxA protects these transgenic mice from viruses even in the absence of functional IFNα/β system [92], a fact, undoubtedly proving that the protein does not need help from other IFN-induced proteins to perform its antiviral activity. MxA is a powerful antiviral agent on its own, once induced and synthesized it works without external help. This makes the protein a paradigm for a GTPase functioning as a cell-autonomous resistance factor.

The mechanism of action of Mx proteins is still unclear. The direct interaction of MxA with viral particles has been demonstrated and proposed to be important for its

function [93]. The protein was shown to block nuclear import of viral nucleocapsids [94] probably by sequestering them into perinuclear complexes [95] in a process involving smooth ER membranes [96]. Like certain other large GTPases, Mx proteins also form highly organized oligomers in nucleotide-dependent manner [97, 98] and exhibit high GTP hydrolysis rate [97, 99]; however, a report on a MxA mutant unable to oligomerize and hydrolyze GTP but still exhibiting antiviral activity, makes the functional significance of these processes questionable [100]. MxA was also shown to self-assemble into rings, which tubulate lipids *in vitro*, but its still unknown if membrane deformation is important for its function [101]. Mouse Mx1 is a nuclear protein accumulating in distinct nuclear dots that frequently associate with promyelocytic leukemia protein (PML) nuclear bodies. However, recently the protein was shown to be functionally independent from them [102].

1.5.2   p65-kDa GBPs

GBPs represent a family of GTPases conserved in vertebrates [103]. They are highly induced by IFNγ and less by IFNα/β [103]. The function of the members of this family is still not completely clear. When stably expressed in HeLa cells human GBP1 (hGBP1) shows activity against vesicular stomatitis virus (VSV) and encephalomyocarditis virus (ECMV) [104]. A similar but smaller effect against these two viruses was also recently reported for murine GBP2 (mGBP) [105]. GBPs were also shown to be involved in regulation of cell proliferation: mGBP2 alters the growth characteristics of fibroblasts [106] and hGBP1 controls proliferation and angiogenic capability of endothelial cells [107, 108] only in the presence of a functional GTP-binding domain. Some family members are isoprenylated at the C-terminus and this appears to be necessary for targeting to intracellular vesicular structures [109]; the functional importance of this modification for the GBP proteins is, however, still unclear.

1.5.3   Very large inducible GTPases (VLIGs)

The VLIGs are the most recently discovered family of IFN-inducible GTPases [110]. In mice, this family consists of at least six genes, in humans there is only one homologue. The prototype VLIG, VLIG-1, is a cytosolic and nuclear protein which is induced by both type I and type II IFNs and has a canonical GTP-binding domain.

The molecular mass of VLIG-1 is 280 kDa, which makes it the largest known GTPase in any species. No resistance function for this protein has been shown so far but VLIG-1 displays highest homology to the GTPases mediating cell-autonomous resistance. This, in addition to the IFN inducibility, suggests a possible role of the VLIGs in intracellular defense mechanisms.

1.5.4   p47 (IRG) GTPases

Extensive data generated in the last few years clearly show that the p47 GTPases are among the most efficient cell-autonomous resistance mediators found in the mouse so far [111]. The family consists of 23 members in C57BL/6 mice [112], six of which have been previously described, namely TGTP/Mg21 [113], IRG-47 [114], IIGP1 [103], GTPI [103], IGTP [115] and LRG-47 [116]. IIGP1, TGTP and IRG-47 contain the three classical GTP binding motifs [117]: GX_4GKS/T (G1; phosphate binding P loop), DXXG (G3) and (N/T)(K/Q)XD (G4; responsible for the base specificity). In the three other published members the universally conserved G<u>K</u>S sequence in the P loop is substituted by G<u>M</u>S, which is so far a unique feature among all known GTPases. The substitution correlates with other sequence similarities between these three proteins and defines a distinct GMS subgroup in the family [103]. p47 GTPase families with different degree of complexity are found in jawed fish and mammals [112]. Only two genes are present in humans: a homologue of mCINEMA, called hCINEMA, and a gene fragment homologous to the members of the mouse GMS subgroup [112]. Recently a new general nomenclature for the p47 GTPase family was introduced [112]. It is based on phylogenetic principles and the names of the genes originate from the stem name IRG (Immunity-Related GTPases). The family tree shown in Fig. 2 presents the new, as well as the old names of the members of the mouse p47 GTPase (IRG) family. The old names will to be used in this thesis.

The p47 GTPases are classified as immediate-early genes because their expression does not require *de novo* protein synthesis of transcription factors [118, 116, 111]. A hallmark feature of the members of the p47 family is their strong and rapid induction in response to IFNγ stimulation from almost undetectable basal levels in all cell lines and primary cells tested [115, 114, 103, 116, 112]. The only exception in this respect is CINEMA, which is not IFN inducible [112]. IFNα/β and LPS also induce the expression of the p47 GTPases but less than IFNγ [116, 119]. Other bacterial cell wall

components also stimulate synthesis of some family members, probably via TLR signaling and indirect secretion of IFNβ [120]. The p47 GTPases seem not to be induced by other cytokines, including some interleukins (IL-1α and β, IL-2, IL-4, IL-6, IL-10), tumor necrosis factor α (TNFα) and granulocyte-macrophage colony stimulating factor (GM-CSF) [116, 118, 119]. The p47 GTPases are also shown to be highly induced *in vivo* after infection with bacteria and protozoa [103, 121, 122]. Interestingly, at least the six published family members have low but detectable basal expression levels in almost all mouse organs tested and apparently this basal production does not depend on IFN, as it is still present in mice lacking receptors for IFNα/β or/and IFNγ (Jia Zeng, personal communication). The *in vivo* expression pattern of CINEMA is also an exception from the rule: the protein is expressed only in
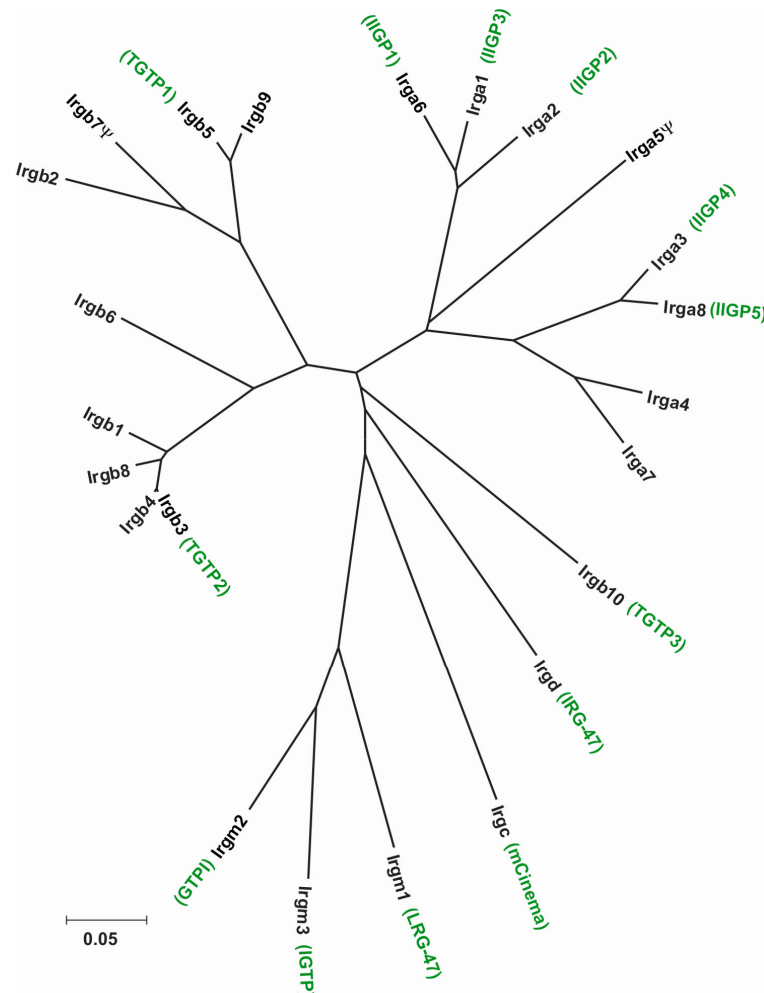
Figure 2: Unrooted tree of nucleotide sequences of the G-domains of the 23 members of the mouse p47 GTPase (Irg) family (p-distance based on a Neighbour-Joining method). The names generated according to the new nomenclature [112] are depicted in black, the old names, in green (courtesy to Cemalettin Bekpen)

10

testis in both mouse and man ([112] and Christoph Rohde, personal communication). Mice with targeted deletions of three individual members of the p47 GTPase family, namely IGTP, IRG-47 and LRG-47, display complete loss of resistance to several intracellular pathogens of bacterial and protozoan origin despite having an intact and functional adaptive immune system and IFNγ production [111, 121, 122]. The data on susceptibility of these deficient mice is summarized in Table 2.

Mouse	Intracellular protozoa			Intracellular bacteria			
	T. gondii	*L. major*	*T. cruzi*	*L. monocytogenes*	*S. typhimurium*	*M. tuberculosis*	*M. avium*
Wild-type	R	R	R	R	R	R	R
IFN-γ knockout	S (acute)	S	S	S	S	S	S
Igtp knockout	S (acute)	S	R	R	R	R	R
Lrg47 knockout	S (acute)	S	N.T.	S	S	S	S
Irg47 knockout	S (chronic)	N.T.	N.T.	R	R	R	N.T.

Table 2. This table (from Taylor et al. [111]) summarizes the phenotypes of the three available p47 GTPase deficient mice in comparison to the IFNγ deficient mouse (S, susceptible, R, resistant, N.T., not tested)

The cellular mechanisms underlying the essential resistance functions of the p47 GTPases are not yet understood. Currently available data is concentrated mainly on the interactions between LRG-47 and phagosomes. The protein was reported to co-purify with phagosomes from *Mycobacterium*-infected macrophages and promote the acidification, and thus maturation of these phagosomes [123]. In resting cells, LRG-47 was shown to localize to *cis*-Golgi and ER [124]. Upon phagocytosis LRG-47 translocates to the plasma membrane at the forming phagocytic cups and in fibroblasts also at phagocytosis-induced membrane ruffles; the protein then stays associated with the maturing phagosome and reaches the lysosomal compartment [124]. Other family members have also been shown to associate with intracellular membrane compartments: IIGP1 and IGTP both localize to the ER [124, 125], GTPI is a Golgi protein [126] and TGTP1 partitions between intracellular membranes and cytosol [126]. The intracellular behavior of the p47 GTPases suggests that these proteins work by interfering with the lifestyle of pathogens whose survival and propagation in host cells is critically dependent on exploitation of membrane compartments.

1.5.4.1 IIGP1

From all published members of the p47 GTPase family IIGP1 is the best characterized with respect to biochemical properties and enzymatic activity *in vitro,* features, which relate the protein to the large GTPases including dynamins and p65 GBPs [127-129]. Purified recombinant IIGP1 binds GDP and GTP in the micromolar range, hydrolizes

GTP to GDP in a cooperative manner and forms enzymatically active oligomers in presence of GTP *in vitro* [130]. In contrast to the large GTPases, however, IIGP1 has higher affinity for GDP than for GTP; its intrinsic enzymatic activity is also relatively low, which suggests that the protein might need additional help for GTPase activation. Such GAP (GTPase-activating protein) activity is an intrinsic feature of the related dynamins and p65 GBPs [127, 131, 132]. It is possible that the IIGP1 molecules are activated *in trans* during the oligomerization process.

The crystal structure of IIGP1 shows a typical Ras-like G domain between an N-terminal three-helix bundle and a complex system of C-terminal helices and loops [133]. The protein crystallizes as a dimer, which is required for cooperative GTP hydrolysis and GTP-dependent oligomerization as shown by analysis of dimer interface mutants. Sequence comparison and secondary structure prediction suggests that the structure of IIGP1 can be a valid model for the p47 GTPase family.

IIGP1 associates to the endoplasmic reticulum in fibroblast, macrophage and hepatocyte cell lines [124]; it was also previously reported to be a predominantly Golgi protein in bone-marrow derived macrophages [119]. Notably, IIGP1 translocates to the parasitophorous vacuole (PV) in primary astrocytes infected with *Toxoplasma gondii* and this process correlates with subsequent disruption of the PV [134]. IIGP1 behaves as a classical peripheral membrane protein with relatively weak interactions to the membrane [124]. The protein is partly membrane associated but it also has a substantial cytosolic pool. IIGP1 is targeted to membranes by N-terminal myristoylation. There is, however, also a residual membrane interaction signal because the non-myristoylated IIGP1 mutant is still partly membrane-bound. IIGP1 probably could interact directly with lipids in cellular membranes as suggested by its ability to bind to synthetic phosphatidylserine lipid vesicles *in vitro* [124].

The only interaction partner of IIGP1 reported until now is the microtubule binding protein Hook3 (mHk3) [135]. The interaction was identified by yeast-two-hybrid screen using the complete IIGP1 protein as a bait. It was also confirmed by co-immunoprecipitation of the two proteins in lysates of IFNγ-activated bone marrow-derived macrophages. The hook proteins were previously proposed to participate in proper assembly and/or positioning of membranous compartments and contribute to their ordered dynamic formation, maturation and trafficking [136]. Therefore, the interaction between IIGP1 and mHk3 was reported as evidence for participation of IIGP1 in intracellular trafficking [135].

1.6   Aims of this study

The introductory remarks in the previous chapter summarized our current knowledge about IIGP1 with respect to biochemical characteristics and intracellular behavior. Our aim was to investigate the proposed defense function of the protein by generating an IIGP1 deficient mouse strain and analyzing the susceptibility of these animals to infection with different pathogens. We also planned to characterize in detail the expression profile of IIGP1 and the genomic organization of its homologous genes.

2 MATERIALS AND METHODS

2.1 Chemicals and reagents

All chemicals were purchased from Aldrich (Steinheim), Amersham-Pharmacia (Freiburg), Applichem (Darmstadt), Baker (Deventer, Netherlands), Boehringer Mannheim (Mannheim), Fluka (Neu-Ulm), GERBU (Gaiberg), Merck (Darmstadt), Pharma-Waldhof (Düsseldorf), Qiagen (Hilden), Riedel de Haen (Seelze), Roth (Karlsruhe), Serva (Heidelberg), Sigma-Aldrich (Deisenhofen) or ICN biochemicals, Oxoid, (Hampshire UK).

2.1.1 Oligonucleotides

Oligonucleotidess were purchased from Invitrogen (Carisbad, USA) and are listed in Table 3

Table 3

Name	Sequence 5'- 3'	Usage
RT1.1FA	TGCTTCCTGAAGCTGAACTA	Real-Time PCR (IIGP1A)
RT1.2FA	ACCGAGGGCTATTCCTCTCA	Real-Time PCR (IIGP1B)
RT1R	CAGAGAAGGGATGATATTCAC	Real-Time PCR (IIGP1A and B)
mHPRT FA	ATTAGCGATGATGAACCAGG	Real-Time PCR (HPRT)
mHPRT R2A	TGGCCTATAGGCTCATAGTG	Real-Time PCR (HPRT)
5HAF	CCGCTCGAGGTACTGTTGAAAGCAATGATT	Targeting vector (5' homology arm)
5HAR1	CCGCTCGAGGAATTCTATACAAAACTTTCCCAGTAG	
3HAF	CAGGATCCCGCAGAAGGTTTG	Targeting vector (3' homology arm)
3HAR	CGCGGATCCATAATGTTTTCATCTCTAATC	
5DEL	TTGTTATTCAGGGAAGCTAAG	IIGP1 mouse typing
3DEL	TGTCTGGTGATTCTCATTAGC	
5'EX2	CTCAGGTTATCTAACATTCTG	
G6PDH 1f	ACAGGGACAGAGGGAGAA	Real-Time PCR *A. phagocytophilum* detection
G6PDH 1r	AACGCAAAGCTGAAGTGA	
CL Forward	GGA GGC TGC AGT CGA GAA TCT	Real-Time PCR *C. trachomatis* detection
CL Reverse	TTA CAA CCC TAG AGC CTT CAT CAC	

2.1.2 Enzymes

Restriction Enzymes were purchased from New England Biolabs (Bad Schwalbach); T4 DNA ligase (New England Biolabs); RNase A (Sigma); shrimp alkaline

phosphatase (SAP) (USB, Amersham); *Thermus aquaticus* (Taq) polymerase was prepared by Rita Lange; *Pyrococcus furios*us (Pfu) DNA Polymerase (Promega, Mannheim)

2.1.3   Kits

Plasmid Maxi and Midi kit (Qiagen, Hilden), Terminator-cycle Sequencing kit version 3 (ABI), Rapid PCR product purification Kit (Boehringer, Ingelheim), pGEM-T Easy Vector System I (Promega, Madison, USA), Ladderman labeling kit (TaKaRa) RNeasy Mini Kit (Qiagen, Hilden), Oligotex mRNA Mine Kit (Qiagen, Hilden), SuperScript First-Strand Synthesis System (Invirtogen, Carisbad, USA), QuantiTect SYBR Green PCR KIT (Qiagen, Hilden)

2.1.4   Serological reagents.

2.1.4.1   Primary antibodies and antisera (Table 4)

name	target	species	dilution	origin
10D7	IIGP1	mouse monoclonal	IB: 1:1000 IF: 1:200	Jens Zerrahn, Berlin
A20	TGTP1	goat polyclonal	IF: 1:100	Santa Cruz Biotechnology, Santa Cruz, CA
I68120	IGTP	mouse monoclonal	IF: 1:250	BD Transduction Laboratories, Lexington, KY
5-241-178	GRA7	mouse monoclonal	IF: 1:30000	R. Ziemann, Abbott Laboratories, Abbott Park, IL

2.1.4.2   Secondary antibodies and antisera

goat anti-mouse Alexa 546/488, goat anti-rabbit Alexa 546/488, donkey anti-goat Alexa 546/488, donkey anti-mouse Alexa 488, goat anti-mouse Alexa 680 (all Molecular Probes), goat anti-mouse HRP (Amersham)

2.2   Media

2.2.1   Luria Bertani (LB) medium

10g bactotryptone, 5g yeast extract, 10g NaCl, 1l dH_2O

2.2.2   LB agar medium

10g bactotryptone, 5g yeast extract, 10g NaCl, 15g agar, 1l dH_2O

2.2.3 EF medium

DMEM (Dulbecco's Modified Eagle Medium) with Glutamax (no sodium piruvate, 4500 mg glucose, with pyridoxine) supplemented with 10% EF FCS, 1 mM sodium piruvate, 100 µg/ml penicillin/streptomycin (optional)

2.2.4 ES medium

DMEM (Dulbecco's Modified Eagle Medium) supplemented with 15% ES FCS (tested for germline transmission), 1 mM sodium piruvate, 2 mM L-glutamine, 1x non-essential amino acids, 1 mM β-mercaptoethanol, 100 µg/ml penicillin/streptomycin (optional, not recommended), LIF (leukemia inhibitory factor; a supernatant from LIF-transfected CHO cells line 8/24 720 LIFD(.1) from Genetics Institute, Cambridge, Massachusetts; the amount used depends on the concentration of the batch)

Mammalian tissue culture media and supplements were bought from Gibco BRL, (Eggelstein), ES and EF FCS from Gibco BRL, (Eggelstein), LIF was provided by the Center for Mouse Genetics, Institute for Genetics, Cologne

2.2.5 Freezing medium

10% DMSO, 90% FCS, sterile filtered, kept in aliquots at -20°C

2x Freezing media (for 96 well plates)

20% DMSO, 80% FCS, sterile filtered, kept in aliquots at -20°C

2.3 Cells and cell lines

2.3.1 Bacterial strains

Escherichia coli DH5α: *80dlacZΔM15*, recA1, gyrA96, thi-1, hsdR17 (r_B^-, m_B^+), supE44, relA1, deoR, *Δ(lacZYA-argF)*U196

2.3.2 Bacterial pathogens

Listeria monocytogenes strain EDG, serotype 1/2a

Chlamydia trachomatis L2

Anaplasma phagocytophilum strain MRK

2.3.3 Protozoan parasites

Toxoplasma gondii strain ME49, DX

Plasmodium berghei strain ANKA

Leishmania major clone V1 (MHOM/IL/80/Friedlin)

2.3.4 Mammalian cells and cell lines

Embryonic feeder (EF) cells: primary, prepared from day 13-14 embryos from 129 mouse strain harboring pSV2 neo [137]

Embryonic stem (ES) cells: Bruce4 cell line derived from C57BL/6 mouse strain [138]

2.4 Methods

2.4.1 Molecular biology

All common methods molecular biology methods were performed according to standard protocols [139] or cited references.

2.4.1.1 Preparation of competent Cells

Competent *Escherichia coli* DH5α or BL21 cells were prepared according to the protocol of Inoue et al. [140] and used in heat shock transformations of plasmid DNA.

2.4.1.2 Isolation of Plasmid DNA

Plasmid DNA was isolated from transformed bacteria with an alkaline lysis method [141] following the standard protocol [139]. Plasmid DNA of a higher amount and purity was prepared with Oiagen Plasmid Midi kit (Qiagen, Hilden) following the supplier's instructions. BAC DNA was isolated using Oiagen Plasmid Midi kit (Qiagen, Hilden) following the protocol for preparation of very low copy number plasmids provided by the company.

2.4.1.3 Isolation of Genomic DNA from mouse tissues and cells

Mouse tissue was incubated o/n at 56°C in lysis buffer (l0 mM NaC1, 10 mM Tris-HCl pH 7.5, l0 mM EDTA, 0.2% SDS, 0.4 mg/mI Proteinase K [freshly added each time]). Debris were pelleted by centrifugation and supernatant was mixed with an equal volume of isopropanol to precipitate DNA. DNA was washed with 70% EtOH, dried and resuspended in ddH$_2$O or TE buffer.

Preparation and restriction digest of ES cell DNA in 96 well plates was performed as follows. 50 µl of lysis buffer (l0 mM NaC1, 10 mM Tris-HCl pH 7.5, l0 mM EDTA, 0.5% Sarcosyl, 0.4 mg/mI Proteinase K [freshly added each time]) was added to each well of the 96 well plate. The plate was wrapped in parafilm, transferred to pre warmed at 56°C humidified chamber and incubated at 56°C overnight. At the next day, the plate was allowed to cool down at room temperature for 1 hour. 100 µl of 100% EtOH were added to each well and the plate was let to sit at room temperature for 1 hour during which the DNA strands became visible at lower magnification. The plate was inverted and carefully drained on paper towels allowing DNA to remain attached to the plastic walls of the wells. The plate was washed 3 times with 100µl 70% EtOH and dried at room temperature. 35 µl restriction mix (1x restriction buffer, 1 mM spermidine, 1 mM DTT, 100 µg/ml BSA, 20-30 units of restriction enzyme per reaction) were added to each well and the plate was incubated overnight at the appropriate temperature in a humidified chamber. At the next day, the digested DNA samples were fractionated on agarose gel.

2.4.1.4 Agarose gel electrophoresis purification of DNA fragments from agarose gels

Size of DNA fragments was analyzed by agarose gel electrophoresis. DNA was run on 0.7% - 2% gels in 1 x TAE [139] and stained with 0.3 µg/ml ethidium bromide; migration of the DNA molecules was visualized by using Bromophenol blue or Orange G. DNA fragments were eluted from the gel with the rapid PCR purification Kit (Boehringer) according to the manufacture's protocol. Purity and yield of the DNA was determined by agarose gel electrophoresis and measurement of OD260.

2.4.1.5 Quantification of nucleic acids

The concentration of DNA and total RNA was determined by measuring the absorption of the sample at 260 nm in a spectrophotometer (Pharmacia). An OD260 of 1 corresponds approximately to 50 µg/ml for double stranded DNA or 40 µg/ml RNA.

2.4.1.6 Polymerase Chain Reaction

2.4.1.6.1 General PCR protocol

Polymerase chain reaction (PCR) [142] was used for the cloning of the short and long arm of homology of the targeting vector, screening for deleted clones after *in vitro* neo deletion and typing of transgenic mouse strains. All PCR reactions except the amplifications of the homology arms were made with *Thermus aquaticus* (Taq) DNA polymerase prepared by Rita Lange; for the homology arms 1:20 mix of KlenTherm Taq (BIOFIDAL, Vaulcs-En-Velin, France) and *Pyrococcus furiosus* (Pfu) DNA Polymerase (Promega, Mannheim) was used. The general reaction mix contained 1 µl DNA, 1x Hepes PCR buffer, 10 pM of each primer, 200 pM dNTP-mix, various amount of 50 mM $MgCl_2$, 2,5U Taq-Polymerase, and water up to 50 µl. Primers were bought from Invitrogen and are listed in Table 3

2.4.1.6.2 Mouse typing PCR for IIGP1 deletion

The reaction mix contained 1 µl genomic tail DNA, 1x Hepes PCR buffer, 10 pM of each primer (5DEL, 3DEL, 5'EX2) (Table 3), 200 pM dNTP-mix, 3 mM $MgCl_2$, 2,5U Taq-Polymerase, and water up to 50 µl. The PCR program was 94°C for 2 min, followed by 35 cycles of 94°C for 30 sec, 58° for 30 sec and 72°C for 45 sec. The sizes of the amplified bands were 260, 330 and 500 bp for wild type, floxed and deleted IIGP1 allele, respectively.

2.4.1.7 Cloning of PCR products

Amplified PCR products were purified using the rapid PCR purification Kit (Boehringer). DNA yield was monitored by agarose gel electrophoresis. Purified fragments were cloned in pGEMTeasy vector according to supplier's protocol.

2.4.1.8 Ligation

Vector was cut with the respective restriction enzyme(s) (10U/1µg DNA) usually for 1h under temperature and buffer conditions optimal for the enzyme(s) used. After the first hour the same amount of restriction enzyme(s) and 0.1U of shrimp alkaline phosphatase were added to the reaction followed by 1.5h incubation under the same conditions. Following restriction DNA fragments were ran on agarose gel and purified using the rapid PCR purification Kit (Boehringer). DNA yield after purification was monitored by agarose gel electrophoresis. Vector and insert were mixed at a ratio of

1:3 and ligated with T4-DNA ligase in total volume of 10µl at 16°C over night according to the manufacture's protocol. Two control reactions were set in parallel: a ligation of vector without insert (control for dephosphorylation of the vector) and a ligation of insert only (control for purity of the insert). At the next day 5 µl of each ligation reaction were transformed in competent bacteria.

2.4.1.9 DNA sequencing

Plasmid DNA and PCR products were sequenced using the *ABI Prism*ᴿ *BigDye*™ Terminator Cycle Sequencing Ready Reaction Kit (PE Applied Biosystems) and the automatic sequencers ABI373 and ABI377 with the help of Rita Lange. The method is based on the dideoxy-chain termination reaction with fluorescently labeled dNTPs [143].

2.4.1.10 Southern Blot analysis

Gels were treated subsequently with 0.25 M HCl and 0.4 M NaOH for 20 min and placed onto a prewet Hybond N+ thansfer membrane (Amersham). The membrane was placed on stacks of paper towels covered with 3 prewet Whatman paper sheets. The gels were overlaid with prewet Watman paper sheets and connected via a Wantman paper bridge to a reservoir with transfer solution (0.4 M NaOH, 0.6 M NaCl). Transfer for performed for at least four hrs, then the blot was dissembled. The membrane was incubated with hybridization solution (1 M NaCl, 50 mM Tris pH 7.5, 10% Dextransulfat, 1% SDS, 250 µg/ml sonicated salmon sperm DNA) over night or at least 2 hrs at 65ºC in a hybridization oven (Techne Hybridizer HB-1D, Techne, Cambridge, UK). Probes were labeled with Ladermann labeling kit (Takara, Japan) according to manufacturers instructions, cleaned from residual radioactive nucleotide over ProbeQuant G-50 Micro Columns (Amersham Biosciences, UK) added to the hybridization solution and incubated overnight at 65ºC in hybridization oven. At the next day blots were subsequently washed for 10 min at 65ºC with 2xSSC, 1xSSC, 0.5xSSC 1%SDS for 10 min at 65ºC. Radioactive signals were measured with Fujix BAS 1000 phosphoimager and analyzed with Aida Image Analyser v.3.43 software.

2.4.1.11 Preparation of total RNA from mouse tissues and cells

Mice were killed with CO_2; tissues were prepared and immediately placed in the appropriate amount of RNAlater RNA Stabilization Reagent (Qiagen). According to

manufacturer's instructions, tissues were kept in the reagent overnight at 4°C and later processed or kept for archival storage at -20°C.

Total RNA from tissues was prepared with RNeasy Mini Kit (Qiagen); the only exceptions were testis and brain tissue, which were processed with RNeasy Lipid Tissue Kit (Qiagen). In all cases, the procedures recommended by the manufacturer were followed including an additional on-column DNaseI digestion with RNase-Free DNase Set (Qiagen). Prior to RNA preparation tissues were mechanically disrupted in the appropriate volume of lysis buffer from the kit and homogenized through QIAshredder Homogenizers (Qiagen).

Total RNA from cells was also prepared with RNeasy Mini Kit (Qiagen) following manufacturer's instructions.

The integrity and size of purified total RNA was evaluated by agarose gel electrophoresis and ethidium bromide staining. RNA was stored at -80°C in water.

2.4.1.12 Preparation of mRNA

PolyA mRNA was prepared from total RNA with Oligotex mRNA kit (Qiagen) according to the procedure recommended by the supplier. mRNA was stored at -80°C.

2.4.1.13 cDNA synthesis

cDNA was synthesized from mRNA using SuperScript First-Strand Synthesis System (Invirtogen) according to manufacturers instructions. 10 to 100 ng mRNA was used as template; synthesis was primed by Oligo-dT. cDNA diluted in water 1:1 to reduce the concentration of MgCl$_2$, which might interfere with further amplification and stored at -20°C.

2.4.1.14 Real-Time PCR

2.4.1.14.1 Quantification of IIGP1 transcripts

The amount of IIGP1A and IIGP1B transcripts was detected by a quantitative PCR assay using the LightCycler System (Roche). cDNA was used as a template. Fragments from IIGP1A (969 bp) and IIGP1B (972 bp) transcripts were amplified using primer pairs RT1.1FA/RT1R and RT1.2FA/RT1R, respectively. The amount of measured transcripts was normalized to the amount of the mouse HPRT transcript in the probes. The 827 bp fragment from this transctipt was amplified in a separate

reaction using the primers mHPRT FA and mHPRT R2A. The sequences of all primers are listed in Table 3.

The PCR reaction mixtures (20 µl) contained 1x QuantiTect SYBR Green PCR Master Mix (Qigen, Hilden), 10 pM of each primer, 2 µl of template cDNA and 1U Taq polymerase (prepared by R.Lange). The LightCycler PCR program consisted of 95°C for 3 min followed by 35 cycles of 95°C for 30 s, 60°C for 30 s, and 72°C for 1 min and 78°C for 1 min; additional melting step was added at the end of each run (95°C for 15 min). Melting curve analysis was performed after each run. The quantitation of all transcripts was achieved by external standards, five serial tenfold dilutions of IIGP1A containing pGEMTeasy plasmid; the dilutions were ranging from 10^6 to 10^2 plasmid copies/dilution.

2.4.1.14.2 Detection of *A. phagocytophilum*

This analysis was preformed in the laboratory of Prof. Christian Bogdan, Institute of Medical Microbiology and Hygiene, University of Freiburg

A. phagocytophilum was detected by a quantitative PCR assay using the LightCycler System (Roche). The 444-bp fragment of the *A. phagocytophilum ankA* gene was amplified using the primers LA1 and LA6 [144]. For the sequence-specific detection of the amplicon the hybridization probes Ephago-HP-3 and Ephago-HP-4 were used. The amount of bacterial DNA was normalized to the amount of mouse genomic DNA in the probes. The 429-bp fragment of the mouse glucose-6-phosphate dehydrogenase gene (G6PDH) was amplified in a separate reaction using the primers G6PDH 1f and G6PDH 1r (Table 3). The amplicon was detected by the hybridization probes G6PDH-HP-3 and G6PDH-HP-4. The hybridization probes were synesized by TIB MOLBIOL (Berlin) and had the following sequence:

Ephago-HP-3   TAAAGCATGTAAAATACTACTAAAGTCT-fluorescein
Ephago-HP-4   LC Red 640-CGTCAGTATCAGTCGTGAATGTAGA-Ph
G6PDH-HP-3   TCATTACGCTTGCACTGTTGGTGGA-fluorescein
G6PDH-HP-4   LC Red 640-TCACCTGCCACGTCTCGGAACTGC-Ph

The PCR reaction mixtures (20 µl) contained 1×LightCyclerFastStart DNA Master Hybridization Probes (Roche), 3 mM MgCl2, 0.5 µM of each primer, 0.2 µM of the respective hybridization probes, and 2 µl of template DNA. The LightCycler PCR

program consisted of 95°C for 10 min followed by 50 cycles of 95°C for 10 s, 55°C for 20 s, and 72°C for 30 s. The quantitation of bacterial DNA and mouse genomic DNA was achieved by external DNA standard preparations, which consisted of five serial tenfold dilutions (ranging from 10^6 to 10^2 plasmid copies/dilution).

2.4.1.14.3 Detection of *C. trachomatis*

C. trachomatis was detected by a quantitative PCR assay by amplifying a fragment of the *C. trachomatis* 16s gene using primers CL Forward and CL Reverse (Table 3). For the sequence-specific detection of the amplicon, the following hybridization probe was used:

5'-[6-FAM]-TCG TCA GAC TTC CGT CCA TTG CGA-[TAMRA]-3'

The amount of bacterial DNA was normalized to the amount of mouse genomic DNA in the samples by amplifying a fragment of the mouse GAPDH gene in a separate reaction using primers and probe from Applied Biosystems.

2.4.2 Cell biology
2.4.2.1 ES cell culture

ES cell culture was performed according to the protocols published in *Laboratory Protocols for Conditional Gene Targeting* [145] with modifications used in the laboratory of Ari Waisman.

2.4.2.1.1 Thawing of cells

Cells were thawed fast at 37°C in a water bath, immediately transferred in 10 ml media to dilute DMSO and pelleted by centrifugation for 5 min 1200 rpm, 4°C. The pellet was resuspended in appropriate amount of media and plated.

2.4.2.1.2 Freezing of cells

Plates were washed 2 times with PBS and trypsinized for 3-5 min at 37°C. The reaction was stopped by adding equal volume of media. Cells were pelleted for 5 min 1200 rpm, 4°C. The pellet was resuspended in 1 ml freezing media, immediately transferred on ice and slowly frozen at -80°C. At the next day, the frozen tubes were transferred in liquid nitrogen for storage.

2.4.2.1.3   Mitomycin C treatment of EF cells

ES cells were grown on a layer of EFs, mitotically inactivated by treatment with mitomycin C (MMC). Mitomycin C was diluted in EF media to final concentration 10 µg/ml and aliquoted. Aliquotes were kept at -20°C. EFs were grown to confluence on 15 cm tissues culture plates and treated with 10 ml MMC media for 3 hours. After the treatment, cells were washed 2 times with PBS, trypsinized, counted and plated on gelatinized 9 cm tissue culture plates.

2.4.2.1.4   Transfection of ES cells

2 individual transfections were made. 30 µg of linearized pEF-IIGP1 were used for each transfection. ES cells were fed with fresh media 4 hours before transfection. DNA was dried under sterile hood and dissolved in 0.8 ml RPMI without phenol rot. ES cells were trypsinized and counted. 10^3 cells were plated for ES cell viability control and 2 aliquots of 10^7 cells were kept for transfection. These cells were centrifuged for 10 min at 1200 rpm, 4°C. The cell pellet was dissolved in 0.4 ml RPMI without phenol rot and 0.4 ml of dissolved DNA was added. The mix was transferred to an electroporation cuvette, allowed to sit for 10 min at room temperature and electroporated at 240V/500µF. 10^3 cells from each transfection were plated on individual EF covered 6 cm tissue culture plates to control the survival rate of the ES cells after the transfection; additional 10^5 cells were pated for stringency of selection control. The rest of the transfected cells were diluted in media and plated on 10 cm tissue culture plates with MMC treated EF (5 plates per transfection). The cells were grown for 2 days with normal ES media. At day 2 the G418 process started.

The cell viability controls were analyzed by counting and comparing the number of colonies formed from the transfected and non-transfected ES cells. For both transfections the cell survival was around 10 %.

2.4.2.1.5   G418 selection (positive selection)

For Bruce4 ES cells, G418 is generally used in final active concentration 200 µg/ml. The activity differs between the batches of G418 and has to be experimentally assessed for each new batch. The stock used for the experiments in this thesis was 70% active, i.e. 1.4 ml G418 were used per bottle (600 ml) of ES media. G418 was kept in aliquots at -80°C. The selection process started at day 2 after transfection.

2.4.2.1.6   Gancyclovir (GANC) selection (negative selection)

GANC was used in working concentration $2x10^{-6}$ M and prepared fresh every day from a stock kept at -80°C. To prepare the stock 4.3 mg GANC sodium salt were dissolved in 80 µl ddH$_2$O to obtain a concentration $2x10^{-1}$ M. 10 µl of the stock were further diluted in 1 ml of ES media, sterilized by filtering through a 0.22 µm filter, kept at -20°C and used for preparation of the final working dilution of GANC. The selection process took 3 days from day 5 to day 8 after transfection with the targeting vector.

2.4.2.1.7   ES colony picking

At day 9-10 after transfection with the targeting vector plates with ES cells were washed three times with PBS and left in PBS after the last washing. Colonies were picked in a sterile hood. Individual colonies were taken with a P20 pipette and transferred to individual wells of a 96 well round bottom plate previously filled with 50µl trypsin/EDTA. After 20 min of picking, the plates incubated at 37°C for 3-4 min. Subsequently trypsinization process was stopped by adding 150µl of ES cell media and picking was continued. After one hour of picking the trypsinized ES cells were distributed into three gelatinized and EF covered flat bottom 96 well tissue culture plates and the wells were filled with media up to 200µl. At least 300 colonies were picked from each transfection.

The cells were grown for 2 to 3 days; two plates were frozen on two subsequent days and kept at -80°C. The third plate was washed 2 times with PBS and trypsinized. The cells were equally distributed to three gelatinized flat bottom 96 well tissue culture plates and grown to complete confluence. The wells were subsequently washed 2 times with 100µl PBS and the plates were frozen at -20°C.

2.4.2.1.8   Freezing of 96 well plates

The wells were washed 2 times with 100 µl PBS. The colonies were incubated for 3-5 min with 50 µl trypsin/EDTA. The reaction was stopped by adding 50 µl ice cold 2x freezing media. The plates were immediately placed on ice, wrapped in parafilm and frozen slowly (in Styrofoam box) at -80°C.

2.4.2.1.9 Thawing and expansion of clones from 96 well plates

The 96 well plates were thawed by incubation at 37°C in a water bath or on a heating block. Immediately after thawing the cells were transferred to previously prepared tubes with 5 ml ES media and centrifuged for 5 min at 1200 rpm, 4°C. Each cell pellet was dissolved in 1 ml ES media and plated in an individual well of gelatinized and EF covered 24 well tissue culture plate. Clones were expanded by subsequent transfer to gelatinized and EF covered 6 well tissue culture plates, 6- and 9 cm tissue culture dishes with growing for 2 to 3 days between the transferring steps. Three aliquots were frozen from each individual ES clone.

2.4.2.1.10 His-TAT-NLS-Cre transduction of ES cells

$2x10^5$ ES cells were plated in individual wells of gelatinized 6 well tissue culture plate. Cells were allowed to attach for 4-5 hours and media was aspirated. His-TAT-NLS-Cre protein was diluted to 1 mM or 2 mM final concentration in ES media without FCS and sterile filtered. 600 µl were added per well and the plates were incubated for 20 hours at 37°C. After the incubation His-TAT-NLS-Cre containing media was changed with normal ES cell media and cells were grown to confluence. His-TAT-NLS-Cre protein was kindly provided by Thomas Wunderlich.

2.4.2.1.11 Preparation of ES cells for blastocyst injection

ES cells were thawed and plated on gelatinized and EF covered 9 cm tissue culture dishes 2 days prior injection. At the day of injection, plates were washed 2 times with PBS and trypsinized for 4-5 min at 37°C. The reaction was stopped by adding equal volume of ES media. Cells were pelleted for 5 min at 1200 rpm, 4°C, and resuspended in 10 ml ES media. The cell suspension was plated on gelatinized 9 cm tissue culture plate and incubated for 30 min at 37°C to deplete from EF cells. After incubation, the supernatant containing the ES cells was centrifuged for 5 min at 1200 rpm, 4°C and the cell pellet was resuspended in 1 ml injection media. The plate was washed with 10 ml ES media to harvest potentially weakly attached ES cells. This media was also centrifuged for 5 min at 1200 rpm, 4°C and the cell pellet was resuspended in 1 ml injection media. ES cells from both pellets were compared under microscope and usually both were used for blastocyst injection.

2.4.2.2 FACS analysis

Single cell suspensions were stained with FITC-, PE-, APC- and biotin-conjugated antibodies. Staining with these fluorescently labeled antibodies was performed as described elsewhere [146]. Briefly, $2x10^6$ cells were stained with antibodies diluted in PBS/1% BSA/0.01% NaN3 (PBA) for 15 min at 4°C. All antibodies were titrated in separate experiments before use. After washing with PBA either a second staining step including Streptaviding-Cychrome, -APC, -Cy7-PE or analysis was performed immediately after resuspending of the cells in 200–400 µl of PBA. Analysis was done FACScalibur (BecktonDickinson). Dead cells were excluded by adding Topro-3 (1 nM). All antibodies were kindly provided by Ari Waisman.

2.4.2.3 In vitro passage of *Toxoplasma gondii*

T. gondii infection experiments were performed under the supervision of Dr. Gaby Reichmann, Institute for Medical Microbiology and Hygiene, University of Duesseldorf.

Toxoplasma gondii tachyzoites, strain ME49, were passaged *in vitro* in HS27 human foreskin fibroblasts. Confluent fibroblast monolayers in 25 cm^2 flasks were inoculated with $1x10^6$ parasites in IMDM supplied with 5% FCS, 2 mM L-Glutamin and 50 µM β-mercaptoethanol. Under these conditions, parasites actively invade the host cells, replicate intracellularly and egress from the cells approximately 3 days later. At this time point extracellular parasites were harvested with the supernatant and purified from host cell debris by differential centrifugation procedure consisting of 2 steps: 5´at 500g and 15' at 1500g, both steps performed at room temperature. Parasites were resuspended in culture medium, counted in a Neubauer chamber and immediately used for inoculation of host cells.

2.4.2.4 Preparation and culture of murine primary astrocytes (mixed glial cell cultures)

Mixed glial cell cultures contain approximately 90 % glial fibrillary acidic protein (GFAP)-positive astrocytes and less than 10% microglia (as controlled by immunofluorescence staining). The cultures were prepared as follows.

1 day old mice were killed in CO2, desinfected in 70 % ethanol and decapitated. Cortices were prepared and meninges were removed under a binocular. Brain tissue was placed in DMEM and mechanically disrupted by repeated passage through a

Pasteur pipette until a homogenous cell suspension was obtained. The suspension was filtered through a 70µm cell strainer and centrifuged for 10´at 220g, 4°C. The pellet was resuspended in DMEM supplied with 10 % FCS, 2mM L-glutamine, 50µM 2-mercaptoethanol and seeded in 6-well plates at density of $1x10^6$ cells per well. Medium was exchanged every 3-4 days. At day 10, when a confluent glial cell monolayer had developed, cells were harvested, depleted from microglia using CD11b MACS columns and replated in 6-well plates. After reaching confluence again, the cells were seeded at density of $1x10^5$ cells/well in 48-well plates for growth assay or onto glass cover slips for immunofluorescence. When monolayers reached confluence they were used for experiments.

2.4.2.5 *Toxoplasma gondii* growth assay

Murine primary astrocytes plated in 48 well plates were stimulated with 1 to 100 U/ml IFN-γ for 24h; control cells were left untreated. Cultures were then inoculated at different multiplicities of infection (MOI) with *T. gondii* ME49 tachyzoites for 24 hours. Cultures were then labelled with 1µCi/well [^{3}H]-uracil (Hartmann analytical) for further 24 h and frozen at -80°C to release the parasites. After thawing the parasites were harvested with the media and moved to 96 well plates; the wells of the 48 well plates were washed two times with 300 µl 0.1% SDS to harvest all remaining tachyzoites. The parasites were then moved to paper filters using a cell harvester. The filters were dried at 100°C, sealed in plastic bags with scintillation liquid and the amount of incorporated uracil, directly corresponding to the parasite growth [147], was determined by liquid scintillation counting.

2.4.2.6 Infection of primary astrocytes with *T. gondii* for immunofluorescence

Murine primary astrocytes were grown in 48-well plates on glass cover slips to confluence and stimulated with 100 U/ml IFN-γ for 24h; control cells were left untreated. Cultures were then inoculated at a MOI 10 with *T. gondii* ME49 tachyzoites. Non-invaded parasites were removed 2h later by extensive washing with PBS (3-5 times, 1ml/well) and cells were fixed with 3% paraformaldehyde (PFA) in PBS for 20 min at room temperature. After one wash with PBS, fixed cultures were stored with PBS at 4°C until immunostaining was performed.

2.4.2.7 Indirect immunofluorescence

Cells were grown on coverslips, fixed with 3% paraformaldehyde (PFA) in PBS for 20´ and subsequently washed 4 times with PBS. Cells were permeabilized with 0.1% saponin in PBS (washing buffer) followed by a blocking step with 0.1% saponin, 3% BSA fraction V, 0.1% gelatin in PBS (blocking buffer) for 1h. Cover slips were then incubated with the appropriate primary antibodies (Table 4) diluted in blocking buffer for 1h and washed three times with washing buffer for 5 min. Cells were then incubated with secondary antibodies for 30 min and washed as described above. Cover slips were mounted on slides with embedding media (ProLong antifade reagent, Molecular Probes, USA), sealed with nail polish and kept at 4°C in the dark. Images were taken with a Zeiss Axioplan II fluorescence microscope equipped with a cooled CCD camera (Quantix) using the Metamorph software (version 4.5r3, Universal Imaging Corp.); the same software was used for general processing of raw images. Overlays of fluorescence images were created using Adobe Photoshop version 5.5

2.4.3 Mouse infection experiments

2.4.3.1 Preparation of *Toxoplasma gondii* cysts from mouse brain

Mice chronically infected with *Toxoplasma gondii* ME49 or DX strains were killed in CO_2; brains were prepared and washed with PBS to remove blood. Brains were then cut in small pieces with scissors and homogenized in 4 ml PBS by subsequent passage through needles (18, 20, 22 and 23 gauge). Brain suspension was pelleted by centrifugation for 5 min at 500 rpm, RT and resuspended in 15 ml PBS. Cysts were isolated from the brain suspension in a Ficoll gradient (10 ml Ficoll) by centrifugation for 25 min at 2500 rpm, RT; under these conditions cysts are pelleted under the Ficoll and cell debris are kept in the interface between Ficoll and PBS. Cysts were resuspended in PBS and 10 μl of the suspension were counted under an 18x18 mm glass cover slip.

2.4.3.2 Infection of mice with *Toxoplasma gondii*

Mice were infected with *Toxoplasma gondii* bradyzoites isolated from the brains of chronically infected CD1 mice. Freshly isolated cysts were lysed in 0.5 ml Trypsin/EDTA solution to release the bradyzoites; lysis was observed under

microscope. After all cysts were lysed the reaction was stopped by adding equal volume of FCS. Bradyzoites were washed with 2 ml PBS, pelleted at 1800 rpm, 15 min, RT and immediately used for infection. Each mouse was infected i.p. with bradyzoites from five cysts in 200 µl PBS.

2.4.3.3   Infection of mice with *Plasmodium berghei*

P. berghei infection experiments were performed in the laboratory of Prof. Achim Hoerauf under the supervision of Dr. Michael Saeftel, Institute for Parasytology, University of Bonn.

P. berghei strainANKA was maintained by periodic passages through the vector A. stephensi. For infection with sporozoites, mosquitoes were prepared that had been infected from identical frozen aliquots of parasites. Mice were infected by intravenous (i.v.) injection into the tail of a phosphate-buffered saline (PBS) suspension of 50 sporozoites per animal. For infection with parasitized erythrocytes, mice were infected with the identical frozen aliquots of parasite. The percentage of parasitemia was calculated by examining Giemsa-stained smears under a microscope with an oil immersion lens (x1,000). The parasitized blood was diluted in PBS and injected intraperitoneally (i.p.) into mice. Mice were observed daily for disease symptoms and time of death.

2.4.3.4   Preparation of *Leishmania major* metacyclic promastigotes and infection of mice

L. major infection experiments were performed in the laboratory of Dr. Esther von Stebut, Institure for Dermatology, University of Mainz.

L. major clone V1 (MHOM/IL/80/Friedlin) was cultured in 199 medium supplemented with 20% FCS (Hyclone Laboratories Inc., Logan, UT), 100 U/ml penicillin, 100 µg/ml streptomycin, 2 mM Lglutamine, 40 mM Hepes, 0.1 mM adenine (in 50 mM Hepes), 5 µg/ml hemin (in 50% triethanolamine) and 1 µg/ml 6-biotin (in 95% EtOH). Infective-stage promastigotes (metacyclic promastigotes) of *L. major* were isolated from stationary cultures (5–6 days old) by their lack of agglutination with peanut agglutinin (Vector Laboratories Inc., Burlingame, CA). Prior to infection, promastigotes were opsonized with 5% C5-deficient serum obtained from B10.D2/OsNj mice, by incubation at 37 °C for 30 min.

Experimental mice were infected by injection of 10 µl of PBS containing the appropriate dose of parasites into the dorsal dermis of the left ears.

2.4.3.5   Infection of mice with *Listeria monocytogenes*

L. monocytogenesi infection experiments were performed under the supervision of Dr. Olaf Utermohlen, Institute for Medical Microbiology, Immunology and Hygiene, University of Cologne.

L. monocytogenes, strain EGD, serotype 1/2a was freshly prepared for each experiment from aliquots of log-phase growing cultures kept frozen at -80°C. The aliquots were thawed and grown overnight in brain-heart infusion (BHI) medium, resuspended in fresh BHI medium, and harvested during mid-log phase. Bacteria were washed in PBS once and their density was estimated by OD measurement at 600 nm. The inocula were adjusted to the desired density and injected i.p. in 0.5 ml PBS; serial dilutions of the inocula were plated on bloodagar plates to quantify the CFU.

2.4.3.6   Measurement of *L. monocytogenes* load in spleen and liver

At day 3 p.i. mice were euthanized by cervical dislocation and specimens of liver and spleen were examined for bacterial titers. Organs were homogenized in 0.1% Triton X100 in water and 10-fold serial dilutions were plated on blood-agar plates. The plates were incubated at 37°C and 48 h later the CFU were counted to determine the bacterial load, which was presented as CFU/g organ.

2.4.3.7   Infection of mice with *A. phagocytophilum*

A. phagocytophilum infection experiments were performed in the laboratory of Prof. Christian Bogdan, Institute of Medical Microbiology and Hygiene, University of Freiburg

The *A. phagocytophilum* strain MRK (formerly Ehrlichia equi MRK) was cultured in HL60 cells grown in RPMI 1640 medium supplemented with 1% fetal calf serum with 5% CO2. Experimental animals were infected with 100 µl blood from infected C.B17 SCID mice by i.p. injection; before the injection the infected blood was diluted 1:5 in PBS. C.B17 SCID mice were infected i.p. with 10^6 *A. phagocytophilum* MRK cells and infection was maintained through continuous passage of infected blood.

Mice were sacrificed at different time points after infection. EDTA-anticoagulated blood, spleen and lung were collected from each mouse. DNA was extracted from blood using the High Pure PCR Template Preparation Kit (Roche, Mannheim,

Germany) and from the organs using the QIAamp tissue kit (Qiagen, Hilden, Germany). *A. phagocytophilum* was detected by a Real-Time PCR as described in section 3.4.1.14.2 (Detection of *A. phagocytophilum*)

2.4.3.8 Infection of mice with *C. trachomatis*

C. trachomatis infection experiments were performed in the laboratory of Prof.W. Dietrich, Harvard Medical School, Boston, USA

Mice were infected with 10^7 CFU of *C. trachomatis* strain L2. by i.v.injection into the tail vain. Animals were sacrificed at 29h p.i., spleens were isolated form each animal and the amount of *C. trachomatis* in the samples was measured by Real-Time PCR assay as described in section 3.4.1.14.3 (Detection of *C. trachomatis)*

3 RESULTS

3.1 IIGP1 has seven homologues

At the time this project was started two genes homologous to IIGP1, namely IIGP2 and IIGP3, were already known. A subsequent screening of the NCBI mouse EST database revealed two other homologues, later named IIGP4 and IIGP5. It was however still unclear if the mouse genome contained more IIGP1 homologous genes and if these genes were clustered together or located on different chromosomes.

In order to obtain information about the genomic structure of the IIGP1-related group of genes we analyzed three genomic bacterial artificial chromosome (BAC) clones, 20620, RP23-19A12 and RP24-335D4. The 20620 BAC was previously identified as an IIGP1 containing clone by Doris Luedke [218]; this clone originated from a 129Sv mouse genomic library. The other two BAC clones were identified by search of the NCBI Nucleotide database, which showed that the ends of these clones contained part of the coding sequence (CDS) of IIGP3 and IIGP2, respectively. Both clones originated from C57BL/6 derived mouse genomic libraries.

To analyze the order of the IIGP1-related genes DNA from all BAC clones was digested with HindIII and subjected to Southern blot analysis. The PCR amplified CDS of IIGP1 and its homologues were used as probes. We started with the analysis of the positions of IIGP1, 2 and 3 and observed that in addition to IIGP3, which was part of the end of RP23-19A12, this BAC clone also contained IIGP1 and 2 (Fig. 3a). Due to the high homology between these three genes (75-85%), the corresponding probes showed strong cross-hybridization. Nevertheless, every gene could be individually identified by the size of the corresponding band and the strength of the signal on the blot. The 20620 BAC clone did not contain IIGP2 and 3, the signals of the two corresponding probes were due to cross-hybridization to the IIGP1 band (Fig. 3a). Therefore, we positioned IIGP1 at the end of the cluster. The analysis of these two BAC clones showed that IIGP1, 2 and 3 were clustered in the mouse genome. The first gene in this group was IIGP3, followed by IIGP2 and IIGP1 (Fig. 3b). The next step was to find the positions of IIGP4 and 5 in the IIGP cluster. The alignment of the sequences of these two genes showed that they were 95% identical. Therefore, it was not possible to distinguish between them on a Southern blot and to find their position
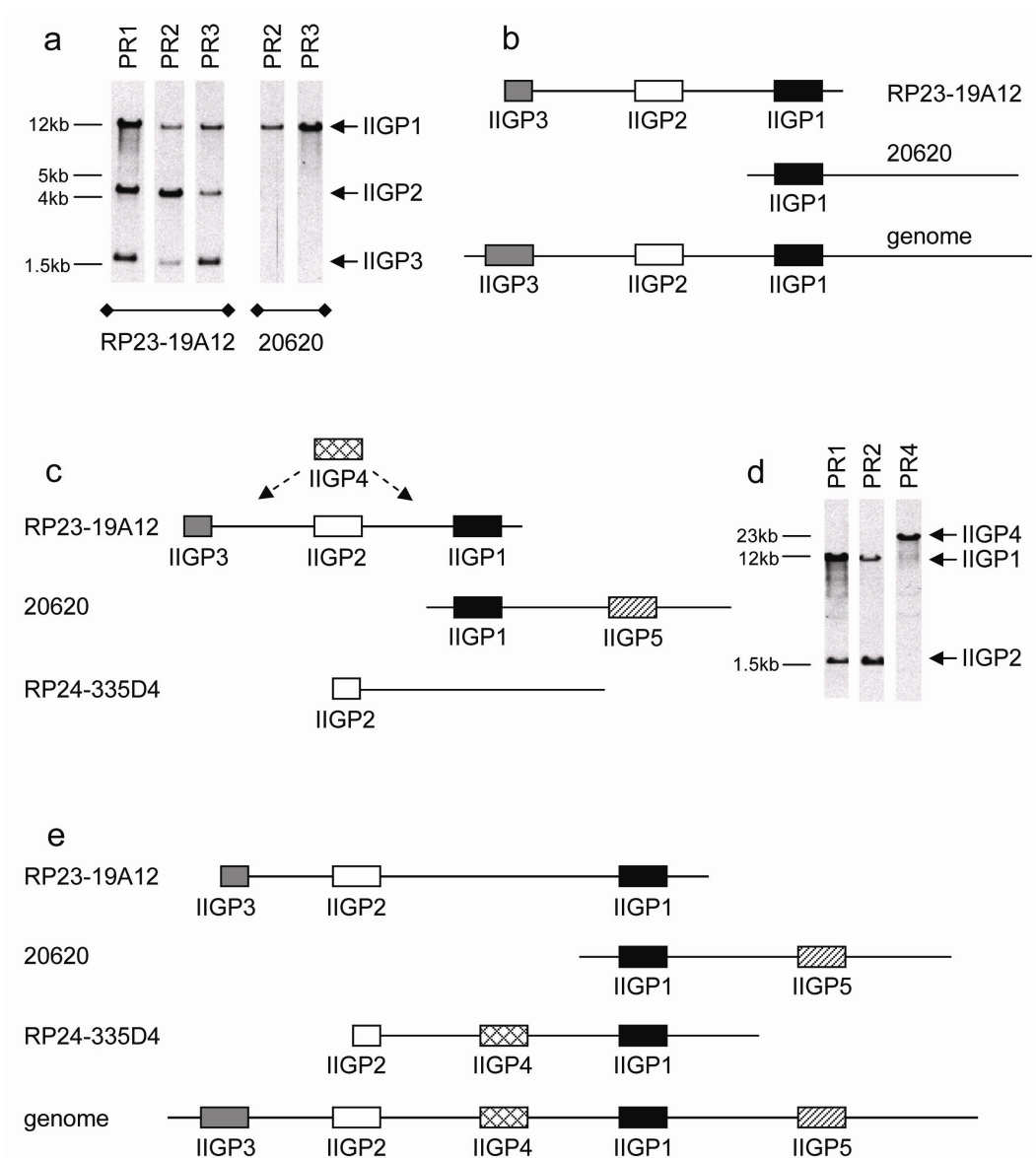
Figure 3: Structure of the IIGP cluster

DNA from RP23-19A12, 20620 (a) and RP24-335D4 (d) BAC clones was digested with HindIII and subjected to Southern blot analysis. PR1, 2, 3 and 4 were the probes for IIGP1, IIGP2, IIGP3 and IIGP4, respectively. The arrows show the bands corresponding to the indicated genes. (b), (c) and (e) presents the subsequent steps in the elucidation of the structure of the IIGP1 cluster based on the information obtained from the analysis of the BAC clones. The schemes are not in scale.

we chose a PCR approach. We used primers, which could amplify both genes, and DNA from RP23-19A12 or 20620 as a template. The PCR products were sequenced and the analysis of the sequences showed that RP23-19A12 and 20620 contained IIGP4 and IIGP5, respectively (not shown). This result positioned IIGP5 at the 3' end of the IIGP cluster but the position of IIGP4 relative to IIGP2 was still unknown (Fig. 3c). To find this position we analyzed DNA from the RP24-335D4 BAC clone by

Southern blot using IIGP4 as a probe and found that this clone contained the gene (Fig. 3d). We therefore concluded that IIGP4 was positioned 3' from IIGP2 in the IIGP cluster. Together the analysis of the three BAC clones revealed that the IIGP cluster consisted of five genes in the order depicted in Figure 3e.

The first complete sequence of the mouse genome was published soon after the end of this analysis. The sequence published in the ENSEMBL database confirmed the order we found but also showed that there are three additional IIGP1 homologues, which belong to the same cluster [112].

3.2 IIGP1 has two splice variants originating from two individual promoters

Analysis of IIGP1 mRNA and EST (expressed sequence tags) sequences available in the GenBank database showed that there are at least two splice variants (Fig. 4a). They will be further referred to as IIGP1A and IIGP1B. Both variants encode the same protein, as they both contain the IIGP1 coding exon (exon 3). The two molecules however significantly differed in the sequence of the first exons (exon 1A and exon 1B). Extensive analysis of the 5' ends of the available ESTs showed that there is no other exon positioned further 5' from exon 1A and 1B. We therefore concluded that the IIGP1A and IIGP1B originate from different promoters. Some rare ESTs however contained an additional exon between exons 1 and 3 (Fig. 4b). Together this analysis showed that the IIGP1 gene has 4 exons (Fig. 4c), two leading non-coding exons (1A and 1B) with two different promoters, a non-coding and possibly rarely used exon 2 and a coding exon 3. This structure was later confirmed by analysis of the IIGP1 genomic sequence available in the ENSEMBL database [112]. Further analysis of the available EST sequences showed that the ESTs for IIGP1A seemed to be more abundant. The transcript was found in EST libraries from spleen, liver, kidney, skin, heart, lung and lymph node. There were only a few ESTs encoding IIGP1B and they originated from liver and spleen. This suggested that the two IIGP1 splice variants might have a differential expression profile in mouse tissues.

```
IIGP1A AJ007971    1 -----CTCATGTGAAGAGCCTGTAGCAGTGAAGGTTGCTTCCTGAAGCTGAACTACAGTA
IIGP1B BC004649    1 GTAGACTCAAGCCAAGAGCA------CACCGAGGGCTA-TTCCT----CTCAGGAGCAGTG

                                              exon 1A/B ◄──────► exon 3
       AJ007971   56 AACAAATCCAGTGGACACAGGAGTTTCTGTGCCTTTATTGCTTGAAGTCATGGGTCAGCT
       BC004649   51 AGTGCATCCACTGGACACAGGATTTTCTGTGCCTTTATTGCTTGAAGTCATGGGTCAGCT
  a

       AJ007971  116 GTTCTCTTCACCTAAGAGTGATGAGAATAATGATTTGCCCTCCAGCTTTACTGGTTATTT
       BC004649  111 GTTCTCTTCACCTAAGAGTGATGAGAATAATGATTTGCCCTCCAGCTTTACTGGTTATTT


       AJ007971  176 TAAGAAATTTAATACGGGAAGAAAAATCATTTCTCAAGAGATCCTCAATTTGATT..............
       BC004649  171 TAAGAAATTTAATACGGGAAGAAAAATCATTTCTCAAGAGATCCTCAATTTGATT..............



IIGP1A  AJ007971    1 CTCATGTGAAGAGCCTGTAGCAGTGAAGGTTGCTTCCTGAAGCTGAACTACAGTAAACAA
IIGP1Am BI152144    1 CTCATGCGAAGAGCCTGTAGCAGTGAAGGTTGCTCCCTGAAGCTGAACTACAGTAAACAA

                                         exon 1A ◄──────► exon 2
        AJ007971   61 ATCCAGTGGACACAGGAGTTTCTG------------------------------------
        BI152144   61 ATCCAGTGGACACAGGAGTTTCTGGATTTCTCTGCTTCTGCTGCTCTGGCTGTCCTGGAA
  b

        AJ007971   85 ------------------------------------------------------------
        BI152144  121 CTCATCCTGTAGACCAGGCTGGCCTCAAACTCACAGAGATCTGCATACCTCTGCCTGTGA

                             exon 2 ◄──────► exon 3
        AJ007971   85 ----------------TGCCTTTATTGCTTGAAGTCATGG...........................
        BI152144  181 AAGGTAGGGATTAAAGTGCCTTTATTGCTTGAAGTCATGG...........................
```

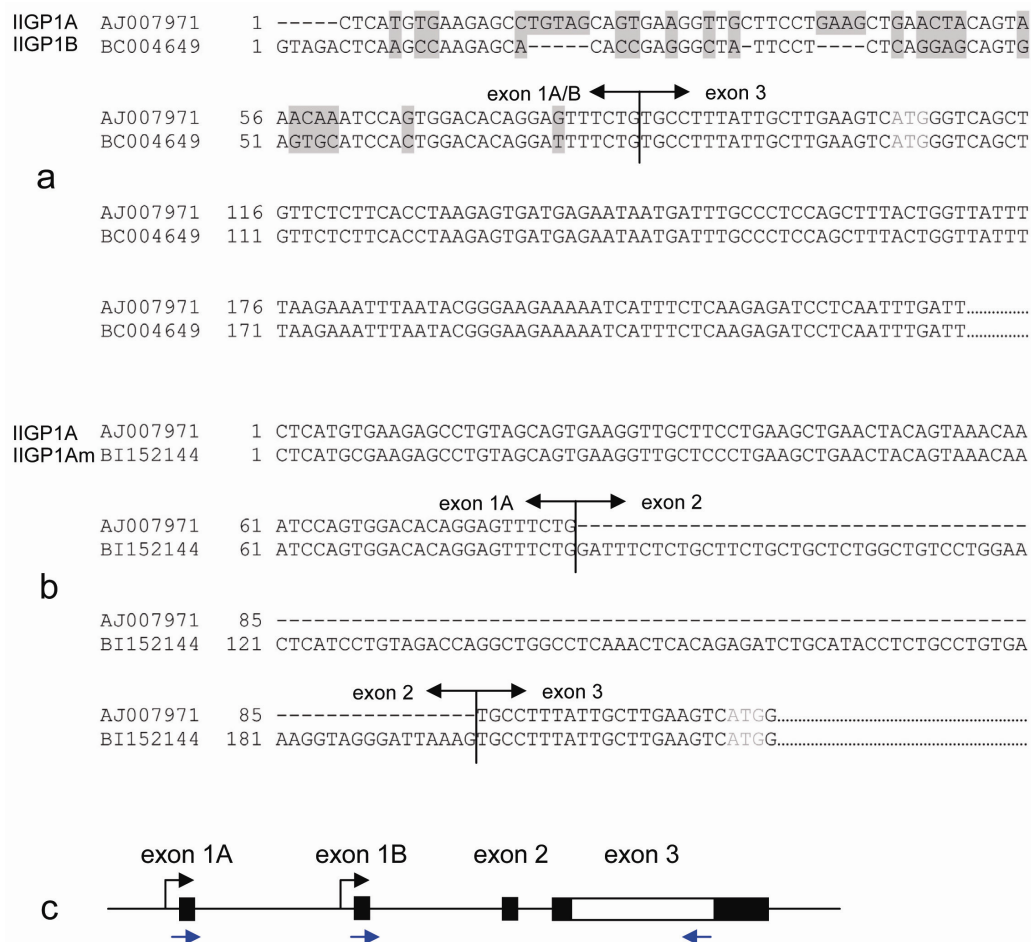c   exon 1A   exon 1B   exon 2   exon 3

Figure 4: Structure of the IIGP1 gene

Presented are alignments of mRNA sequences encoding IIGP1 splice variants. IIGP1A and IIGP1B (a) originate from two alternative promoters and differ in the sequence of their first exons, which are non-coding. In some rare mRNAs exon 1 splices to exon 2 (b), which is also non-coding. Shown are the borders between the exons. The beginning of the CDS (ATG) is written in gray. The differences between the sequences in a) are highlighted in grey. The differences in the nucleotides in positions 7 and 35 in b) (not highlighted) are probably due to sequencing errors. c) shows a scheme of the IIGP1 gene based on the alignment of available mRNA and EST sequences. Black blocks indicate exons, white box- CDS, black arrows- promoter regions, blue arrows- positions of primers used for Real-Time PCR.

3.3   IIGP1A and IIGP1B have similar basal expression levels in all mouse organs except the liver

In order to analyze qualitative and quantitative differences between the IIGP1A and B transcripts in different organs of healthy and infected mice the amount of these transcripts was measured by two-step Real-Time PCR. mRNA was isolated from mouse organs and used as a template for cDNA synthesis primed by Oligo-dT. The

cDNA samples were diluted 1:1 with water to reduce the concentration of MgCl$_2$, which might interfere with further amplification, and used as templates for Real-Time PCR on LightCycler (Roche). The number of molecules in each sample was calculated using a standard curve generated by amplification of known concentrations of an IIGP1A containing plasmid. The expression of the measured transcripts was normalized between the different organs to the expression level of the mouse hypoxanthine guanine phosphoribosyl transferase 1 gene (HPRT). The expression of HPRT was measured for each sample and set as 1 unit; the amounts of IIGP1A and B were calculated for each sample based on the HPRT unit and are therefore presented here as relative units.

In agreement with the already available IIGP1 protein expression profile (Jia Zeng, personal communication) the amount of both transcripts in all tested organs except brain was low but detectable (Fig. 5a). In all organs except lung and skin, the expression of IIGP1 seemed to be driven preferably by the IIGP1A promoter although in all these cases we could not detect very big differences in the amounts of the two transcripts. The only organ, which showed significant differences in expression level and ratio between IIGP1A and IIGP1B, was the liver. The expression level of IIGP1 in the liver was exceptionally high, being approximately equal to the expression of the HPRT gene in this organ (Fig. 5b), while the highest level in other organs reached only up to 0.05 relative units (Fig. 5a). Furthermore, the high expression in the liver was driven exclusively by the IIGP1B promoter (Fig. 5b). This data was confirmed by the analysis of IIGP1A and IIGP1B expression in primary hepatocytes (Fig. 6a, b). The basal expression of IIGP1 in these cells was also high, although not as high as in the liver, and was driven by the IIGP1B promoter (Fig. 6b).

3.4 The response of the IIGP1A but not IIGP1B promoter to IFNγ induction is very strong

Another important difference between the two IIGP1 promoters was revealed by the analysis of the amount of the two transcripts in organs from mice infected with *L. monocytogenes*. In agreement with previously published data [103, 119] we observed upregulation of IIGP1 expression in spleen and liver of mice 24 hours after infection with *L. monocytogenes* (Fig. 5c, d). Notably, in liver the IIGP1A transcription
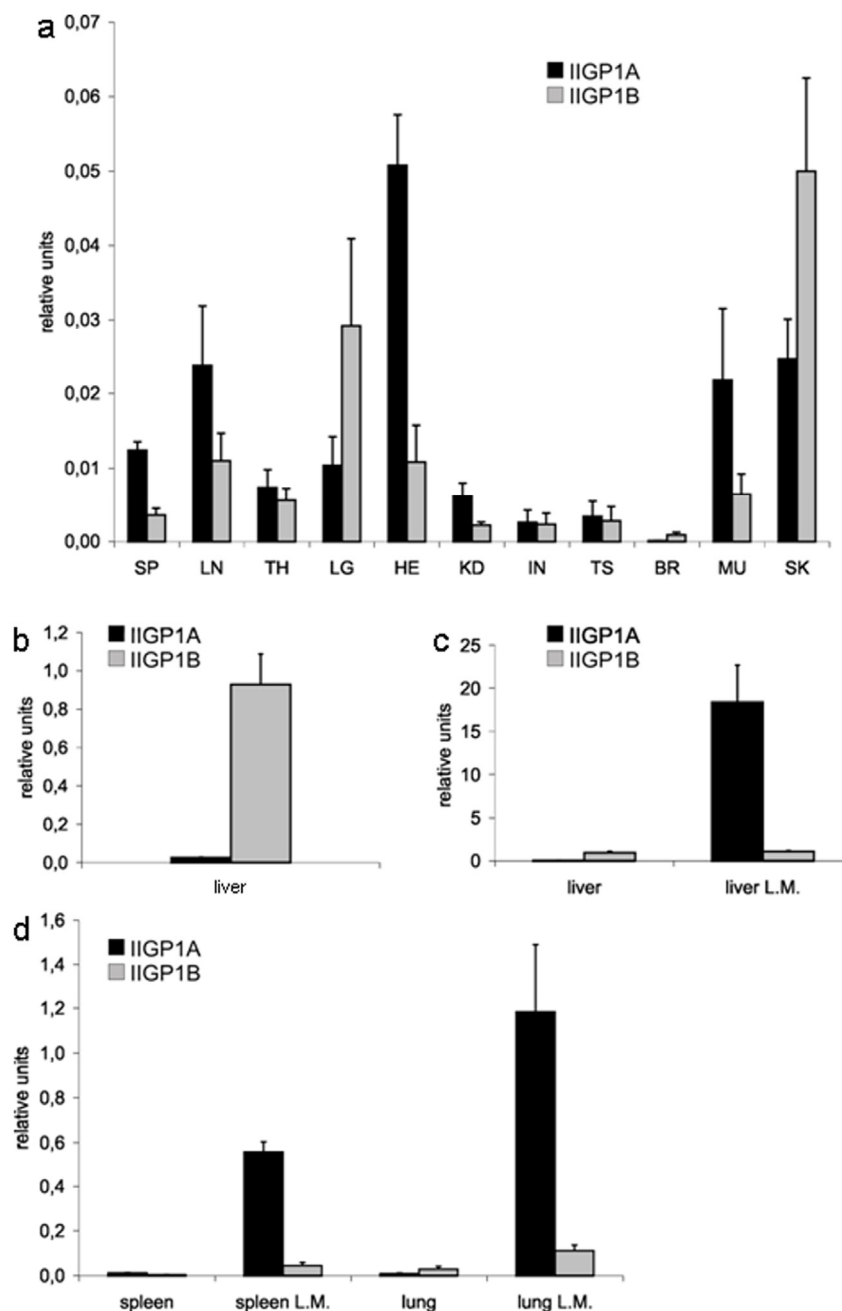
Figure 5: Expression profile of IIGP1A and IIGP1B splice variants in mouse organs

mRNA was isolated from organs of healthy (a, b) and *L. monocytogenes* infected (c, d) C57BL/6 mice and subjected to Real-Time PCR analysis. Presented are the mean values and standard deviations from 4 to 5 individual measurements. The amounts of both transcripts were similar in all organs (a) except liver, which showed exceptionally high expression driven by the IIGP1B promoter (b). The IIGP1A promoter exhibited strong induction by infection, while the IIGP1B promoter was barely inducible (c, d). SP-spleen, LN- lymph nodes, TH- thymus, LG- lung, HE-heart, KD- kidney, IN- intestine, TS- testis, BR- brain, MU- muscle, SK- skin

was strongly induced while the IIGP1B promoter did not respond to the induction (Fig. 5c). In spleen, there was a slight increase in the level of the IIGP1B transcript but the strong upregulation of IIGP1 in this organ was also mainly driven by the

IIGP1A promoter (Fig. 5d). A similar induction profile was observed in infected lung (Fig. 5d). The analysis of the induction of IIGP1 by IFNγ and in primary hepatocytes also showed high inducibitiy of the IIGP1A promoter and no induction of the IIGP1B promoter (Fig. 6c, d). Taken together our analysis of the inducibility of the two IIGP1 promoters indicates that they are probably regulated by different factors. The IIGP1A promoter is responsible for the IFNγ inducibility of the IIGP1 gene in all organs. The IIGP1B promoter is barely inducible by IFNγ but its high activity in the liver suggests that it is probably regulated by liver-specific transcription factors. This conclusion was later confirmed by *in silico* analysis of the two promoter sequences, which showed that the IIGP1A promoter has multiple IFNγ inducible elements (GAS and ISRE) [112], while the IIGP1B promoter includes only a single GAS site but also binding sites for liver-specific transcription factors ([112] and Jia Zeng, personal communication).
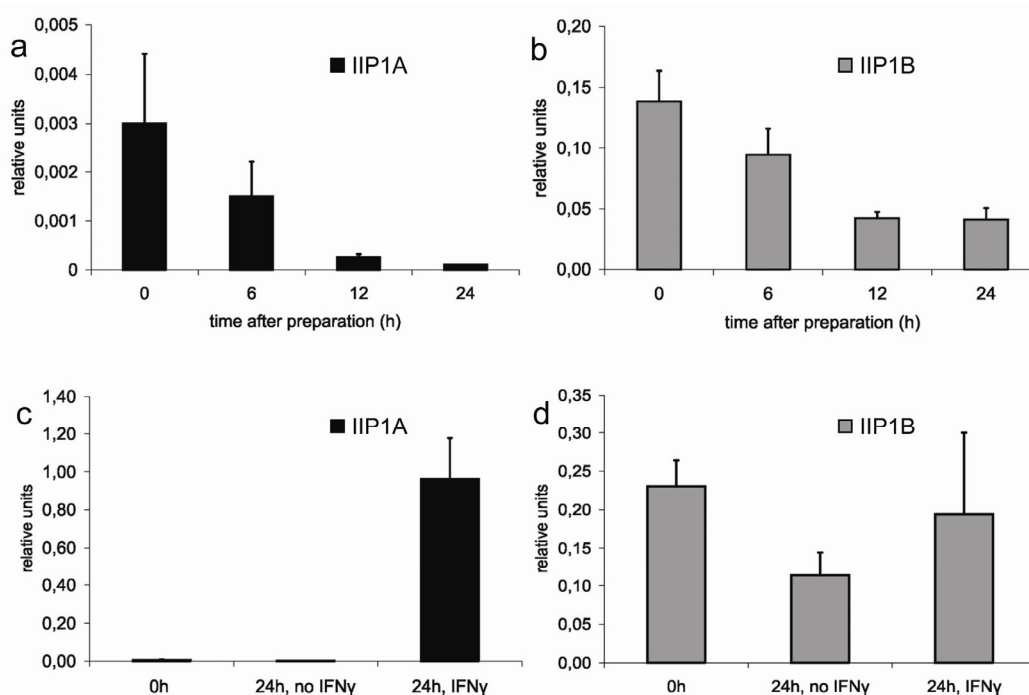
Figure 6: Expression profile of IIGP1A and IIGP1B splice variants in primary hepatocytes

Primary hepatocytes were isolated from livers of adult mice and immediately processed or cultured up to 24h. Cells were left untreated (a, b) or induced with 100U/ml IFNγ for 24h (c, d) and harvested at the indicated time points. mRNA isolated form the cells was subjected to Real-Time PCR analysis. Presented are the mean values and standard deviations from 3 individual measurements. In agreement with the observed liver expression profile the basal expression of IGP1B was high, while IIGP1A showed low basal expression but strong IFNγ induction. Primary hepatocytes were kindly provided by Jia Zeng.

3.5 Generation of a conditional IIGP1 allele and an IIGP1-deficient mouse

The IIGP1 gene is located on mouse chromosome 18 [112]. The complete CDS of the protein is part of exon 3. In order to generate an IIGP1 conditional allele (IIGP1^{FN}), a targeting vector, which allowed placing of this coding exon between two loxP sites in the mouse genome had to be designed and cloned (Fig. 7A).

The genomic DNA used for generation of the targeting vector was obtained from a C57BL/6 genomic BAC clone (RP23-19A12) containing the almost complete IIGP cluster. The genomic sequences were cloned into the vector pEasyFlox as follows. 4kb BamHI fragment containing exon 2, 5' UTR and polyA signal of IIGP1 was subcloned from the BAC and cloned blunt into the previously SalI digested and blunted pEasyFlox. The two arms of homology were generated by PCR from two subclones of the BAC. The PCR primers contained the restriction sites needed for the subsequent cloning of the homology arms in the targeting vector; the 3' primer of the long arm of homology contained also an additional EcoRI site, which was later used for screening for homologous recombinant ES cell clones. The 5' and 3' arms of homology were cloned into the XhoI and NotI sites of pEasyFlox, respectively. The integrity of the targeting vector was proven by multiple restriction digests; all important elements of the vector, including the three loxP sites, IIGP1 coding sequence, polyA signal and all borders between the cloned genomic fragments, were sequenced.

10^7 Bruce4 ES cells [138] derived from C57Bl/6-Thy1.1 mice were transfected with SfiI linearized targeting vector, cultured and selected as described in Materials and Methods. Out of 300 G418 and gancyclovir resistant colonies 2 were identified as homologous recombinants by Southern blot analysis of EcoRI digested genomic DNA with probe p1 (not shown). Homologous recombination in the 3' region was confirmed with HindIII restriction digest and probe p2 (not shown); this digest also proved co-integration of the third loxP site. Additionally, random integration of the targeting vector was excluded by hybridization with an internal probe specific for the neomycin-resistance gene (probe p3; not shown). *In vitro* deletion of the sequence between the external loxP sites after incubation of the cells with membrane-permeable Cre protein (His-TAT-NLS-Cre) [148] showed that they are functional (not shown).
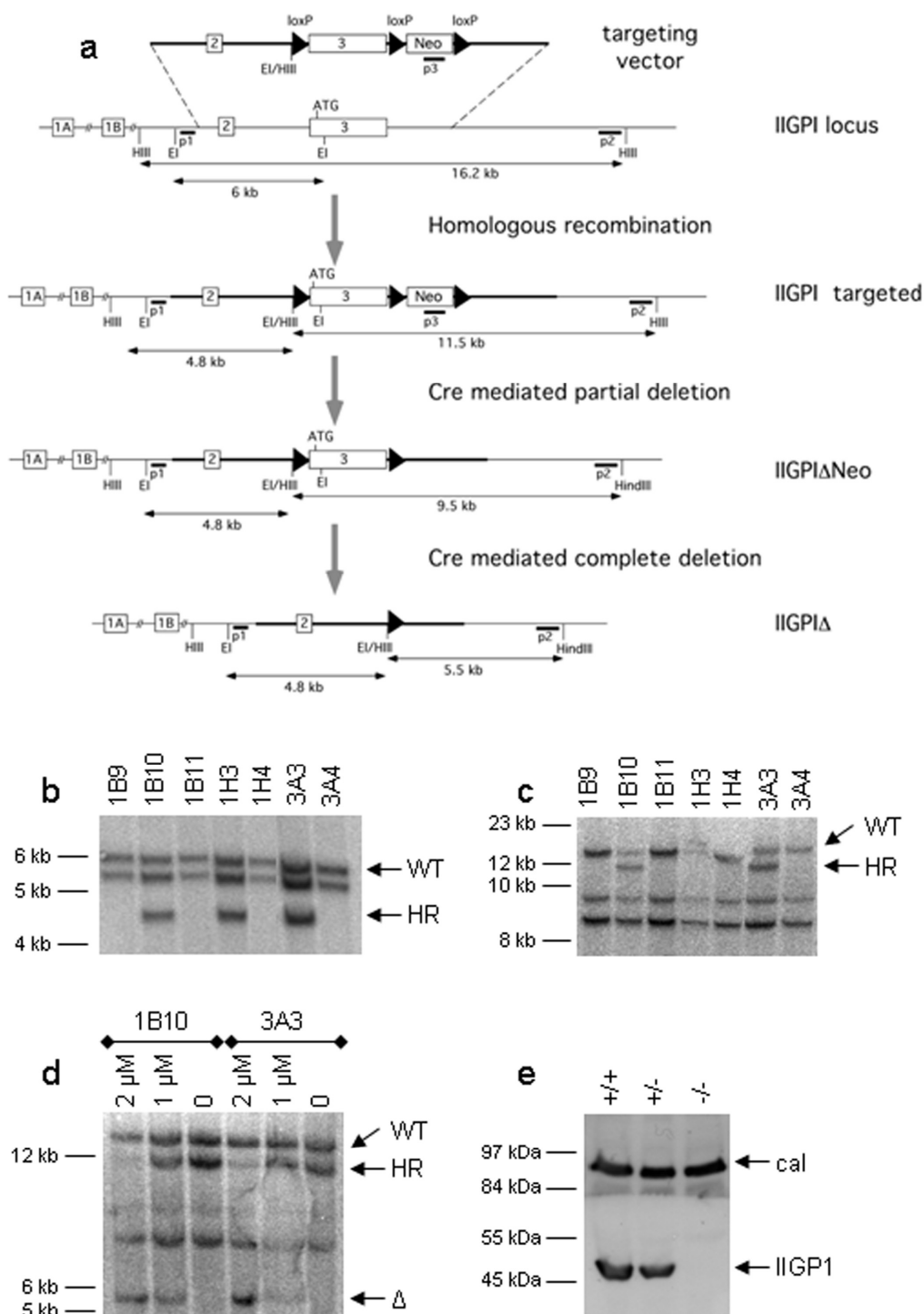
Figure 7: Generation of IIGP1-deficient ES cells

(a) Insertion of the targeting vector into the IIGP1 locus by homologous recombination generates a targeted IIGP1 allele. The neo cassette and the exon placed between two loxP sites are excised by partial and complete Cre mediated deletion, respectively. Sizes of DNA fragments are indicated under the two-sided arrows; white boxes represent exons; Neo, neomycin resistance gene; p1,2 and 3, Southern blot probes; EI, EcoRI restriction site; HIII, Hind III restriction site. (b), (c) Homologous recombination was confirmed by Southern blot analysis after EcoRI digest and

hybridization with p1 (b) and HindIII digest and hybridization with p2 (c). The respective wild type (WT) and homologous recombinant (HR) bands and the names of the clones are indicated. Additional bands are due to crossreactivity of the probes to IIGP1 homologous genes. (d) Recombinant ES cells from clones 1B10 and 3A3 were treated with the indicated concentrations of His-TAT-NLS-Cre. Complete deletion after Cre treatment was confirmed by Southern blot analysis after HindIII restriction digest and hybridization with p2. The respective WT, HR and complete deletion (Δ) are indicated (e) Lack of expression of IIGP1 after IFNγ induction was confirmed by Western blot analysis of lysates from mouse embryonic fibroblasts. The respective IIGP1 and calnexin (cal) bands are indicated.

ES cells from both clones were injected into CB20 blastocysts by Sonja Becker (Center for Mouse Genetics, Cologne). As a result, mice with chimerism between 10 and 30% were generated from both clones. Seven chimaeras were bred for germline transmission of the IIGP1 targeted allele (IIGP1^{FN}) to C57BL/6 animals. The IIGP1^{FN} failed to be transmitted through the germline. Therefore, a second transfection of Bruce4 ES cells was performed in conditions identical to the first one. Out of 350 G418 and gancyclovir resistant colonies 3 were identified as homologous recombinants by Southern blot analysis of EcoRI digested genomic DNA with probe p1 (Fig. 7b). Probe p2 showed that one of these clones was a partial integrant (Fig. 7c), therefore the work continued with the other two (1B10 and 3A3). Random integration of the targeting vector was excluded by hybridization with probe p3 (not shown). *In vitro* deletion of the sequence between the external loxP sites after treatment of the cells with His-TAT-NLS-Cre showed that they are functional (Fig. 7d). Cells from these two clones were injected in CB20 blastocysts and mice with chimerism between 30 and 90 percent were generated. The chimeric mice were bred for germline transmission of the IIGP1^{FN} allele to C57BL/6 animals. Two of the chimeras generated from clone 1B10 transmitted the allele in 100% of the progeny.

In order to generate a complete IIGP1 deficient mouse the germline-transmitted offspring were crossed to C57BL/6 Cre-deleter mice [149]. The progeny were screened for deletion of IIGP1 by PCR and/or Southern blot (not shown) and the positive heterozygous (IIGP1$^{+/-}$) animals were crossed for homozygocity. The latter breeding produced all expected genotypes (IIGP1$^{-/-}$, IIGP1$^{+/-}$ and IIGP1$^{+/+}$) in mendelian ratio. The intercross of the IIGP1$^{-/-}$ offspring showed that these animals were fertile.

The inability of the generated IIGP1$^{-/-}$ mice to produce IIGP1 protein upon IFNγ induction was demonstrated by a Western blot analysis of lysates from primary embryonic fibroblasts prepared from these animals. 24 h after stimulation with 100

U/ml IFNγ the IIGP1 deficient cells did not produce any detectable IIGP1 protein (Fig. 7e).

IIGP1 deficient mice did not have any apparent anatomical abnormalities. An initial analysis of the adaptive immune system by flow cytometry showed the presence of all major cell types in normal numbers. Single cell suspensions of spleen and mesenteric and inguinal lymph nodes were stained with fluorescent antibodies and analysed on a FACScalibur flow cytometer. CD19 expressing B cells and TCRβ expressing T cells were observed in normal numbers (Fig.8a). In addition, the T cell subpopulations characterized by CD4 (helper T cells) and CD8 (cytotoxic T cells) were found to be unaltered (Fig.8b). Analysis with the markers NK1.1 and CD11c also confirmed the presence of normal numbers of NK cells and dendritic cells, respectively (Fig. 9).

An IIGP1 conditional mutant mouse was generated by crossing the IIGP1[FN] germline transmitted animals to Partial Cre-deleter mice [220]. The conditional mutant animals were not used in this study.
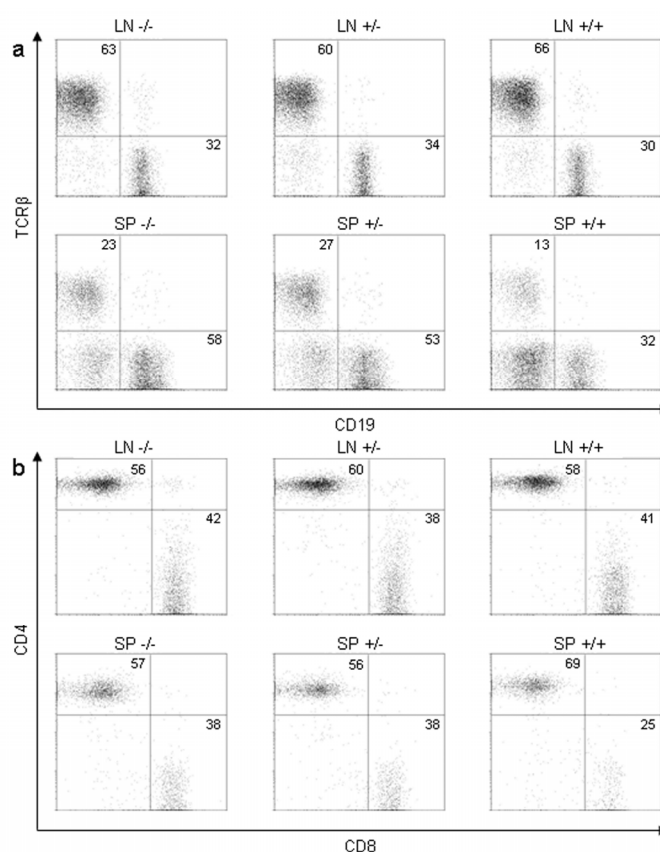
Figure 8: Initial analysis of the adaptive immune system of IIGP1-deficient mice

Single cell suspensions were prepared from spleen and lymph nodes of IIGP1^{-/-}, IIGP1^{+/-} and IIGP1^{+/+} mice and the expression of lineage-specific surface markers was analyzed by flow cytometry under exclusion of dead cells by Topro-3. The percentages of the different cell populations are shown in the respective quadrants. All analyzed cell populations, B- and T-cells (a), CD4 and CD8 positive T cells (b) were present in normal numbers. SP- spleen, LN- lymph nodes

43
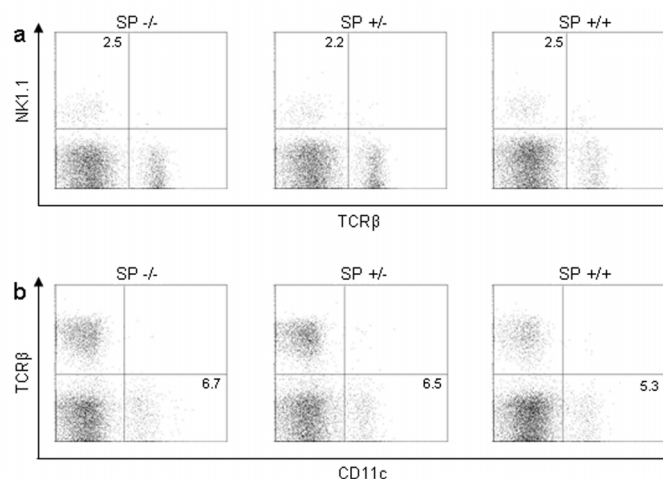
Figure 9: Analysis of NK cells and DCs in IIGP1-deficient mice

Single cell suspensions were prepared from spleen of IIGP1$^{-/-}$, IIGP1$^{+/-}$ and IIGP1$^{+/+}$ mice and the expression of lineage-specific surface markers was analyzed by flow cytometry under exclusion of dead cells by Topro-3. The percentages of the different cell populations are shown in the respective quadrants. NK cells (a) and DCs (b) were present in normal numbers. SP- spleen

3.6   Influence of IIGP1 deficiency on resistance against intracellular pathogens

To examine the ability of the IIGP1 deficient mice to mount a response against intracellular pathogens the animals were challenged with several infectious agents from bacterial and protozoan origin. Resistance against all these pathogens has been previously proven to be crucially dependent on IFNγ (Table 1).

3.6.1   IIGP1 deficiency leads to a partial loss of IFNγ-induced inhibition of *Toxoplasma gondii* growth in primary astrocytes.

T. gondii is an obligate intracellular protozoan parasite, which causes one of the most common infections in humans. Infection with *T. gondii* is characterized by an acute phase in which the rapidly proliferating form (tachyzoite) disseminates throughout the host, followed by a chronic phase in which the slowly replicating form (bradyzoite) encysts and persists mainly in the central nervous system (CNS) and muscles. These brain cysts periodically reactivate and rupture releasing bradyzoites. In healthy individuals, parasite replication is limited and the infection is asymptomatic. In immunosuppressed patients, however, upon cyst reactivation the bradyzoites convert into rapidly replicating tachyzoites and cause necrotizing and often fatal encephalitis.

IFNγ is critical for control of both phases of *T. gondii* infection [55, 150]. There seems to be a difference in the set of resistance mechanisms, which IFNγ induces in different types of cells. IFNγ-activated microglia control *T. gondii* growth via a NO-mediated mechanism [151], whereas in murine astrocytes restriction of parasite growth is dependent on the p47 GTPase IGTP [154].

To study the influence of IIGP1 deficiency on the IFNγ-induced protection against *T. gondii* we analyzed the parasite growth in primary astrocytes prepared from brains of neonatal IIGP1$^{-/-}$ and IIGP1$^{+/+}$ littermate mice. The astrocytes were stimulated with different concentrations of IFNγ (1, 10 or 100 U/ml) for 24 h; control cells were left untreated. Cells were then infected with *T. gondii* ME49 tachyzoites at different multiplicity of infection (MOI) (0.1, 0.3, 1 or 3) for 24 h. Cultures were labeled with [^{3}H]-uracil (1 μCi/well Hartmann Analytical) for further 24 h and the amount of incorporated uracil, directly corresponding to the parasite growth [147], was
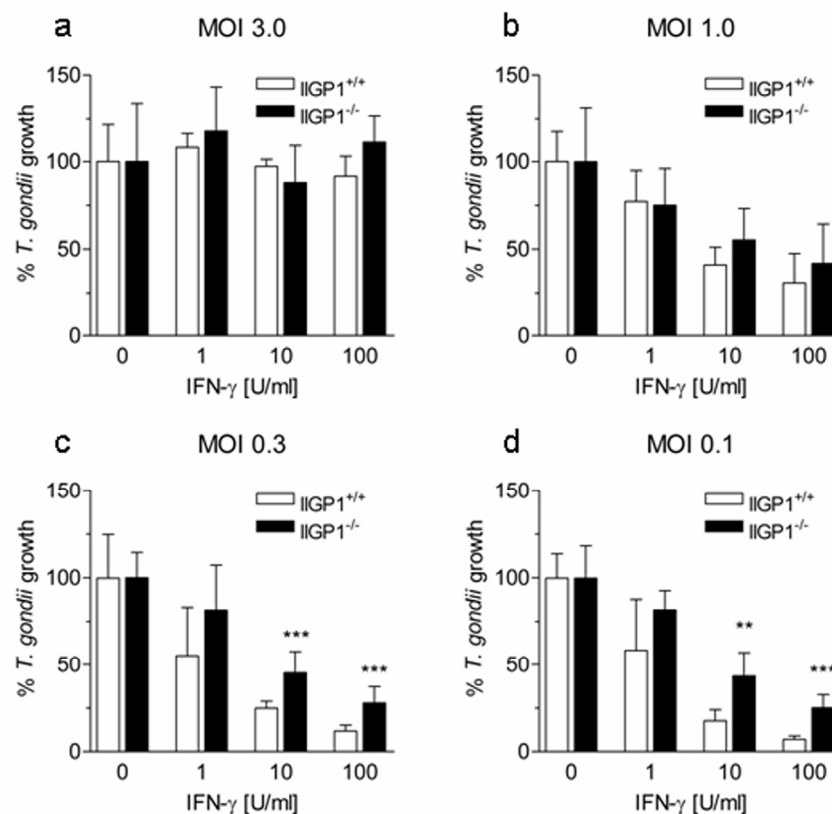
Figure 10: IIGP1 deficient astrocytes show a partial loss of IFNγ-induced inhibition of *Toxoplasma gondii* growth
Primary astrocytes were prepared from brains of neonatal IIGP1$^{-/-}$ and IIGP1$^{+/+}$ littermate mice, stimulated with the indicated concentrations of IFNγ for 24 h and infected with *T. gondii* ME49 tachyzoites at MOI 3 (a), 1 (b), 0.3 (c) or 0.1 (d) for total of 48h. Parasite growth was monitored by uracil incorporation assay. The higher parasite growth at MOI 0.1 and 0.3 indicated the reduced ability of IIGP1$^{-/-}$ astrocytes to inhibit intracellular *T. gondii* (P values: ** 0.0015, *** 0.0001 by unpaired Student's T-test). Results are representative of 3 experiments. MOI, multiplicity of infection

determined by liquid scintillation counting. The results are presented as percentages of *T. gondii* growth calculated separately for each set of conditions (MOI and genotype) with the radioactive signal measured in non-induced cells set to 100%. The initial experiment showed that an infection at MOI 3 could not be controlled even by IFNγ-stimulated IIGP1$^{+/+}$ astrocytes (Fig. 10a) while at MOI 1 or lower an IFNγ-induced anti-parasitic effect was detectable in IIGP1$^{-/-}$ and IIGP1$^{+/+}$ cells (Fig. 10b). At MOI 0.1 and 0.3 parasite growth was higher in the IIGP1$^{-/-}$ astrocytes compared to the one in IIGP1$^{+/+}$ control cells (Fig. 10c,d) indicating a reduced ability of IIGP1$^{-/-}$ astrocytes to inhibit intracellular *T. gondii*. Although only partial, the loss of resistance in the IIGP1$^{-/-}$ cells was significant, as controlled by unpaired Student's T-test. The effect of IIGP1 deficiency on inhibitory capacity of astrocytes is smaller than the one reported for IGTP [154]. This suggests that IIGP1 might be partially redundant to other IFNγ-inducible resistance factors, at least in the inhibition of *T. gondii* growth by murine astrocytes.

3.6.2 The accumulation of other p47 GTPases at the membrane of *T. gondii* parasitophorous vacuoles does not depend on IIGP1

T. gondii actively invades cells [155] and replicates in a parasitophorous vacuole (PV) formed by invagination of the host cell plasma membrane during entry [156]. During the formation of the PV, most of the host proteins are excluded from its membrane and the PV escapes fusion with the endocytic compartment [157, 158]. After entry of the parasite into the host cell IIGP1 rapidly translocates to the PV and massively accumulates around it [134]. A similar behavior has also been observed for other members of the p47 GTPase family [134].

In order to explore possible interactions of IIGP1 with other p47 GTPases at the PV we analyzed the localization of TGTP1 and IGTP in *T. gondii* infected IIGP1$^{-/-}$ and IIGP1$^{+/+}$ astrocytes. Cells were stimulated with 100 U/ml IFNγ for 24 hours and infected with *T. gondii* ME49 tachyzoites at MOI 10 for 2 hours. The cells were then extensively washed with PBS to remove extracellular parasites, fixed with 3 % PFA, and stained with the appropriate antibodies (Table 4). Vacuoles containing intracellular parasites were visualized by indirect immunostaining for *T. gondii* GRA7, a 29kDa predicted transmembrane protein, which is released in the PV by parasites shortly after cell invasion and associates with the PV membrane (PVM) [159]. The nuclei of host cells and parasites were visualized by DAPI staining. In

agreement with previous data [134], TGTP1 massively accumulated around the PV in IIGP1$^{+/+}$ cells (Fig. 11d). Similar association of TGTP1 with the PV was observed in IIGP1$^{-/-}$ cells (Fig. 11b). The localization of IGTP in IIGP1$^{-/-}$ astrocytes (Fig. 11a) was also indistinguishable from that in IIGP1$^{+/+}$ cells (Fig. 11c). Preliminary data shows that GTPI and IRG-47 also associate with the PV in IIGP1$^{-/-}$ astrocytes in a manner similar to the one in IIGP1$^{+/+}$ cells but this has to reconfirmed. Together these data indicate that IIGP1 is not required for the accumulation of at least some other p47 GTPases at the PV.
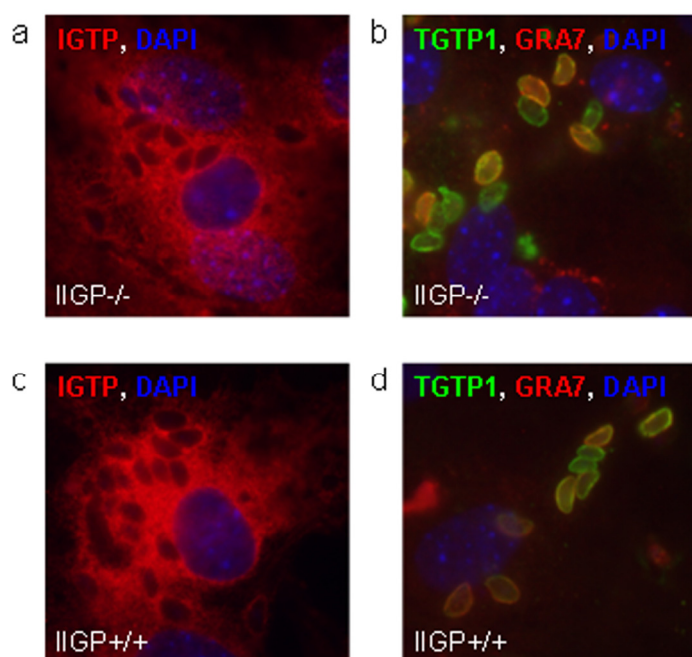
Figure 11: The association of IGTP and TGTP1 with *T. gondii* PV in IIGP1$^{-/-}$ astrocytes is indistinguishable from that in IIGP1$^{+/+}$ cells

Astrocytes were stimulated with 100 U/ml IFNγ for 24 hours and infected with *T. gondii* ME49 tachyzoites at MOI 10 for 2 hours. The cells were then extensively washed with PBS to remove extracellular parasites, fixed with 3 % PFA, and stained with the appropriate antibodies. The localization of IGTP in IIGP1$^{-/-}$ astrocytes (a) was indistinguishable from that in IIGP1$^{+/+}$ cells (c). The association of TGTP1 with the PV in IIGP1$^{-/-}$ cells (b) was also similar to that in IIGP1$^{+/+}$ astrocytes.

3.6.3 The effect of IIGP1 deficiency on susceptibility of mice to *T. gondii* is not yet clear

Groups of 4 to 7 IIGP1$^{-/-}$, IIGP1$^{+/-}$ and IIGP1$^{+/+}$ littermate mice were infected with *T. gondii* bradyzoites freshly prepared from cysts isolated from the brains of chronically infected CD1 mice. Two avirulent strains of *T. gondii* (ME49 and DX) were used. Each animal was infected i.p. with bradyzoites prepared from 5 cysts of strain DX or

20 cysts of strain ME49. The mice were observed daily for disease symptoms and their weight was measured every 2-3 days. The results obtained were similar regardless of the *T. gondii* strain used for infection. In both experiments all infected IIGP1$^{+/-}$ and IIGP1$^{+/+}$ animals survived the acute phase of the infection, while one mouse from the IIGP1$^{-/-}$ group died in each experiment, at day 11 during the DX infection and day 14 after infection with ME49 parasites. During the chronic phase of infection, all animals lost weight comparably and around week 7 p.i., they all developed neurological symptoms (ataxia, deviation of the head). During infection with ME49 one IIGP1$^{+/-}$ mouse died at day 54 p.i., while all animals infected with strain DX survived until the end of week 8 p.i. At that time point (day 56 p.i.), all surviving mice were sacrificed. *T. gondii* cysts were isolated from the brains and their number was counted. Following infection with strain DX, the brain parasite load was similar in IIGP1$^{-/-}$, IIGP1$^{+/-}$ and IIGP1$^{+/+}$ mice (Fig. 12a). After infection with strain ME49 one IIGP1$^{-/-}$ and one IIGP1$^{+/-}$ animals had a very high parasitic load in the brain, while the cyst numbers in the remaining animals were comparable to these of IIGP1$^{+/+}$ mice (Fig. 12b). The results from these *in vivo* infection experiments are not yet conclusive. The possibility that a higher *T. gondii* growth in IIGP1$^{-/-}$ astrocytes may lead to a higher mortality rate of IIGP1$^{-/-}$ compared to IIGP1$^{+/+}$ mice cannot be excluded. The expected effect on survival is, however, relatively small. Therefore, the infection experiments have to be conducted on a larger scale.
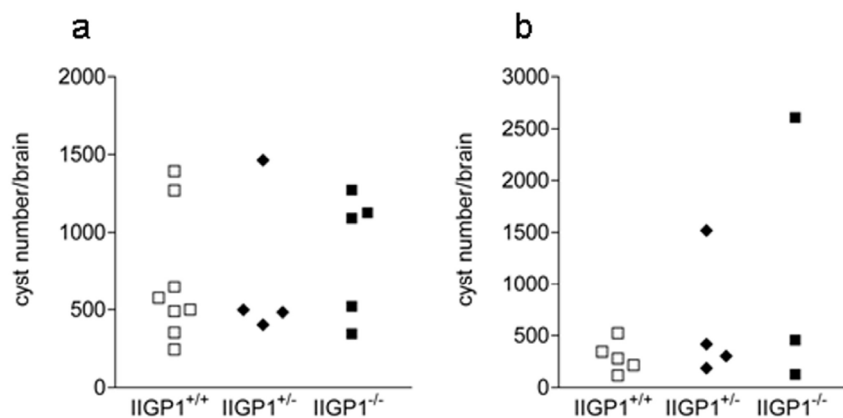
Figure 12: *T. gondii* load in brains of infected mice

Mice were infected with freshly prepared *T. gondii* strain DX (a) or ME49 (b) bradyzoites. At day 56 p.i., all animals were sacrificed., *T. gondii* cysts were isolated from the brains and their number was counted. After infection with strain DX, the brain parasite load was similar in IIGP1$^{-/-}$, IIGP1$^{+/-}$ and IIGP1$^{+/+}$ mice. Following infection with strain ME49 one IIGP1$^{-/-}$ and one IIGP1$^{+/-}$ animals had a very high parasitic load in the brain, while the cyst numbers in the remaining animals were comparable to these of IIGP1$^{+/+}$ mice.

3.6.4 IIGP1 deficient mice have higher incidence of development of cerebral malaria

Malaria is caused by infection with different members of the *Plasmodium* genus. These protozoan parasites have a very complex life cycle [160], which includes diverse stages infecting different tissues of the host. The disease has two stages, pre-erythrocytic (sporozoite/liver) and erythrocytic. During the pre-erythrocytic stage, the *Plasmodium spp.* sporozoites invade the liver and amplify in hepatocytes producing merozoites. At the end of this stage, the merozoites leave the liver and infect erythrocytes thus starting the erythrocyte stage, which is responsible for all symptoms and pathology of malaria. The immune response against malaria is extremely complex and it is apparent that different components of the immune system operate at the pre-erythrocytic and erythrocytic stages of the parasite. IFNγ secreted by CD8+ T cells and NK cells and inducing NO production in hepatocytes mediates the former [161, 162]. The latter varies in different hosts infected with different parasites but is largely dependent on protective antibodies, NO and γδT cells [163, 162, 164].

In many mouse strains, malaria progresses into a brain vascular pathology known as cerebral malaria (CM). CM is characterized by sequestration of parasitized red blood cells by brain microvascular endothelial cells, which leads to vessel obstruction and hypoxia; the disease is also accompanied by vessel disruption and brain hemorrhages [165, 166]. Host-derived inflammatory cytokines play a key role in the pathogenesis of CM in both mice and humans [164, 167].

To study the influence of the IIGP1 deficiency on development of cerebral malaria we infected mice with either sporozoites of *Plasmodium berghei* strain ANKA or blood of mice previously infected with this parasite. The infection with sporozoites mimics the natural route of transmission of the disease. The injected sporozoites infect hepatocytes; in mice, the liver stage of malaria continues around two days, after which the merozoites egress the liver and start the blood stage. Some of the infected mice develop neurological disease symptoms of cerebral malaria (deviation of the head, ataxia and convulsions) at day 8-9 p.i.; the sick animals die fast, usually in 1 or 2 days after the first symptoms. The period of development of cerebral malaria continues until day 14 p.i. The animals, which survive this period, do not develop cerebral malaria anymore. They die between day 25- 30 p.i. from anemia caused by very high blood parasitemia. When mice are infected with parasitized blood all manifestations of the disease start two days later in comparison to the liver stage infection. In the

presented liver stage infection experiment groups of 7 to 11 IIGP1$^{-/-}$, IIGP1$^{+/-}$ and IIGP1$^{+/+}$ littermate mice were infected by injection of 500 µl PBS containing 50 sporozoites in the tail vein; the sporozoites were freshly prepared from the salivary glands of infected *Anopheles stephensi* mosquitoes. In the presented blood stage infection experiments groups of 10 to 13 IIGP1$^{-/-}$, IIGP1$^{+/-}$ and IIGP1$^{+/+}$ littermate mice were infected with 50 000 parasitized erythrocytes. The animals were observed daily for symptoms of cerebral malaria and time of death. The three groups of mice infected with parasitized blood showed similar survival rates (Fig. 13a). The mortality of the IIGP1$^{-/-}$ animals was slightly higher but the closer analysis of the data with Kaplan-Meier test showed that this difference is not significant (p=0.77). The sporozoite infection, however, revealed a 30% higher mortality of IIGP1$^{-/-}$ mice compared to IIGP1$^{+/-}$ and IIGP1$^{+/+}$ control animals (Fig. 13b). The statistical analysis of this data showed that the difference in survival between the IIGP1$^{-/-}$ and IIGP1$^{+/+}$ in this experiment had a high tendency to be significant (p<0.1 by Kaplan-Meier test) but in order to confirm the result the experiment had to be conducted on a larger scale.
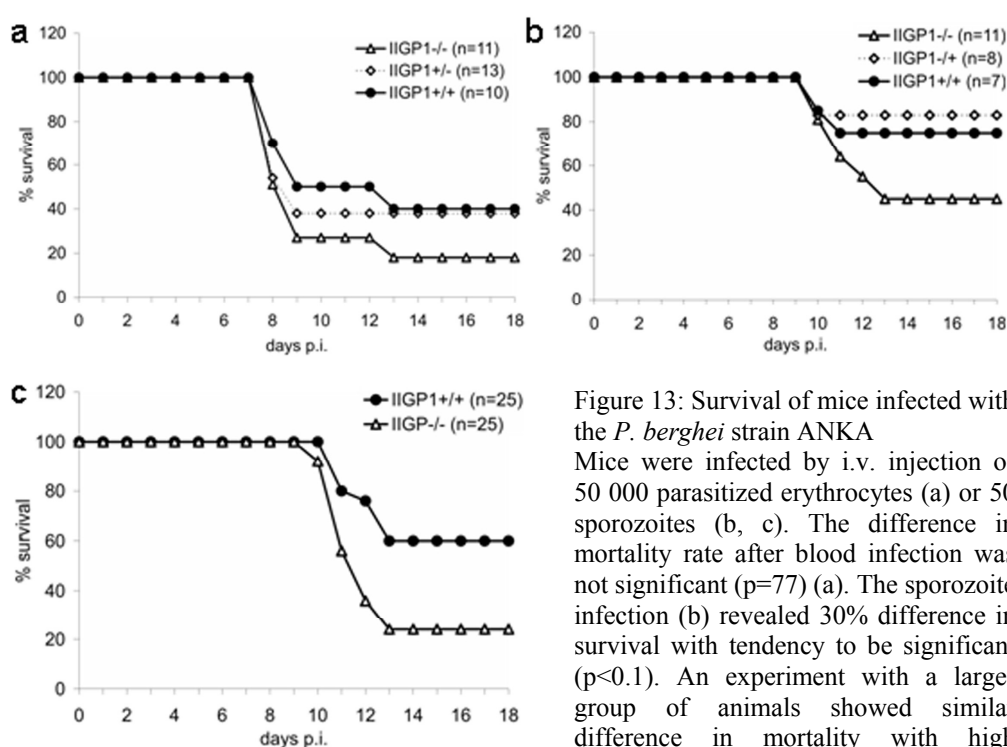
Figure 13: Survival of mice infected with the *P. berghei* strain ANKA
Mice were infected by i.v. injection of 50 000 parasitized erythrocytes (a) or 50 sporozoites (b, c). The difference in mortality rate after blood infection was not significant (p=77) (a). The sporozoite infection (b) revealed 30% difference in survival with tendency to be significant (p<0.1). An experiment with a larger group of animals showed similar difference in mortality with high significance (p=0.01).

Therefore, we challenged groups of 25 IIGP1^{-/-} and IIGP1^{+/+} mice with the same sporozoite dose (50 sporozoites per mouse) and monitored their survival. The difference in mortality rate detected in this experiment was in the same range, 35% (Fig. 13c) and the statistical analysis showed that the result is highly significant (p=0.01 by Kaplan-Meier test). Together these experiments indicate that IIGP1 contributes to host defense against *P. berghei.*

3.6.5 Resistance of C57BL/6 mice against *Leishmania major* is not affected by the lack of IIGP1

L. major is a protozoan pathogen causing cutaneous disease in humans and rodents, which is transmitted by sand flies and characterized by development of localized skin lesions that eventually heal. It is well established that inbred mouse strains are genetically predisposed for susceptibility or resistance to *L. major* and the predisposition correlates with the dominance of T_H1 or T_H2 responses in the respective strains. T_H1 cells are required for protection and differentiate naturally in genetically resistant strains of mice, such as C57BL/6, whereas T_H2 cells cause disease progression and differentiate naturally in genetically susceptible mouse strains, such as BALB/c [168, 169]. IFNγ secreted by T_H1 cells is the leading factor generating protective immunity against *L. major* [58, 59].

To test the potential effect of IIGP1 deficiency on resistance to *L. major* groups of 4 IIGP1^{-/-}, IIGP1^{+/-} and IIGP1^{+/+} littermate mice were challenged with infective-stage (metacyclic) promastigotes of *L. major* clone V1 (MHOM/IL/80/Friedlin). The mice were infected by injection of 10 µl of PBS containing the parasites into the dorsal dermis of the left ears. Lesion volumes were measured weekly in three dimensions using a caliper.

In the presented experiments two infectious doses were used, a high dose ($2x10^5$) and a low dose ($1x10^3$). Most studies on the host response against *L. major* employ high doses of promastygotes because in such a set-up the lesions appear and resolve very fast. In the low dose model, the disease develops slower. It has an initial silent phase characterized by increasing load of parasites in the dermis but no histopathological changes; after the end of this phase, around week 4 p.i., the lesions develop. The advantage of the low dose model is that it is much closer to the natural transmission of the disease. In the experiments presented here the development of the lesions in the IIGP1^{-/-} mice was not significantly different from the one in the control animals for

both infectious doses (Fig. 13). The lesions appeared at the same time, developed to the same maximal size and healed in all infected animals regardless of their genotype.
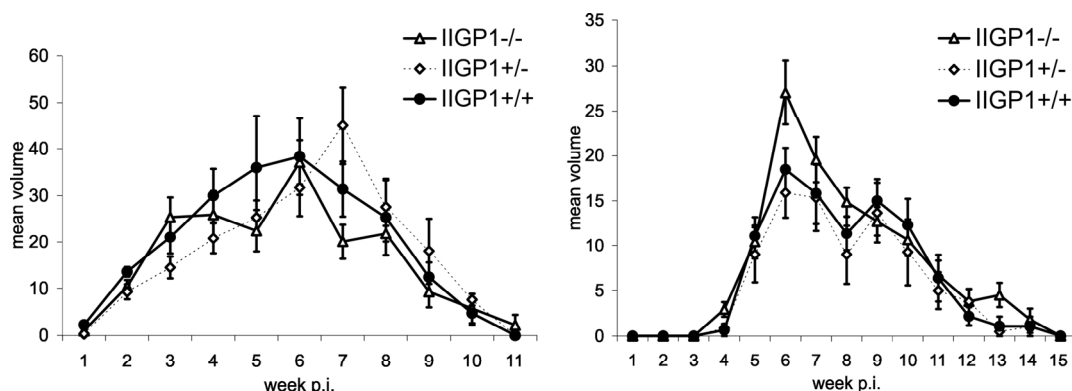

Figure 14: Disease onset in *L. major* infected mice

Groups of 4 IIGP1$^{-/-}$, IIGP1$^{+/-}$ and IIGP1$^{+/+}$ littermate mice were infected with $2x10^5$ (a) or 10^3 (b) metacyclic promastigotes of *L. major* clone V1 (MHOM/IL/80/Friedlin). Lesion volumes were measured weekly in three dimensions using a caliper. Presented are the mean volumes with standard errors. There was no significant difference in disease outcome between the groups of experimental animals.

3.6.6 IIGP1 deficient mice are not susceptible to infection with Listeria monocytogenes

L. monocytogenes is a bacterial pathogen with a very broad host range. It causes food born disease, which is particularly dangerous for immunocompromised individuals and pregnant women. Early resistance to infection with *L. monocytogenes* is attributed to the rapid triggering of innate immune responses and especially IFNγ production [170, 171].

To analyze the effect of IIGP1 deficiency on host response against *L. monocytogenes* we infected IIGP1$^{-/-}$ and IIGP1$^{+/+}$ littermate mice by i.p. injection of 10^3 or 10^4 CFU of *L. monocytogenes*, strain EDG, serotype 1/2a. Following infection mice were monitored daily for disease symptoms and time of death. The infectious dose of 10^4, which equals to LD$_{50}$ of *L. monocytogenes* strain EDG in C57BL/6 mice, showed similar mortality rate in both groups of animals (Fig. 15). All mice infected with 10^3 bacteria (n=8 for both genotypes) survived the infection. At day 3 p.i., four mice from each genotype infected with 10^3 bacteria were sacrificed and specimens of liver and spleen were examined for bacterial titers. Organs were homogenized in 0.1% Triton X100 and 10-fold serial dilutions from the homogenates were plated on blood-agar plates. 48 h later the CFU were counted to determine the bacterial load, which was

presented as CFU/g organ. The two groups of animals had similar bacterial burden in spleen, $20 \pm 12.3 \times 10^3$ and $31.5 \pm 11.6 \times 10^3$ CFU/g (mean $\pm$ standard deviation) for IIGP1$^{+/+}$ and IIGP1$^{-/-}$, respectively. The amount of bacteria in the liver was under the detection limit ($< 2 \times 10^2$) and the infection in this organ at day 3 p.i. was probably already cleared in all mice. Thus, the lack of IIGP1 does not affect resistance of mice against infection with *L. monocytogenes.*
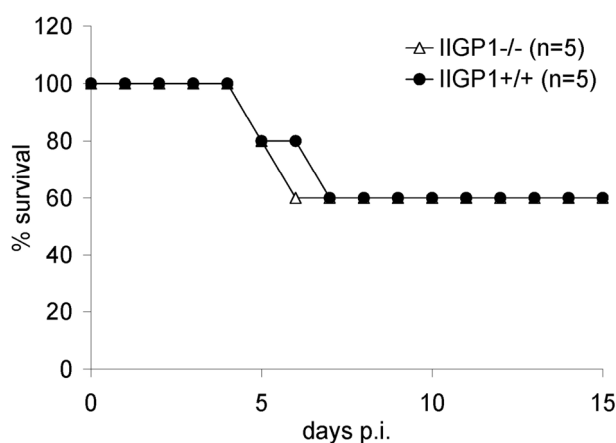

Figure 15: Survival of mice infected with *L. monocytogenes*

Mice were infected by i.p. injection of 10^4 CFU of *L. monocytogenes*, strain EDG, serotype 1/2a. The infectious dose equals to LD$_{50}$ for strain EDG in C57BL/6 mice. Animals were monitored daily for disease symptoms and time of death. The two experimental groups showed similar mortality rate.

3.6.7 IIGP1 deficient mice are resistant to infection with *Anaplasma phagocytophilum*

Anaplasma phagocytophilum is an obligate intracellular bacterium that is transmitted by ticks. It belongs to the order *Rickettsiales* and is recognized as the causative agent of human granulocytic anaplasmosis (HGA) [172]. Unique feature of *A. phagocytophilum* is its ability to replicate within the hostile environment of its host cell, the neutrophil. Resistance to *A. phagocytophilum* in mice is dependent on IFNγ [173, 174].

Groups of nine IIGP1$^{-/-}$ and C57BL/6 control mice were infected by i.p. injection of 100 µl blood from C.B17 SCID mice infected with *A. phagocytophilum* strain MRK; before the injection the infected blood was diluted 1:5 in PBS. Mice were sacrificed at day 3, 7 and 14 after infection and EDTA-anticoagulated blood, spleen and lung were collected from each animal. DNA was extracted from all samples and *A. phagocytophilum* was detected by a quantitative PCR assay. The amount of bacterial DNA was normalized to the amount of mouse genomic DNA in the probes by amplifying the mouse glucose-6-phosphate dehydrogenase gene (G6PDH). The

results are presented in Fig. 16 There was no significant difference in the bacterial load between the IIGP1^{-/-} and the control animals at any of the analyzed time points and at day 14 p.i. all mice had cleared the infection. Therefore, we concluded that IIGP1 deficiency does not influence resistance of mice to *A. phagocytophilum.*
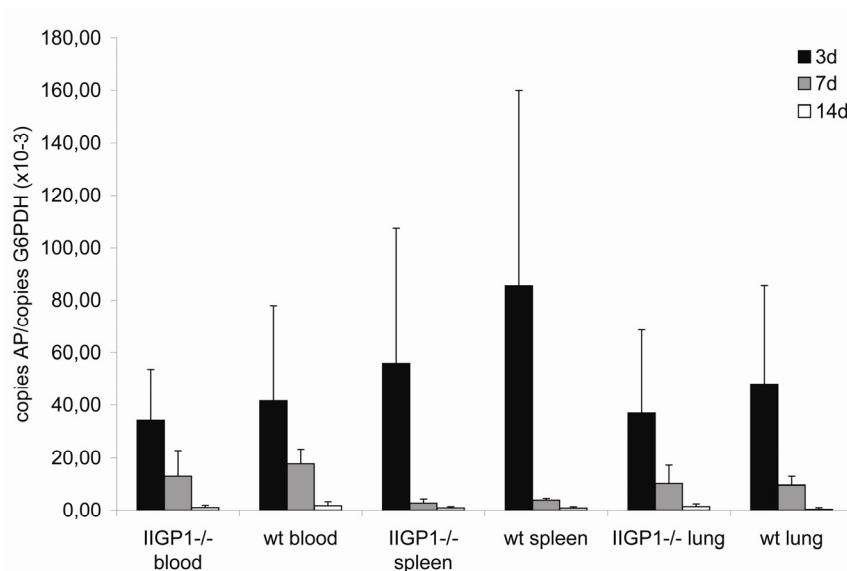
Figure 16: *A. phagocytophilum* load in organs of infected mice

Mice were infected by i.p. injection of 100 μl *A. phagocytophilum* strain MRK infected blood. and sacrificed at the indicated time points. DNA was extracted from blood, spleen and lung and *A. phagocytophilum* was detected by a quantitative PCR assay. The amount of bacterial DNA was normalized to the amount of mouse genomic DNA in the probes by amplifying the mG6PDH. Presented are the mean values and standard deviations from three animals. There is no significant difference in the bacterial load between both experimental groups of animals at any of the analyzed time points.

3.6.8 IIGP1 deficient mice are not susceptible to infection with Chlamydia trachomatis

C. trachomatis is an obligate intracellular bacterium that causes sexually transmitted diseases in humans. Infections with different serovars of the bacterium can lead to infectious blindness and infertility [175]. Resistance against *Chlamydia* depends on IFNγ [43, 44]. The protective mechanisms of IFNγ are not completely understood but it is well established that this cytokine controls the *in vitro* growth of *Chlamydia* by inducing the production of IDO and iNOS [176, 177]. However, IFNγ also plays a role in pathogenesis of *Chlamydia* by inducing persistence [40].

Groups of four IIGP1^{-/-} and control mice were infected by i.v.injection of 10^7 CFU of *C. trachomatis* L2. The control group consisted of two IIGP1^{+/-} and two

IIGP1^{+/+}animals. Mice were sacrificed at 29h p.i. and spleens were isolated form each animal. The amount of *C. trachomatis* in the samples was measured by Real-Time PCR assay by amplifying the *C. trachomatis* 16s gene. The amount of bacterial DNA was normalized to the amount of mouse genomic DNA in the probes by amplifying the mGAPDH gene. There was no significant difference in the bacterial load between the two experimental groups (Fig. 17). Thus, IIGP1 deficiency does not influence resistance of mice to *C. trachomatis*.
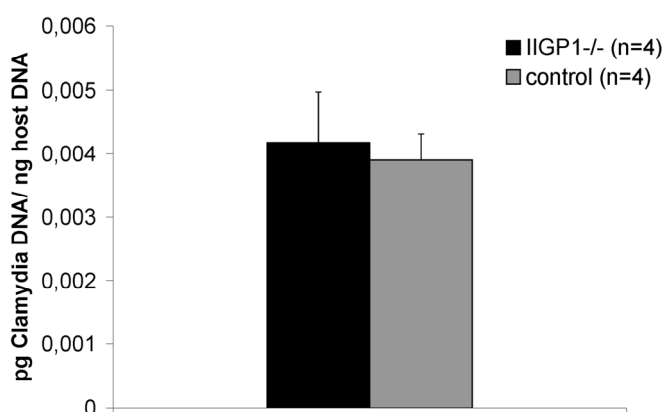
Figure 17: *C. trachomatis* load in spleens of infected mice
Mice were infected with 10^7 CFU of *C. trachomatis* L2 by i.v. injection. 29h p.i. spleens were isolated from each animal and the amount of *C. trachomatis* was measured by Real-Time PCR assay. The amount of bacterial DNA was normalized to the amount of mouse genomic DNA in the probes by amplifying the mG6PDH gene. No significant difference in the bacterial load between the two experimental groups was detected.

4 DISCUSSION

This thesis describes the initial attempt to reveal the role of the p47 GTPase IIGP1 in host defense against intracellular pathogens. The pathogens included in this study have developed different strategies of evading host defense mechanisms and surviving in the hostile environment of their host cell. The data presented will be discussed in the context of our current knowledge about these pathogens and the effect of the p47 GTPases on their survival in host cells.

The resistance against all pathogens included in this analysis has been shown to be critically dependent on IFNγ (Table 1). Our choice of pathogens was influenced initially by the high basal expression and inducibility of IIGP1 in the liver (Fig. 5b, c). The importance of the liver for innate and adaptive immunity is becoming increasingly appreciated [178, 179]. This organ is constantly exposed to a variety of pathogens, which enter the body through the gastrointestinal tract and is an important barrier against their further dissemination. A paradigmatic example for such a pathogen is the bacterium *L. monocytogenes.* The liver is also an initial homing organ for *Plasmodium spp.* sporozoites and provides a niche in which these pathogens replicate before spreading into the blood. The high liver basal expression of IIGP1, which we observed indicated that IIGP1 might provide resistance against liver-specific pathogens at a very early time point, probably even before other IFNγ-inducible factors are produced. The group of pathogens analyzed was later enlarged by including other intracellular pathogens from protozoan and bacterial origin and the data obtained formed our current view on the role of IIGP1 in host resistance.

4.1 IIGP1 is required for resistance against some intracellular protozoan parasites

In this study, we analyzed the effect of IIGP1 deficiency on mouse resistance against three intracellular protozoan parasites. *Toxoplasma gondii* and *Plasmodium berghei* belong to the same phylum, *Apicomplexa,* and have strikingly similar mechanisms of cell invasion and intracellular survival. The phylogenetically distant relative of the apicomplexans *Leishmania major* has a significantly different intracellular lifestyle.

4.1.1 IIGP1 and *Toxoplasma*

T. gondii is an obligate intracellular protozoan parasite with an extremely large host range. It can infect virtually all nucleated cells from a variety of vertebrate hosts [180]. The parasite utilizes a distinct form of actin/myosin-dependent movement, known as gliding motility, which facilitates dissemination throughout the host and active penetration of target cells [155, 181]. The process of cell invasion is very rapid (20-30 s) and does not involve the endocytic machinery of the host cell; it employs the actin cytoskeleton of the parasite but not of the host [182, 183]. The invasion process is facilitated by proteins secreted from specialized apical secretory organelles of the parasite, known as rhoptries and micronemes. During entry *T. gondii* squeezes through a moving junction, which is formed between the host cell plasma membrane and the parasite and controls internalization of host cell membrane components into the forming parasitophorous vacuole (PV) [157, 184]. The lipid components of the PV membrane (PVM) originate from the host cell plasma membrane (PM) [156] and flow freely past the moving junction during the formation of the PV [157]. In contrast, the moving junction selectively excludes many transmembrane (TM) proteins by a mechanism that is still unknown but depends on their membrane anchoring [157]. Subsequently, the PVM is extensively modified by secreted parasite proteins [185]. These remodeling processes render the PV completely non-fusogenic; it resists fusion with both endocytic and exocytic host cell vesicles. After invasion, the formed PV tightly associates with host cell endoplasmic reticulum and mitochondria [186]. The PV contains pores, which allow small molecules to diffuse through the membrane [187]. The PV thus provides *T. gondii* with an intracellular niche in which the parasite is supplied with nutrients and can multiply without being endangered by the host cell lysosomal compartment.

The p47 GTPases proved to be potent factors in host defense against *T. gondii* infection. All three proteins analyzed so far, LRG-47, IGTP and IRG-47 play distinct and non-redundant roles in resistance against this pathogen [121, 122]. IGTP and LRG-47 are required for resistance during the acute phase of infection, while IRG-47 is needed during the chronic phase. Furthermore, for normal resistance IGTP expression is required in both haematopoetic and non-haematopoetic cells [188] and the protein was shown to be an essential mediator of IFNγ-induced inhibition of *T. gondii* growth in astrocytes [154]. The same effect was observed in IGTP-deficient

macrophages [111]. However, the mechanisms through which these three proteins promote the IFNγ-induced *T. gondii* clearance are still unknown.

IIGP1 shows a markedly dynamic behavior in *T. gondii* infected astrocytes. In IFNγ-induced non-infected cells, the protein associates with the ER membrane [124]. Upon *T. gondii* infection, IIGP1 rapidly translocates to the PV and accumulates around it [134]. Already at 15 min p.i., IIGP1 associates with approximately 30% of the PVs; by 2 h p.i., this number increases to 75% and then begins to drop. The dynamic association of IIGP1 with the PV correlates with maturation of the PVs, disintegration of the PVM and damage of the parasite PM [134]. Furthermore, overexpression of IIGP1 leads to accelerated maturation and disintegration of the PVs, while the expression of a dominant negative mutant of IIGP1 (K82A) partially inhibits the *T. gondii* killing by IFNγ stimulated astrocytes [134]. All these observations pointed to a potential role of IIGP1 in IFNγ-dependent *T. gondii* in astrocytes.

Our analysis of *T. gondii* growth in IFNγ-induced IIGP1$^{-/-}$ astrocytes did indeed show a partial loss of resistance to the parasite (Fig. 10c, d). The effect of IIGP1 deficiency on the inhibitory capacity of astrocytes differed from the one showed for IGTP [154]. This study reported an uncontrollable growth of *T. gondii* in IFNγ stimulated IGTP$^{-/-}$ astrocytes at MOI 5. In our system we could not use such a high MOI because already at MOI 3 the infection could not be controlled even by the IFNγ-induced IIGP1$^{+/+}$ cells. This is possibly due to the different genetic background of the astrocytes; we used C57BL/6 cells, while the astrocytes used by Halonen et al. were derived from mice with a mixed C57BL/6x129Sv background. We observed a loss of resistance to *T. gondii* at lower MOI and the effect was smaller than the one reported for IGTP. The latter suggests that IIGP1 might be partially redundant with other IFNγ-inducible resistant factors at least in the inhibition of *T. gondii* growth in mouse astrocytes. In addition to IIGP1, four other p47 GTPases associate with *T. gondii* PVs after infection; this association is very pronounced for TGTP1, GTPI and IRG47 but not so strong for IGTP ([134] and Fig. 11c, d). Furthermore, here we showed that TGTP1 and IGTP accumulated at the PV in IIGP1$^{-/-}$ astrocytes in a manner at least qualitatively indistinguishable from the one in IIGP1$^{+/+}$ cells (Fig. 11a, b). Thus, their association with the PV does not depend on IIGP1. Preliminary data suggests a similar PV associaton dynamics of GTPI and IRG-47 in IIGP1$^{-/-}$ and IIGP1$^{+/+}$ astrocytes. It is therefore possible that one or more of these p47 GTPases could at

least partly take over the defense function of IIGP1 and compensate the effect of the lack of this molecule in the IIGP1$^{-/-}$ astrocytes.

It is still unclear whether IIGP1 recognizes the PVs directly or is recruited to the PVM by another factor. It is however evident that the recruitment of IIGP1 to the PV is stimulated by active invasion because the protein does not associate with phagosomes formed upon internalization of heat-killed parasites [134]. The mechanism used by IIGP1 to promote disintegration of the PV is still unknown but there are already hints that at least some of the biochemical properties of the protein could be critical for this process. Intact GTP-binding is important for both association with the PV and subsequent disruption of this vacuole because the IIGP1K82A dominant negative mutant, which is deficient in GTP-binding, does not translocate to the PV and partially inhibits *T. gondii* killing in astrocytes [134]. It has been suggested that the N-terminal myristoylation of IIGP1 could facilitate disruption of the PVM by introducing positive curvature into this membrane and thus causing its vesiculation [134]. Future experiments employing transfection of IIGP1 mutants into IIGP1-deficient cells will show whether other properties of the protein such as GTP hydrolysis and GTP-dependant oligomerization also play a role in the process of IIGP1-promoted PV disintegration.

The results from the *T. gondii* infections in mice are not yet conclusive. All IIGP1$^{+/+}$ animals infected with both *T. gondii* avirulent strains used in the presented experiments (DX and Me49) survived until week 8 p.i., while one IIGP1$^{-/-}$ mouse died in each experiment during the acute phase. The brain cyst burden at the end of week 8 p.i. was increased in only one IIGP1$^{-/-}$ and one IIGP1$^{+/-}$ mouse, while the remaining animals had similar cyst numbers (Fig. 12). These results are difficult to interpret because the number of animals used in the two experiments was not big enough to allow registering of small effects on parasite burden or mouse survival. An experiment in a larger scale might show an increased cyst burden in some of the IIGP1$^{-/-}$ mice, which would be in agreement with the promoted growth of *T. gondii* tachyzoites in IIGP1$^{-/-}$ astrocytes. Such an increased parasite burden might in turn lead to increased mortality of the IIGP1$^{-/-}$ animals at a time point later than the end of week 8 p.i. The latter however indicates that we might have to infect IIGP1 deficient animals from a different genetic background. C57BL/6 mice are generally susceptible to infection with *T. gondii.* These animals start loosing weight during the chronic phase of infection and die earlier than other mouse strains, usually around week 8 to 9

p.i. It is therefore possible that the small difference in survival, which we expect, would be undetectable in the C57BL/6 strain.

4.1.2   IIGP1 and *Plasmodium*

The causative agents of malaria, the *Plasmodium spp.* parasites, also belong to the phylum *Apicomplexa*. Despite having a host range restricted to only two types of host cells, hepatocytes and erythrocytes, the *Plasmodium* parasites share the basic invasion features and intracellular life-style with *Toxoplasma*. Like *Toxoplasma, Plasmodium* extensively migrates through the host utilizing an actin-dependent gliding motility [189]. Host cell invasion is also an active process; however, during parasite entry into erythrocytes, additional signaling through host β_2-adenergic receptors is required for successful penetration [190]. During entry into hepatocytes and erythrocytes, the two invasive forms of *Plasmodium* (sporozoites and merozoites) form PVs. The process of PV formation is very similar to that of *Toxoplasma* [185]. It starts with the formation of a moving junction and is accompanied by selective exclusion of most host cell TM proteins [191, 192], while the PVM lipids are largely derived from the PM of the host cell [193, 194]. However, the biological functions of the PVM differ in hepatocytes and erythrocytes due to the specific features of these two types of host cells. Hepatocytes are nucleated cells with complete biosynthetic machinery and therefore the function of the PVM in these cells is very similar to that of *Toxoplasma* PVM; it resists fusion to endosomes and lysosomes and provides the parasite with essential nutrients. Erythrocytes however lack a nucleus and are incapable of protein, nucleic acid or lipid synthesis, as well as endocytosis. Therefore, many molecules essential for the parasite development have to be obtained from outside the host cell. In infected erythrocytes, the PVM extends into the host cytosol as a network of so-called tubovesicular membranes (TVM). The TVM is believed to be an intracellular transport system, which forms junctions with the erythrocyte membrane and facilitates import of specific nutrients [195].

The similarity in the intracellular life-style of the two apicomplexan parasites used in this study suggests that the model of IIGP1-dependent killing of *Toxoplasma* in astrocytes [134] could also be relevant for defense against at least the hepatocyte invasive stage of *Plasmodium.* IIGP1 has high basal expression in primary hepatocytes (Fig. 6b) and accumulates at the PVs after infection of these cells with *T. gondii* (Jia Zeng, personal communication). It is therefore possible that in hepatocytes

IIGP1 associates also with the PVs formed during the invasion of *Plasmodium* sporozoites and facilitates their disintegration and the killing of the parasites. Such a model underlines the possibility for an important role of the basal expression of IIGP1 in early defense against malaria. The sporozoites, which enter the body with the mosquito bite, are transported with the blood stream and rapidly reach the liver, within 2 min after the bite. Once in the liver, the parasites breach through a few hepatocytes and stop in a final cell, which they enter by forming a PV [196]. IIGP1, which is already synthesized in these cells, might facilitate the killing of the parasites very early after invasion, before the IFNγ response is stimulated and fully functional. If IIGP1 is indeed required for the killing of the sporozoites in the liver, then the lack of this protein in the IIGP1 deficient animals could lead to increased survival of the sporozoites in this organ followed by a release of more merozoites in the blood after the end of the liver stage and a higher blood parasitemia. This might be the reason for the observed higher incidence of cerebral malaria (CM) in these animals (Fig. 13b, c) because the risk of developing CM correlates with the level of parasitemia, at least in humans [197]. The possible role of IIGP1 in defense of hepatocytes against sporozoites remains to be explored.

At the present stage of this analysis, we cannot exclude the possibility that IIGP1 deficiency could also influence the blood stage of malaria. The difference in survival of IIGP1$^{-/-}$ and IIGP1$^{+/+}$ animals, which we observed after erythrocyte infection is small (Fig. 13a). However, an experiment in a larger scale might render this difference significant. The IIGP1-dependent disintegration of the PV as discussed above is not applicable for the malaria blood stage because the infected erythrocytes are not capable of protein synthesis. However, the infected erythrocytes move with the blood stream and pass through the spleen, which was shown to be very important for defense against the disease [198]. The spleen plays a major role in generation of antimalarial immunity but also is largely responsible for removal of parasitized erythrocytes from the blood probably through the resident macrophages of the red pulp [199, 200]. IIGP1 synthesized in the spleen might facilitate the process of parasite clearance and thus influence the blood stage of malaria. Conversely, the lack of IIGP1 then might lead to decreased parasite clearance, higher parasitemia and increased incidence of CM.

Our hypothesis for increased parasite survival leading to higher parasitemia is only one possible explanation for the observed higher mortality of IIGP1-deficient animals.

Alternatively, IIGP1 deficiency might influence the vascular pathology and brain inflammation associated with development of CM. Pathogenesis of CM is a very complex process the underlying mechanisms of which despite extensive analysis are still largely unclear [164]. It is however evident that the brain vascular pathology associated with CM is mediated by pro-inflammatory cytokines, mainly TNF family members and IFNγ. So far, we did not analyze the effect of IIGP1 deficiency on the brain cytokine profile following infection. However, the existence of such an effect seems unlikely because cytokine production is not affected in the available p47 GTPase-deficient mice. Nevertheless, the development of CM-associated brain pathology in IIGP1 deficient mice remains to be studied in detail.

4.1.3 IIGP1 and *Leishmania*

Leishmania is also a protozoan parasite but the mechanisms it utilizes to infect and exploit host cells are very different from the ones used by the apicomplexians. *Leishmania* is not capable of entering cells actively and therefore infects exclusively professional phagocytes, mainly macrophages, with the exception of fibroblasts, DCs and neutrophils [201]. The parasites are taken up by macrophages via conventional receptor-mediated phagocytosis facilitated by the opsonization of the parasites [202, 203]. In contrast to the apicomplexian parasites *Leshmania* amastigotes do not modify the phagosome and it rapidly (within 30 minutes) fuses with late endosomes or lysosomes [204] thus generating a PV that maintains low pH and intact hydrolytic activity. Promastigotes, which are considered more sensitive to acid, seem to delay phagosomal maturation until they have differentiated into amastigotes; when this transformation has occured, the block on phagosomal maturation is lifted and the amastigotes multiply in the formed acidic PV.

Our experiments showed similar disease onset in all *L. major* infected mice regardless of their genotype for both infectious doses (Fig. 14). We therefore concluded that IIGP1 is not required for host defense against *L. major* infection. In contrast to IIGP1-, LRG-47- and IGTP-deficient mice were both found to be acutely susceptible to *L. major* developing lesions and increased parasite burdens [111]. The mechanisms by which these two p47 GTPases protect mice from *L. major* are however still unknown.

Our analysis of the role of IIGP1 in resistance against intracellular protozoan parasites shows an important trend. IIGP1 is involved in resistance against two apicomplexan

parasites, which extensively modify their PVs and survive in cells by inhibiting fusion of the PV with lysosomes; in contrast, IIGP1 is dispensable in defense against *Leishmania*, which does not modify the PV and delays but does not completely block its fusion with lysosomes. This observation suggests that IIGP1 is probably involved specifically in cellular defense against apicomplexan parasites residing in non-fusogenic PVs.

4.2 IIGP1 seems not to be required for defense against intracellular bacteria

In this study, we analyzed the influence of the IIGP1 deficiency on mouse resistance against three intracellular pathogenic bacteria, *Listeria monocytogenes, Chlamydia trachomatis* and *Anaplasma phagocytophilum.* These pathogens differ in the mechanisms they utilize to invade host cells and to facilitate their intracellular survival and replication.

L. monocytogenes employs a cell entry strategy used by a variety of invasive bacteria [205]. It actively induces its own uptake in normally non-phagocytic cells by means of surface proteins, which are known as internalins and mimic the ligands of host cell receptors [206]. Binding of *L. monocytogenes* to these receptors induces the uptake of the bacterium by phagocytosis. After the invasion, *L. monocytogenes* escapes destruction in the host cell endocytic pathway by a rapid (within 30 min) lysis of the phagosome and escape in the cytoplasm. This process is facilitated by a pore-forming bacterial toxin called listeriolysin-O (LLO) [207] or in some cells by bacterial phospholipases [208]. *Listeria* replicates in the cytoplasm and spreads to neighboring cells by an actin-based motility process enabled by the polar expression of an actin-assembly inducing protein, ActA [209, 210]. When *Listeria* reaches the PM, it induces the formation of a protrusion, which is endocytosed by a neighboring cell and leads to a formation of a two-membrane vacuole that in turn is lysed and releases the bacterium it the cytoplasm. Thus, *Listeria* directly spreads from cell to cell and escapes the immune response of the host.

A. phagocytophilum has a unique choice of host cells, it replicates in the hostile environment of neutophils. The bacterium enters neutrophils by phagocytosis and replicates in a phagosome, which completely resists fusion with early and late

endosomes and lysosomes [211]. Furthermore, *A. phagocytophilum* inhibits the NADPH oxidase thus blocking the neutrophil oxidative burst. *A. phagocytophilum* was also shown to delay neutrophil apoptosis thus ensuring itself enough time for replication in these normally short-lived cells.

Chlamydia is also an invasive bacterium but unlike *Listeria* it enters non-phagocytic cells by a process similar to macropinocytosis, which is facilitated by the type III secretion system of the bacterium [212]. The infectious and metabolically inactive form of *Clamydia*, the elementary body (EB), is taken up by mucosal epithelial cells. Upon entry, it forms a unique vacuole, known as inclusion [213, 214]. Like the protozoan PVs, the inclusion blocks fusion with endosomes and lysosomes. However, the *Chlamydia* inclusion is not completely non-fusogenic. Once formed, it is extensively modified by bacterial proteins and this modification process initiates fusion with exocytic vacuoles [215]. The inclusion thus acquires massive amounts of membrane and eventually grows to occupy a significant fraction of the cell. Inside the giant inclusion, the EB transforms into a metabolically active reticulate body (RB), which replicates by binary division. 40-48 hrs after cell invasion the RBs transform into infective EBs, which are released from the inclusion vacuole and infect neighboring cells.

Our analysis showed that IIGP1 is not required for resistance against any of these three intracellular bacterial pathogens. All mice infected with *L. monocytogenes* survived the infection regardless of their genotype. Furthermore, at day 3 p.i. they showed similar bacterial burden in the spleen, while the infection in the liver was already cleared. The infection with *A. phagocytophilum* also showed no difference between IIGP1-deficient and control animals. All mice had similar bacterial burden in spleen, lung and blood at day 3, 7 and 14 p.i. (Fig. 16). All mice infected with *Chlamydia* also had no significant differences in bacterial burden in spleen at 29h p.i. (Fig. 17).

From the members of the p47 GTPase family analyzed so far only LRG-47 was implicated in resistance against bacteria, while IGTP and IRG-47 were shown to be dispensable [111]. LRG-47 has a large antibacterial spectrum including bacteria utilizing different cell entry and intracellular survival strategies. LRG-47 deficient mice are profoundly susceptible to *L. monocytogenes*, *Salmonella typhimurium*, *Mycobacterium tuberculosis* and *Mycobacterium avium* [111, 121, 123]. *Mycobacterium* enters macrophages by phagocytosis and avoids destruction by

blocking fusion of the phagosome with lysosomes. LRG-47 protects macrophages from *M. tuberculosis* by promoting phagosomal acidification and maturation [123]. How LRG-47 counteracts *L. monocytogenes* is still unknown but it was hypothesized that this protein might be involved in the recruitment of the small GTPase Rab5a to *Listeria*-containing vacuoles and thus facilitate bacterial killing by the already established Rab5a-dependent mechanism [216, 217]. *S. typhimurium* does not enter cells by phagocytosis but induces its uptake by a type III secretion system; the formed *Salmonella*-containing vacuole recruits some early and late endosomal markers, acidifies but lacks functional hydrolases. It is possible that LRG-47 counteracts some of the bacterial proteins secreted into the cell by the type III secretion system of *Salmonella* by modulating the function of host cell microtubule associated proteins [216]. LRG-47 is recruited very early to the forming phagocytic cups and stays associated with the phagosomes throughout their maturation pathway [124]. The protein probably marks the phagosomes for rapid maturation thus counteracting the bacterial strategies of escape and maturation arrest. This would explain why LRG-47 is an essential mediator in resistance against various bacteria entering cells by phagocytosis, despite the differences in the evasion mechanisms they could further employ to ensure intracellular survival and replication. In contrast to LRG-47, IIGP1 is not recruited to phagosomes formed after uptake of latex beads [124] indicating that the protein is probably not required for defense against bacteria invading cells by phagocytosis. The lack of susceptibility of the IIGP1 deficient mice to *Listeria* and *Anaplasma* demonstrated in the present study confirms this hypothesis. The here reported resistance of IIGP1 deficient mice to *Chlamydia* together with the observed lack of association of IIGP1 with *Salmonella*-containing vacuoles [126] implicate that the protein is probably dispensable also in defense against bacteria that invade cells by means of type III secretion systems and reside in pathogen-specific vacuoles. Our analysis of the role of IIGP1 in defense against intracellular bacteria is still far from being complete. However, the bacterial pathogens that we used employ diverse cell entry and intracellular survival strategies and IIGP1 seems not to counteract any of these processes. Therefore, the obtained data allows us to hypothesize that IIGP1, like IGTP and IRG-47 might not be required for defense against intracellular bacteria. This hypothesis has to be further proven by challenging the IIGP1 deficient mice with other bacterial pathogens and analysis of the behavior of the protein in infected cells.

The here discussed data allow us to propose a model for the role of IIGP1 in intracellular defense and the place of this protein among the other p47 GTPases. The effect of IIGP1 deficiency on survival of mice following infection is not as profound as the ones reported for the other p47 GTPases, which might be due to a partial functional redundancy, possibly within the family itself. Compared to LRG-47, which is effective against a variety of pathogens, IIGP1 has a more restricted antipathogenic spectrum; in this respect, it is more similar to IGTP and IRG-47. IIGP1 seems to be specifically involved in defense against protozoan parasites residing in non-fusigenic PVs, a function, which it shares with the other family members. Unlike LRG-47, IIGP1 is dispensable for resistance against pathogens entering cells by phagocytosis. Furthermore, this does not seem to depend on the origin of the pathogen because IIGP1 deficiency does not affect both bacteria and protozoa, which invade cells by phagocytosis. Although still not proven, it is possible that like IGTP and IRG-47, IIGP1 is not involved in defense against intracellular bacteria. The role of IIGP1 in defense against viruses remains to be analyzed.

5 REFERENCES

1. Roy, B.A. and J.W. Kirchner, *Evolutionary dynamics of pathogen resistance and tolerance.* Evolution Int J Org Evolution, 2000. **54**(1): p. 51-63.

2. van Baalen, M., *Coevolution of recovery ability and virulence.* Proc R Soc Lond B Biol Sci, 1998. **265**(1393): p. 317-25.

3. Tortorella, D., et al., *Viral subversion of the immune system.* Annu Rev Immunol, 2000. **18**: p. 861-926.

4. Sacks, D. and A. Sher, *Evasion of innate immunity by parasitic protozoa.* Nat Immunol, 2002. **3**(11): p. 1041-7.

5. Gruenheid, S. and B.B. Finlay, *Microbial pathogenesis and cytoskeletal function.* Nature, 2003. **422**(6933): p. 775-81.

6. Gao, L.Y. and Y.A. Kwaik, *The modulation of host cell apoptosis by intracellular bacterial pathogens.* Trends Microbiol, 2000. **8**(7): p. 306-13.

7. Hornef, M.W., et al., *Bacterial strategies for overcoming host innate and adaptive immune responses.* Nat Immunol, 2002. **3**(11): p. 1033-40.

8. Coombes, B.K., Y. Valdez, and B.B. Finlay, *Evasive maneuvers by secreted bacterial proteins to avoid innate immune responses.* Curr Biol, 2004. **14**(19): p. R856-67.

9. Janeway, C.A., Jr. and R. Medzhitov, *Innate immune recognition.* Annu Rev Immunol, 2002. **20**: p. 197-216.

10. Kaisho, T. and S. Akira, *Pleiotropic function of Toll-like receptors.* Microbes Infect, 2004. **6**(15): p. 1388-94.

11. Pearson, A.M., *Scavenger receptors in innate immunity.* Curr Opin Immunol, 1996. **8**(1): p. 20-8.

12. Inohara, N. and G. Nunez, *NODs: intracellular proteins involved in inflammation and apoptosis.* Nat Rev Immunol, 2003. **3**(5): p. 371-82.

13. Clemens, M.J. and A. Elia, *The double-stranded RNA-dependent protein kinase PKR: structure and function.* J Interferon Cytokine Res, 1997. **17**(9): p. 503-24.

14. Kumar, M. and G.G. Carmichael, *Antisense RNA: function and fate of duplex RNA in cells of higher eukaryotes.* Microbiol Mol Biol Rev, 1998. **62**(4): p. 1415-34.

15. Fraser, I.P., H. Koziel, and R.A. Ezekowitz, *The serum mannose-binding protein and the macrophage mannose receptor are pattern recognition*

molecules that link innate and adaptive immunity. Semin Immunol, 1998. **10**(5): p. 363-72.

16.   Gewurz, H., et al., *C-reactive protein and the acute phase response.* Adv Intern Med, 1982. **27**: p. 345-72.

17.   Lehrer, R.I., *Primate defensins.* Nat Rev Microbiol, 2004. **2**(9): p. 727-38.

18.   Zasloff, M., *Antimicrobial peptides of multicellular organisms.* Nature, 2002. **415**(6870): p. 389-95.

19.   Molina, H., *Complement and immunity.* Rheum Dis Clin North Am, 2004. **30**(1): p. 1-18, v.

20.   Guidotti, L.G. and F.V. Chisari, *Noncytolytic control of viral infections by the innate and adaptive immune response.* Annu Rev Immunol, 2001. **19**: p. 65-91.

21.   Isaacs, A. and J. Lindenmann, *Virus interference. I. The interferon.* Proc R Soc Lond B Biol Sci, 1957. **147**(927): p. 258-67.

22.   van Pesch, V., et al., *Characterization of the murine alpha interferon gene family.* J Virol, 2004. **78**(15): p. 8219-28.

23.   Pestka, S., C.D. Krause, and M.R. Walter, *Interferons, interferon-like cytokines, and their receptors.* Immunol Rev, 2004. **202**: p. 8-32.

24.   Mogensen, K.E., et al., *The type I interferon receptor: structure, function, and evolution of a family business.* J Interferon Cytokine Res, 1999. **19**(10): p. 1069-98.

25.   LaFleur, D.W., et al., *Interferon-kappa, a novel type I interferon expressed in human keratinocytes.* J Biol Chem, 2001. **276**(43): p. 39765-71.

26.   Conklin, D., et al., *Interferon-epsilon.* U.S. patent 6,329,175, 2001.

27.   Roberts, R.M., J.C. Cross, and D.W. Leaman, *Unique features of the trophoblast interferons.* Pharmacol Ther, 1991. **51**(3): p. 329-45.

28.   Oritani, K., et al., *Limitin: An interferon-like cytokine that preferentially influences B-lymphocyte precursors.* Nat Med, 2000. **6**(6): p. 659-66.

29.   Lefevre, F., et al., *Interferon-delta: the first member of a novel type I interferon family.* Biochimie, 1998. **80**(8-9): p. 779-88.

30.   Hauptmann, R. and P. Swetly, *A novel class of human type I interferons.* Nucleic Acids Res, 1985. **13**(13): p. 4739-49.

31.   Kotenko, S.V., et al., *IFN-lambdas mediate antiviral protection through a distinct class II cytokine receptor complex.* Nat Immunol, 2003. **4**(1): p. 69-77.

32. Sheppard, P., et al., *IL-28, IL-29 and their class II cytokine receptor IL-28R.* Nat Immunol, 2003. **4**(1): p. 63-8.

33. Young, H.A., *Regulation of interferon-gamma gene expression.* J Interferon Cytokine Res, 1996. **16**(8): p. 563-8.

34. Darnell, J.E., Jr., I.M. Kerr, and G.R. Stark, *Jak-STAT pathways and transcriptional activation in response to IFNs and other extracellular signaling proteins.* Science, 1994. **264**(5164): p. 1415-21.

35. Boehm, U., et al., *Cellular responses to interferon-gamma.* Annu Rev Immunol, 1997. **15**: p. 749-95.

36. Stark, G.R., et al., *How cells respond to interferons.* Annu Rev Biochem, 1998. **67**: p. 227-64.

37. Klamp, T., et al., *A list of genes regulated by IFN-γ (http://www.annurev.org/sup/material.htm).* 1997.

38. Ehrt, S., et al., *Reprogramming of the macrophage transcriptome in response to interferon-gamma and Mycobacterium tuberculosis: signaling roles of nitric oxide synthase-2 and phagocyte oxidase.* J Exp Med, 2001. **194**(8): p. 1123-40.

39. Smythies, L.E., et al., *Helicobacter pylori-induced mucosal inflammation is Th1 mediated and exacerbated in IL-4, but not IFN-gamma, gene-deficient mice.* J Immunol, 2000. **165**(2): p. 1022-9.

40. Rottenberg, M.E., A. Gigliotti-Rothfuchs, and H. Wigzell, *The role of IFN-gamma in the outcome of chlamydial infection.* Curr Opin Immunol, 2002. **14**(4): p. 444-51.

41. Dalton, D.K., et al., *Multiple defects of immune cell function in mice with disrupted interferon-γ genes [see comments].* Science, 1993. **259**(5102): p. 1739-42.

42. Flynn, J.L., et al., *An essential role for interferon gamma in resistance to Mycobacterium tuberculosis infection.* J Exp Med, 1993. **178**(6): p. 2249-54.

43. Johansson, M., et al., *Genital tract infection with Chlamydia trachomatis fails to induce protective immunity in gamma interferon receptor-deficient mice despite a strong local immunoglobulin A response.* Infect Immun, 1997. **65**(3): p. 1032-44.

44. Wang, S., et al., *IFN-gamma knockout mice show Th2-associated delayed-type hypersensitivity and the inflammatory cells fail to localize and control chlamydial infection.* Eur J Immunol, 1999. **29**(11): p. 3782-92.

45. Mastroeni, P., et al., *Interleukin 18 contributes to host resistance and gamma interferon production in mice infected with virulent Salmonella typhimurium.* Infect Immun, 1999. **67**(2): p. 478-83.

46.   Hess, J., et al., *Salmonella typhimurium aroA- infection in gene-targeted immunodeficient mice: major role of CD4+ TCR-alpha beta cells and IFN-gamma in bacterial clearance independent of intracellular location.* J Immunol, 1996. **156**(9): p. 3321-6.

47.   Huang, S., et al., *Immune response in mice that lack the interferon-gamma receptor.* Science, 1993. **259**(5102): p. 1742-5.

48.   Lu, B., et al., *Targeted disruption of the interferon-gamma receptor 2 gene results in severe immune defects in mice.* Proc Natl Acad Sci U S A, 1998. **95**(14): p. 8233-8.

49.   Meraz, M.A., et al., *Targeted disruption of the Stat1 gene in mice reveals unexpected physiologic specificity in the JAK-STAT signaling pathway.* Cell, 1996. **84**(3): p. 431-42.

50.   Harty, J.T. and M.J. Bevan, *Specific immunity to Listeria monocytogenes in the absence of IFN gamma.* Immunity, 1995. **3**(1): p. 109-17.

51.   Way, S.S., et al., *An essential role for gamma interferon in innate resistance to Shigella flexneri infection.* Infect Immun, 1998. **66**(4): p. 1342-8.

52.   Bohn, E., et al., *Ambiguous role of interleukin-12 in Yersinia enterocolitica infection in susceptible and resistant mouse strains.* Infect Immun, 1998. **66**(5): p. 2213-20.

53.   Shinozawa, Y., et al., *Role of interferon-gamma in inflammatory responses in murine respiratory infection with Legionella pneumophila.* J Med Microbiol, 2002. **51**(3): p. 225-30.

54.   Mahon, B.P., et al., *Atypical disease after Bordetella pertussis respiratory infection of mice with targeted disruptions of interferon-gamma receptor or immunoglobulin mu chain genes.* J Exp Med, 1997. **186**(11): p. 1843-51.

55.   Scharton-Kersten, T.M., et al., *In the absence of endogenous IFN-gamma, mice develop unimpaired IL-12 responses to Toxoplasma gondii while failing to control acute infection.* J Immunol, 1996. **157**(9): p. 4045-54.

56.   Tsuji, M., et al., *Development of antimalaria immunity in mice lacking IFN-gamma receptor.* J Immunol, 1995. **154**(10): p. 5338-44.

57.   Aliberti, J.C., et al., *Modulation of chemokine production and inflammatory responses in interferon-gamma- and tumor necrosis factor-R1-deficient mice during Trypanosoma cruzi infection.* Am J Pathol, 2001. **158**(4): p. 1433-40.

58.   Wang, Z.E., et al., *CD4+ effector cells default to the Th2 pathway in interferon gamma-deficient mice infected with Leishmania major.* J Exp Med, 1994. **179**(4): p. 1367-71.

59.   Swihart, K., et al., *Mice from a genetically resistant background lacking the interferon gamma receptor are susceptible to infection with Leishmania major*

but mount a polarized T helper cell 1-type CD4+ T cell response. J Exp Med, 1995. **181**(3): p. 961-71.

60.   Cantin, E., B. Tanamachi, and H. Openshaw, *Role for gamma interferon in control of herpes simplex virus type 1 reactivation.* J Virol, 1999. **73**(4): p. 3418-23.

61.   Nansen, A., et al., *Compromised virus control and augmented perforin-mediated immunopathology in IFN-gamma-deficient mice infected with lymphocytic choriomeningitis virus.* J Immunol, 1999. **163**(11): p. 6114-22.

62.   Presti, R.M., et al., *Interferon gamma regulates acute and latent murine cytomegalovirus infection and chronic disease of the great vessels.* J Exp Med, 1998. **188**(3): p. 577-88.

63.   Meurs, E.F., et al., *Constitutive expression of human double-stranded RNA-activated p68 kinase in murine cells mediates phosphorylation of eukaryotic initiation factor 2 and partial resistance to encephalomyocarditis virus growth.* J Virol, 1992. **66**(10): p. 5805-14.

64.   Lee, S.B. and M. Esteban, *The interferon-induced double-stranded RNA-activated human p68 protein kinase inhibits the replication of vaccinia virus.* Virology, 1993. **193**(2): p. 1037-41.

65.   Chebath, J., et al., *Constitutive expression of (2'-5') oligo A synthetase confers resistance to picornavirus infection.* Nature, 1987. **330**(6148): p. 587-8.

66.   Samuel, C.E., *Antiviral Actions of Interferons.* Clin. Microbiol. Rev., 2001. **14**(4): p. 778-809.

67.   MacMicking, J., Q.W. Xie, and C. Nathan, *Nitric oxide and macrophage function.* Annu Rev Immunol, 1997. **15**: p. 323-50.

68.   Turco, J., et al., *Nitric Oxide-Mediated Inhibition of the Ability of Rickettsia prowazekii To Infect Mouse Fibroblasts and Mouse Macrophagelike Cells.* Infect. Immun., 1998. **66**(2): p. 558-566.

69.   Nussler, A.K. and T.R. Billiar, *Inflammation, immunoregulation, and inducible nitric oxide synthase.* J Leukoc Biol, 1993. **54**(2): p. 171-8.

70.   Bodaghi, B., et al., *Role of IFN-{gamma}-Induced Indoleamine 2,3 Dioxygenase and Inducible Nitric Oxide Synthase in the Replication of Human Cytomegalovirus in Retinal Pigment Epithelial Cells.* J Immunol, 1999. **162**(2): p. 957-964.

71.   Pantoja, L.G., et al., *Inhibition of Chlamydia pneumoniae Replication in Human Aortic Smooth Muscle Cells by Gamma Interferon-Induced Indoleamine 2,3-Dioxygenase Activity.* Infect. Immun., 2000. **68**(11): p. 6478-6481.

72.   Pfefferkorn, E.R., *Interferon gamma blocks the growth of Toxoplasma gondii in human fibroblasts by inducing the host cells to degrade tryptophan.* Proc Natl Acad Sci U S A, 1984. **81**(3): p. 908-12.

73.   Jackson, S., J. Gallin, and S. Holland, *The p47phox mouse knock-out model of chronic granulomatous disease.* J. Exp. Med., 1995. **182**(3): p. 751-758.

74.   Jayan, G.C. and J.L. Casey, *Increased RNA Editing and Inhibition of Hepatitis Delta Virus Replication by High-Level Expression of ADAR1 and ADAR2.* J. Virol., 2002. **76**(8): p. 3819-3827.

75.   Espert, L., et al., *ISG20, a New Interferon-induced RNase Specific for Single-stranded RNA, Defines an Alternative Antiviral Pathway against RNA Genomic Viruses.* J. Biol. Chem., 2003. **278**(18): p. 16151-16158.

76.   Gao, G., X. Guo, and S.P. Goff, *Inhibition of Retroviral RNA Production by ZAP, a CCCH-Type Zinc Finger Protein.* Science, 2002. **297**(5587): p. 1703-1706.

77.   Stremlau, M., et al., *The cytoplasmic body component TRIM5alpha restricts HIV-1 infection in Old World monkeys.* Nature, 2004. **427**(6977): p. 848-53.

78.   Lindenmann, J., C.A. Lane, and D. Hobson, *The Resistance of A2g Mice to Myxoviruses.* J Immunol, 1963. **90**: p. 942-51.

79.   Staeheli, P., et al., *Interferon-regulated influenza virus resistance gene Mx is localized on mouse chromosome 16.* J Virol, 1986. **58**(3): p. 967-9.

80.   Staeheli, P., et al., *Mx protein: constitutive expression in 3T3 cells transformed with cloned Mx cDNA confers selective resistance to influenza virus.* Cell, 1986. **44**(1): p. 147-58.

81.   Staeheli, P. and J.G. Sutcliffe, *Identification of a second interferon-regulated murine Mx gene.* Mol Cell Biol, 1988. **8**(10): p. 4524-8.

82.   Staeheli, P. and O. Haller, *Interferon-induced human protein with homology to protein Mx of influenza virus-resistant mice.* Mol Cell Biol, 1985. **5**(8): p. 2150-3.

83.   Aebi, M., et al., *cDNA structures and regulation of two interferon-induced human Mx proteins.* Mol Cell Biol, 1989. **9**(11): p. 5062-72.

84.   Pavlovic, J., et al., *Resistance to influenza virus and vesicular stomatitis virus conferred by expression of human MxA protein.* J Virol, 1990. **64**(7): p. 3370-5.

85.   Gordien, E., et al., *Inhibition of hepatitis B virus replication by the interferon-inducible MxA protein.* J Virol, 2001. **75**(6): p. 2684-91.

86.   Andersson, I., et al., *Human MxA protein inhibits the replication of Crimean-Congo hemorrhagic fever virus.* J Virol, 2004. **78**(8): p. 4323-9.

87. Frese, M., et al., *Inhibition of bunyaviruses, phleboviruses, and hantaviruses by human MxA protein.* J Virol, 1996. **70**(2): p. 915-23.

88. Staeheli, P., et al., *Influenza virus-susceptible mice carry Mx genes with a large deletion or a nonsense mutation.* Mol Cell Biol, 1988. **8**(10): p. 4518-23.

89. Haller, O., et al., *Genetically determined, interferon-dependent resistance to influenza virus in mice.* J Exp Med, 1979. **149**(3): p. 601-12.

90. Haller, O., et al., *Tick-borne thogoto virus infection in mice is inhibited by the orthomyxovirus resistance gene product Mx1.* J Virol, 1995. **69**(4): p. 2596-601.

91. Pavlovic, J., et al., *Enhanced virus resistance of transgenic mice expressing the human MxA protein.* J Virol, 1995. **69**(7): p. 4506-10.

92. Hefti, H.P., et al., *Human MxA protein protects mice lacking a functional alpha/beta interferon system against La crosse virus and other lethal viral infections.* J Virol, 1999. **73**(8): p. 6984-91.

93. Kochs, G. and O. Haller, *GTP-bound human MxA protein interacts with the nucleocapsids of Thogoto virus (Orthomyxoviridae).* J Biol Chem, 1999. **274**(7): p. 4370-6.

94. Kochs, G. and O. Haller, *Interferon induced human MxA GTPase blocks nuclear import of Thogoto virus nucleocapsids.* PNAS, 1999. **96**: p. 2082-86.

95. Kochs, G., et al., *Antivirally active MxA protein sequesters La Crosse virus nucleocapsid protein into perinuclear complexes.* Proc Natl Acad Sci U S A, 2002. **99**(5): p. 3153-8.

96. Reichelt, M., et al., *Missorting of LaCrosse virus nucleocapsid protein by the interferon-induced MxA GTPase involves smooth ER membranes.* Traffic, 2004. **5**(10): p. 772-84.

97. Richter, M.F., et al., *Interferon-induced MxA Protein.* J. Biol. Chem., 1995. **270**(22): p. 13512-13517.

98. Kochs, G., et al., *Self-assembly of Human MxA GTPase into Highly Ordered Dynamin-like Oligomers.* J. Biol. Chem., 2002. **277**(16): p. 14172-14176.

99. Melen, K., et al., *Enzymatic characterization of interferon-induced antiviral GTPases murine Mx1 and human MxA proteins.* J Biol Chem, 1994. **269**(3): p. 2009-15.

100. Janzen, C., G. Kochs, and O. Haller, *A monomeric GTPase-negative MxA mutant with antiviral activity.* J Virol, 2000. **74**(17): p. 8202-6.

101. Accola, M.A., et al., *The Antiviral Dynamin Family Member, MxA, Tubulates Lipids and Localizes to the Smooth Endoplasmic Reticulum.* J. Biol. Chem., 2002. **277**(24): p. 21829-21835.

102.   Engelhardt, O.G., et al., *Mx1 GTPase accumulates in distinct nuclear domains and inhibits influenza A virus in cells that lack promyelocytic leukaemia protein nuclear bodies.* J Gen Virol, 2004. **85**(Pt 8): p. 2315-26.

103.   Boehm, U., et al., *Two families of GTPases dominate the complex cellular response to IFN-g.* J Immunol, 1998. **161**: p. 6715-6723.

104.   Anderson, S.L., et al., *Interferon-induced Guanylate Binding Protein-1 (GBP-1) mediates an antiviral effect against Vesicular Stomatitis Virus and Encephalomyocarditis Virus.* Virology, 1999. **256**: p. 8-14.

105.   Carter, C.C., V.Y. Gorbacheva, and D.J. Vestal, *Inhibition of VSV and EMCV replication by the interferon-induced GTPase, mGBP-2: differential requirement for wild-type GTP binding domain.* Arch Virol, 2005.

106.   Gorbacheva, V.Y., et al., *The Interferon (IFN)-induced GTPase, mGBP-2. rple in IFN-gamma -induced murine fibroblast proliferation.* J. Biol. Chem., 2002. **277**(8): p. 6080-6087.

107.   Guenzi, E., Topolt, Kristin, Cornali, Emmanuelle, Lubeseder-Martellato, Clara, Jorg, Anita, Matzen, Kathrin, Zietz, Christian, Kremmer, Elisabeth, Nappi, Filomena, Schwemmle, Martin, Hohenadl, Christine, Barillari, Giovanni, Tschachler, Erwin, Monini, Paolo, Ensoli, Barbara, Sturzl, Michael, *The helical domain of GBP-1 mediates the inhibition of endothelial cell proliferation by inflammatory cytokines.* EMBO J., 2001. **20**: p. 5568-5577.

108.   Guenzi, E., et al., *The guanylate binding protein-1 GTPase controls the invasive and angiogenic capability of endothelial cells through inhibition of MMP-1 expression.* EMBO J., 2003. **22**(15): p. 3772-3782.

109.   Vestal, D.J., V.Y. Gorbacheva, and G.C. Sen, *Different subcellular localizations for the related interferon-induced GTPases, MuGBP-1 and MuGBP-2: implications for different functions?* J Interferon Cytokine Res, 2000. **20**(11): p. 991-1000.

110.   Klamp, T., Boehm, U., Schenk, D., Pfeffer K. and Howard J.C., *A giant GTPase, VLIG-1, is inducible by interferons.* J Immunol, 2003. **in press**.

111.   Taylor, G.A., C.G. Feng, and A. Sher, *p47 GTPases: regulators of immunity to intracellular pathogens.* Nat Rev Immunol, 2004. **4**(2): p. 100-9.

112.   Bekpen, C., et al., *The interferon-inducible p47 (IRG) GTPases in vertebrates: loss of the cell-autonomous resistance mechanism in the human lineage.* submitted, 2005.

113.   Carlow, D., et al., *Isolation of a gene encoding a developmentally regulated T cell-specific protein with a guanine nucleotide triphosphate-binding motif.* J Immunol, 1995. **154**(4): p. 1724-34.

114.   Gilly, M. and R. Wall, *The IRG-47 gene is IFN-g induced in B cells and encodes a protein with GTP-binding motifs.* J Immunol, 1992. **148**(10): p. 3275-81.

115. Taylor, G., et al., *Identification of a novel GTPase, the inducibly expressed GTPase, that accumulates in response to interferon gamma.* J Biol Chem, 1996. **271**(34): p. 20399-405.

116. Sorace, J.M., et al., *Identification of an endotoxin and IFN-inducible cDNA: possible identification of a novel protein family.* J Leukoc Biol, 1995. **58**(4): p. 477-84.

117. Bourne, H.R., D.A. Sanders, and F. McCormick, *The GTPase superfamily: conserved structure and molecular mechanism.* Nature, 1991. **349**(6305): p. 117-27.

118. Lafuse, W.P., et al., *Cloning and characterization of a novel cDNA that is IFN-gamma-induced in mouse peritoneal macrophages and encodes a putative GTP-binding protein.* J Leukoc Biol, 1995. **57**(3): p. 477-83.

119. Zerrahn, J., et al., *The IFN-Inducible Golgi- and Endoplasmic Reticulum-Associated 47-kDa GTPase IIGP Is Transiently Expressed During Listeriosis.* J Immunol, 2002. **168**(7): p. 3428-3436.

120. MacMicking, J.D., *IFN-inducible GTPases and immunity to intracellular pathogens.* Trends Immunol, 2004. **25**(11): p. 601-9.

121. Collazo, C.M., et al., *Inactivation of LRG-47 and IRG-47 reveals a family of interferon gamma-inducible genes with essential, pathogen-specific roles in resistance to infection.* J Exp Med, 2001. **194**(2): p. 181-8.

122. Taylor, G.A., et al., *Pathogen-specific loss of host resistance in mice lacking the IFN-gamma-inducible gene IGTP.* Proc Natl Acad Sci U S A, 2000. **97**(2): p. 751-5.

123. MacMicking, J.D., G.A. Taylor, and J.D. McKinney, *Immune control of tuberculosis by IFN-gamma-inducible LRG-47.* Science, 2003. **302**(5645): p. 654-9.

124. Martens, S., et al., *Mechanisms regulating the positioning of mouse p47 resistance GTPases LRG-47 and IIGP1 on cellular membranes: retargeting to plasma membrane induced by phagocytosis.* J Immunol, 2004. **173**(4): p. 2594-606.

125. Taylor, G., et al., *The inducibly expressed GTPase localizes to the endoplasmic reticulum, independently of GTP binding.* J Biol Chem, 1997. **272**(16): p. 10639-45.

126. Martens, S., *Cell-Biology of Interferon Inducible GTPases*, in *Thesis*. 2004.

127. Praefcke, G.J. and H.T. McMahon, *The dynamin superfamily: universal membrane tubulation and fission molecules?* Nat Rev Mol Cell Biol, 2004. **5**(2): p. 133-47.

128. Sever, S., H. Damke, and S.L. Schmid, *Garrotes, springs, ratchets, and whips: putting dynamin models to the test.* Traffic, 2000. **1**(5): p. 385-92.

129. Prakash, B., et al., *Structure of human guanylat-binding protein 1representing a unique class of GTP-binding proteins.* Nature, 2000. **403**(6769): p. 567-71.

130. Uthaiah, R.C., Gerrit J. K. Praefcke, Jonathan C. Howard, Christian Herrmann, *IIGP1, an interferon-g inducible 47 kDa GTPase of the Mouse, showing cooperative enzymatic activity and GTP-dependent multimerisation.* J Biol Chem., 2003. **in press**.

131. Eccleston, J.F., et al., *Oligomerization and kinetic mechanism of the dynamin GTPase.* Eur Biophys J, 2002. **31**(4): p. 275-82.

132. Praefcke, G.J., et al., *Nucleotide-binding characteristics of human guanylat-binding protein 1 (hGBP-1) and identification of the third GTP-binding motif.* J. Mol. Biol., 1999. **292**(2): p. 321-32.

133. Ghosh, A., et al., *Crystal structure of IIGP1: a paradigm for interferon-inducible p47 resistance GTPases.* Mol Cell, 2004. **15**(5): p. 727-39.

134. Martens, S., et al., *Disruption of Toxoplasma gondii parasitophorous vacuoles by the mouse p47 resistance GTPases.* 2005.

135. Kaiser, F., S.H. Kaufmann, and J. Zerrahn, *IIGP, a member of the IFN inducible and microbial defense mediating 47 kDa GTPase family, interacts with the microtubule binding protein hook3.* J Cell Sci, 2004. **117**(Pt 9): p. 1747-56.

136. Walenta, J.H., et al., *The Golgi-associated hook3 protein is a member of a novel family of microtubule-binding proteins.* J Cell Biol, 2001. **152**(5): p. 923-34.

137. Muller, W., R. Kuhn, and K. Rajewsky, *Major histocompatibility complex class II hyperexpression on B cells in interleukin 4-transgenic mice does not lead to B cell proliferation and hypergammaglobulinemia.* Eur J Immunol, 1991. **21**(4): p. 921-5.

138. Kontgen, F., et al., *Targeted disruption of the MHC class II Aa gene in C57BL/6 mice.* Int Immunol, 1993. **5**(8): p. 957-64.

139. Sambrook, j., e.f. Fritsch, and t. Maniatis, *Molecular Cloning.* Cold Spring Harbor Laboratory Press, 1989.

140. Inoue, H., H. Nojima, and H. Okayama, *High efficiency transformation of Escherichia coli with plasmids.* Gene, 1990. **96**(1): p. 23-8.

141. Birnboim, H.C., *A rapid alkaline extraction method for the isolation of plasmid DNA.* Methods Enzymol, 1983. **100**: p. 243-55.

142. Saiki, R.K., et al., *Enzymatic amplification of beta-globin genomic sequences and restriction site analysis for diagnosis of sickle cell anemia.* Science, 1985. **230**(4732): p. 1350-4.

143. Sanger, F., S. Nicklen, and A.R. Coulson, *DNA sequencing with chain-terminating inhibitors.* Proc Natl Acad Sci U S A, 1977. **74**(12): p. 5463-7.

144. Walls, J.J., et al., *Improved sensitivity of PCR for diagnosis of human granulocytic ehrlichiosis using epank1 genes of Ehrlichia phagocytophila-group ehrlichiae.* J Clin Microbiol, 2000. **38**(1): p. 354-6.

145. Torres, R. and R. Kuehn, *Laboratory protocols for conditional gene targeting.* 1997: Oxford university press.

146. Forster, I. and K. Rajewsky, *Expansion and functional activity of Ly-1+ B cells upon transfer of peritoneal cells into allotype-congenic, newborn mice.* Eur J Immunol, 1987. **17**(4): p. 521-8.

147. Pfefferkorn, E.R. and L.C. Pfefferkorn, *Specific labeling of intracellular Toxoplasma gondii with uracil.* J Protozool, 1977. **24**(3): p. 449-53.

148. Peitz, M., et al., *Ability of the hydrophobic FGF and basic TAT peptides to promote cellular uptake of recombinant Cre recombinase: a tool for efficient genetic engineering of mammalian genomes.* Proc Natl Acad Sci U S A, 2002. **99**(7): p. 4489-94.

149. Schwenk, F., U. Baron, and K. Rajewsky, *A cre-transgenic mouse strain for the ubiquitous deletion of loxP-flanked gene segments including deletion in germ cells.* Nucleic Acids Res, 1995. **23**(24): p. 5080-1.

150. Yap, G.S. and A. Sher, *Cell-mediated immunity to Toxoplasma gondii: initiation, regulation and effector function.* Immunobiology, 1999. **201**(2): p. 240-7.

151. Gazzinelli, R.T., et al., *Acute cerebral toxoplasmosis is induced by in vivo neutralization of TNF-alpha and correlates with the down-regulated expression of inducible nitric oxide synthase and other markers of macrophage activation.* J Immunol, 1993. **151**(7): p. 3672-81.

152. Halonen, S.K., F. Chiu, and L.M. Weiss, *Effect of cytokines on growth of Toxoplasma gondii in murine astrocytes.* Infect Immun, 1998. **66**(10): p. 4989-93.

153. Halonen, S.K. and L.M. Weiss, *Investigation into the mechanism of gamma interferon-mediated inhibition of Toxoplasma gondii in murine astrocytes.* Infect Immun, 2000. **68**(6): p. 3426-30.

154. Halonen, S.K., G.A. Taylor, and L.M. Weiss, *Gamma interferon-induced inhibition of Toxoplasma gondii in astrocytes is mediated by IGTP.* Infect Immun, 2001. **69**(9): p. 5573-6.

155. Sibley, L.D., *Intracellular parasite invasion strategies.* Science, 2004. **304**(5668): p. 248-53.

156. Suss-Toby, E., J. Zimmerberg, and G.E. Ward, *Toxoplasma invasion: the parasitophorous vacuole is formed from host cell plasma membrane and*

pinches off via a fission pore. Proc Natl Acad Sci U S A, 1996. **93**(16): p. 8413-8.

157.   Mordue, D.G., et al., *Invasion by Toxoplasma gondii establishes a moving junction that selectively excludes host cell plasma membrane proteins on the basis of their membrane anchoring.* J Exp Med, 1999. **190**(12): p. 1783-92.

158.   Joiner, K.A., et al., *Toxoplasma gondii: fusion competence of parasitophorous vacuoles in Fc receptor-transfected fibroblasts.* Science, 1990. **249**(4969): p. 641-6.

159.   Fischer, H.G., et al., *GRA7, an excretory 29 kDa Toxoplasma gondii dense granule antigen released by infected host cells.* Mol Biochem Parasitol, 1998. **91**(2): p. 251-62.

160.   Bannister, L. and G. Mitchell, *The ins, outs and roundabouts of malaria.* Trends Parasitol, 2003. **19**(5): p. 209-13.

161.   Hoffman, S., et al., *Attacking the infected hepatocyte*, in *Malaria Vaccine Development: A Multi-Immune Response Approach*, H.S. L., Editor. 1996, American Society for Microbiology Press: Washington, DC. p. 35-76.

162.   Good, M.F. and D.L. Doolan, *Immune effector mechanisms in malaria.* Curr Opin Immunol, 1999. **11**(4): p. 412-9.

163.   Berzins, K. and P. P., *Malaria Vaccines: attacking infected erythrocytes*, in *Malaria Vaccine Development: A Multi-Immune Response Approach*, H.S. L., Editor. 1996, American Society for Microbiology Press: Washington, DC.

164.   Good, M.F., et al.,*Development and regulation of cell-mediated immune response to the blood stages of malaria: Implications for Vaccine Research.* Annu Rev Immunol, 2005. **23**: p. 69-99.

165.   Rest, J.R., *Cerebral malaria in inbred mice. I. A new model and its pathology.* Trans R Soc Trop Med Hyg, 1982. **76**(3): p. 410-5.

166.   Lou, J., R. Lucas, and G.E. Grau, *Pathogenesis of cerebral malaria: recent experimental data and possible applications for humans.* Clin Microbiol Rev, 2001. **14**(4): p. 810-20, table of contents.

167.   Clark, I.A., K.A. Rockett, and W.B. Cowden, *Proposed link between cytokines, nitric oxide and human cerebral malaria.* Parasitol Today, 1991. **7**(8): p. 205-7.

168.   Heinzel, F.P., et al., *Reciprocal expression of interferon gamma or interleukin 4 during the resolution or progression of murine leishmaniasis. Evidence for expansion of distinct helper T cell subsets.* J Exp Med, 1989. **169**(1): p. 59-72.

169.   Holaday, B.J., et al., *Reconstitution of Leishmania immunity in severe combined immunodeficient mice using Th1- and Th2-like cell lines.* J Immunol, 1991. **147**(5): p. 1653-8.

170. Tripp, C.S., S.F. Wolf, and E.R. Unanue, *Interleukin 12 and tumor necrosis factor alpha are costimulators of interferon gamma production by natural killer cells in severe combined immunodeficiency mice with listeriosis, and interleukin 10 is a physiologic antagonist.* Proc Natl Acad Sci U S A, 1993. **90**(8): p. 3725-9.

171. Unanue, E.R., *Inter-relationship among macrophages, natural killer cells and neutrophils in early stages of Listeria resistance.* Curr Opin Immunol, 1997. **9**(1): p. 35-43.

172. Dumler, J.S., et al., *Reorganization of genera in the families Rickettsiaceae and Anaplasmataceae in the order Rickettsiales: unification of some species of Ehrlichia with Anaplasma, Cowdria with Ehrlichia and Ehrlichia with Neorickettsia, descriptions of six new species combinations and designation of Ehrlichia equi and 'HGE agent' as subjective synonyms of Ehrlichia phagocytophila.* Int J Syst Evol Microbiol, 2001. **51**(Pt 6): p. 2145-65.

173. Akkoyunlu, M. and E. Fikrig, *Gamma interferon dominates the murine cytokine response to the agent of human granulocytic ehrlichiosis and helps to control the degree of early rickettsemia.* Infect Immun, 2000. **68**(4): p. 1827-33.

174. Martin, M.E., K. Caspersen, and J.S. Dumler, *Immunopathology and ehrlichial propagation are regulated by interferon-gamma and interleukin-10 in a murine model of human granulocytic ehrlichiosis.* Am J Pathol, 2001. **158**(5): p. 1881-8.

175. Schachter, J., *Chlamydia: Intracellular Biology, Pathogenesis and Immunity*, R. Stephens, S., Editor. 1999, American Society for Microbiology Press: Washington DC. p. 139-169.

176. Beatty, W.L., et al., *Role of tryptophan in gamma interferon-mediated chlamydial persistence.* Ann N Y Acad Sci, 1994. **730**: p. 304-6.

177. Ramsey, K.H., et al., *Role for inducible nitric oxide synthase in protection from chronic Chlamydia trachomatis urogenital disease in mice and its regulation by oxygen free radicals.* Infect Immun, 2001. **69**(12): p. 7374-9.

178. Parker, G.A. and C.A. Picut, *Liver immunobiology.* Toxicol Pathol, 2005. **33**(1): p. 52-62.

179. Li, Z. and A.M. Diehl, *Innate immunity in the liver.* Curr Opin Gastroenterol, 2003. **19**(6): p. 565-71.

180. Dubey, J.P. and C.P. Beattie, *Toxoplasmosis of Animals and Man.* Boca Raton, FL, CRC Press, 1988: p. 220.

181. Opitz, C. and D. Soldati, *'The glideosome': a dynamic complex powering gliding motion and host cell invasion by Toxoplasma gondii.* Mol Microbiol, 2002. **45**(3): p. 597-604.

182.   Morisaki, J.H., J.E. Heuser, and L.D. Sibley, *Invasion of Toxoplasma gondii occurs by active penetration of the host cell.* J Cell Sci, 1995. **108 (Pt 6)**: p. 2457-64.

183.   Dobrowolski, J.M. and L.D. Sibley, *Toxoplasma invasion of mammalian cells is powered by the actin cytoskeleton of the parasite.* Cell, 1996. **84**(6): p. 933-9.

184.   Aikawa, M., et al., *Transmission and scanning electron microscopy of host cell entry by Toxoplasma gondii.* Am J Pathol, 1977. **87**(2): p. 285-96.

185.   Lingelbach, K. and K.A. Joiner, *The parasitophorous vacuole membrane surrounding Plasmodium and Toxoplasma: an unusual compartment in infected cells.* J Cell Sci, 1998. **111 (Pt 11)**: p. 1467-75.

186.   Sinai, A.P., P. Webster, and K.A. Joiner, *Association of host cell endoplasmic reticulum and mitochondria with the Toxoplasma gondii parasitophorous vacuole membrane: a high affinity interaction.* J Cell Sci, 1997. **110 (Pt 17)**: p. 2117-28.

187.   Schwab, J.C., C.J. Beckers, and K.A. Joiner, *The parasitophorous vacuole membrane surrounding intracellular Toxoplasma gondii functions as a molecular sieve.* Proc Natl Acad Sci U S A, 1994. **91**(2): p. 509-13.

188.   Collazo, C.M., et al., *The function of gamma interferon-inducible GTP-binding protein IGTP in host resistance to Toxoplasma gondii is Stat1 dependent and requires expression in both hematopoietic and nonhematopoietic cellular compartments.* Infect Immun, 2002. **70**(12): p. 6933-9.

189.   Menard, R., *Gliding motility and cell invasion by Apicomplexa: insights from the Plasmodium sporozoite.* Cell Microbiol, 2001. **3**(2): p. 63-73.

190.   Harrison, T., et al., *Erythrocyte G protein-coupled receptor signaling in malarial infection.* Science, 2003. **301**(5640): p. 1734-6.

191.   Chitnis, C.E. and M.J. Blackman, *Host cell invasion by malaria parasites.* Parasitol Today, 2000. **16**(10): p. 411-5.

192.   Lauer, S., et al., *Vacuolar uptake of host components, and a role for cholesterol and sphingomyelin in malarial infection.* Embo J, 2000. **19**(14): p. 3556-64.

193.   Ward, G.E., L.H. Miller, and J.A. Dvorak, *The origin of parasitophorous vacuole membrane lipids in malaria-infected erythrocytes.* J Cell Sci, 1993. **106 (Pt 1)**: p. 237-48.

194.   Pouvelle, B., J.A. Gormley, and T.F. Taraschi, *Characterization of trafficking pathways and membrane genesis in malaria-infected erythrocytes.* Mol Biochem Parasitol, 1994. **66**(1): p. 83-96.

195.   Lauer, S.A., et al., *A membrane network for nutrient import in red cells infected with the malaria parasite.* Science, 1997. **276**(5315): p. 1122-5.

196.   Mota, M.M., et al., *Migration of Plasmodium sporozoites through cells before infection.* Science, 2001. **291**(5501): p. 141-4.

197.   Molyneux, M.E., et al., *Clinical features and prognostic indicators in paediatric cerebral malaria: a study of 131 comatose Malawian children.* Q J Med, 1989. **71**(265): p. 441-59.

198.   Engwerda, C.R., L. Beattie, and F.H. Amante, *The importance of the spleen in malaria.* Trends Parasitol, 2005. **21**(2): p. 75-80.

199.   Chotivanich, K., et al., *Central role of the spleen in malaria parasite clearance.* J Infect Dis, 2002. **185**(10): p. 1538-41.

200.   Yadava, A., et al., *Trafficking of Plasmodium chabaudi adami-infected erythrocytes within the mouse spleen.* Proc Natl Acad Sci U S A, 1996. **93**(10): p. 4595-9.

201.   Rittig, M.G. and C. Bogdan, *Leishmania-host-cell interaction: complexities and alternative views.* Parasitol Today, 2000. **16**(7): p. 292-7.

202.   Alexander, J. and D.G. Russell, *The interaction of Leishmania species with macrophages.* Adv Parasitol, 1992. **31**: p. 175-254.

203.   Mosser, D.M. and A. Brittingham, *Leishmania, macrophages and complement: a tale of subversion and exploitation.* Parasitology, 1997. **115 Suppl**: p. S9-23.

204.   Courret, N., et al., *Biogenesis of Leishmania-harbouring parasitophorous vacuoles following phagocytosis of the metacyclic promastigote or amastigote stages of the parasites.* J Cell Sci, 2002. **115**(Pt 11): p. 2303-16.

205.   Cossart, P. and P.J. Sansonetti, *Bacterial invasion: the paradigms of enteroinvasive pathogens.* Science, 2004. **304**(5668): p. 242-8.

206.   Cossart, P., J. Pizarro-Cerda, and M. Lecuit, *Invasion of mammalian cells by Listeria monocytogenes: functional mimicry to subvert cellular functions.* Trends Cell Biol, 2003. **13**(1): p. 23-31.

207.   Bielecki, J., et al., *Bacillus subtilis expressing a haemolysin gene from Listeria monocytogenes can grow in mammalian cells.* Nature, 1990. **345**(6271): p. 175-6.

208.   O'Riordan, M., et al., *Innate recognition of bacteria by a macrophage cytosolic surveillance pathway.* Proc Natl Acad Sci U S A, 2002. **99**(21): p. 13861-6.

209.   Domann, E., et al., *A novel bacterial virulence gene in Listeria monocytogenes required for host cell microfilament interaction with homology to the proline-rich region of vinculin.* Embo J, 1992. **11**(5): p. 1981-90.

210. Kocks, C., et al., *L. monocytogenes-induced actin assembly requires the actA gene product, a surface protein.* Cell, 1992. **68**(3): p. 521-31.

211. Carlyon, J.A. and E. Fikrig, *Invasion and survival strategies of Anaplasma phagocytophilum.* Cell Microbiol, 2003. **5**(11): p. 743-54.

212. Fields, K.A. and T. Hackstadt, *Evidence for the secretion of Chlamydia trachomatis CopN by a type III secretion mechanism.* Mol Microbiol, 2000. **38**(5): p. 1048-60.

213. Fields, K.A. and T. Hackstadt, *The chlamydial inclusion: escape from the endocytic pathway.* Annu Rev Cell Dev Biol, 2002. **18**: p. 221-45.

214. Moulder, J.W., *Interaction of chlamydiae and host cells in vitro.* Microbiol Rev, 1991. **55**(1): p. 143-90.

215. Hackstadt, T., et al., *Chlamydia trachomatis interrupts an exocytic pathway to acquire endogenously synthesized sphingomyelin in transit from the Golgi apparatus to the plasma membrane.* Embo J, 1996. **15**(5): p. 964-77.

216. Macmicking, J.D., *Immune control of phagosomal bacteria by p47 GTPases.* Curr Opin Microbiol, 2005. **8**(1): p. 74-82.

217. Prada-Delgado, A., et al., *Interferon-gamma listericidal action is mediated by novel Rab5a functions at the phagosomal environment.* J Biol Chem, 2001. **276**(22): p. 19059-65.

218. Luedke, D., *Erstellung von targeting-Vectoren zur konditionalen Mutagenese der Gene der Interferon-γ-induzierten GTPasen IIGP und GTPI.* Diplomarbeit, 2000

219. Platanias, L., *Mechanisms of type-1 and type-2 interferon-medated signaling.* Nat Rev Immunol, 2005. **5**:p. 375-386

220. Uyttersprot, N. and Rajewsky, K., unpublished

6 SUMMARY

IIGP1 is a member of the p47 GTPase family of IFNγ-induced proteins, which are among the most potent presently known mediators of cell-autonomous resistance against intracellular bacterial and protozoan pathogens in the mouse. From all studied members of this family IIGP1 is the best characterized with respect to biochemical characteristics and enzymatic activity *in vitro,* as well as membrane binding properties and dynamic behavior in cells. The role of the protein in intracellular defense was however, unknown and this study was set as an initial attempt to reveal it.

This thesis describes the generation of an IIGP1 deficient mouse and analysis of the susceptibility of this animal to pathogens from protozoan and bacterial origin, which employ diverse strategies for host cell invasion and intracellular survival and replication. Despite having intact adaptive immune system, the IIGP1 deficient mice showed higher incidence of development of cerebral malaria after infection with *Plasmodium berghei* sporozoites. In addition, IIGP1 deficient astrocytes exhibited a partial loss of IFNγ-induced inhibition of *Toxoplasma gondii* growth. IIGP1 deficient animals were not susceptible to infection with *Leishmania major, Listeria monocytogenes, Chlamydia trachomatis* and *Anaplasma phagocytophilum.*

From the analysis of the obtained data in the context of the intracellular lifestyle of the pathogens involved in this study, we concluded that IIGP1 seems to be specifically involved in defense against protozoan parasites, which like *Pl. berghei* and *T. gondii* reside in non-fusigenic parasitophorous vacuoles after entering cells. The mechanisms of IIGP1-dependent protection of cells against these pathogens remain to be studied.

7 ZUSAMMENFASSUNG

IIGP1 ist ein IFNg-induziertes Protein und Mitglied der p47 GTPase-Familie. Die Mitglieder dieser Familie sind in der Maus hauptverantwortlich für die zellautonome Resistenz gegen intrazelluläre Pathogene, wie Bakterien und Protozoen. Von allen untersuchten Familienmitgliedern ist IIGP1 am Besten charakterisiert, sowohl was die biochemischen Charakteristika, die enzymatische Aktivität *in vitro*, die Membranassoziation wie auch das dynamische Verhalten in der Zelle angehen. Die Rolle des Proteins in der intrazellulären Verteidigung war bisher allerdings unbekannt.

Diese Arbeit beschreibt die Erstellung von IIGP1-defizienten Mäusen und die Analyse dieser Tiere auf Sukzeptibilität gegenüber verschiedenen Pathogenen. Diese Bakterien und Protozoen benutzen eine Reihe verschiedener Strategien für die Invasion von Zielzellen und für das anschliessende Überleben und die Replikation in diesen Zellen. Obwohl IIGP1-defiziente Mäuse ein ansonsten funktionierendes adaptives Immunsystem besitzen, zeigen sie eine höhere Inzidenz zerebraler Malaria nach Infektion mit *Plasmodium berghei* Sporozoiten. Ausserdem zeigten IIGP1 – defiziente Astrozyten einen partiellen Verlust von IFNinduzierter Inhibition des Wachstums von Toxoplasma gondii. IIGP1-defiziente Tiere zeigten hingegen keine erhöhte Sukzetibilität für Infektionen mit *Leishmania major*, *Listeria monocytogenes*, *Chlamydia trachomatis* und *Anaplasma phagocytophilum*.

Aufgrund unserer Analysen erscheint es daher, dass IIGP1 spezifisch in der Verteidigung gegen intrazelluläre Protozoen, die wie wie *Plasmodium berghei* und *Toxoplasma gondii* in einer nicht-fusigenen parasitophoren Vakuole leben, eine zentrale Rolle spielt. Der Mechanismus des IIGP1-abhängigen Schutzes der Zellen gegen diese Pathogene muss nun weiter untersucht werden.

8 ACKNOWLEDGEMENTS

9 ERKLAERUNG

Ich versichere, dass ich die von mir vorgelegte Dissertation selbstaendig angefertigt, die benutzten Quellen und Hilfsmittel vollstaendig angegeben und die Stellen der Arbeit – einschließlich Tabellen, Karten und Abbildungen-, die anderen Werken im Wortlaut oder dem Sinn nach entnommen sind, in jedem Einzelfall als Entlehnung kenntlich gemacht habe; dass diese Dissertation noch keiner anderen Fakultaet oder Universitaet zur Pruefung vorgelegen hat; dass sie abgesehen von den unten angegebenen Teilpublikationen noch nicht veroeffentlicht worden ist, sowie, dass ich eine solche Veroeffentlichung vor Abschluss des Promotionsverfahrens nicht vornehmen werde.

Die von mir vorgelegte Dissertation ist von Prof. Dr. Jonathan C. Howard betreut worden.

Koeln, im Mai 2005

10 LEBENSLAUF

<u>Name:</u>	Iana Angelova Parvanova
<u>Geburtsdatum:</u>	15.03.1976
<u>Geburtsort:</u>	Veliko Tarnovo, Bulgarien
<u>Staatsangehoerigkeit:</u>	Bulgarisch
<u>Familienstand:</u>	Ledig

<u>Ausbildung:</u>

1983-1990	Grundschule, Veliko Tarnovo, Bulgarien
1990-1995	Mathematisch-Naturwissenschaftliche Gymnasium, Veliko Tarnovo, Bulgarien
1995	Immatrikulation an der Biologischen Fakultaet der Universitaet zu Sofia „St. Kliment Ohridski", Bulgarien. Diplomstudiengang: Molekularbiologie
1995-1999	Studium der Biologie an der Universitaet zu Sofia „St. Kliment Ohridski", Bulgarien
1999-2000	Diplomarbeit Biochemie (Fachrichtung Molekularbiologie) an der Biologischen Fakultaet der Universitaet zu Sofia „St. Kliment Ohridski", Bulgarien in der Abteilung fuer Molekularimmunologie Thema: „Charakterisierung der Bindung von C1q an Immunoglobuline der Klasse M"
ab WS 2000/2001	Promotionsstudiengang Biologie (Fachrichtung Genetik) am Institut für Genetik, Universität zu Köln, Abteilung von Prof. Dr. Jonathan C. Howard